MODELING PACKAGED HEAT PUMPS IN A QUASI-STEADY STATE ENERGY SIMULATION PROGRAM

By

TANG, CHIH CHIEN

Bachelor of Science

Oklahoma State University,

Stillwater, Oklahoma

2003

Submitted to the Faculty of the
Graduate College of the
Oklahoma State University
in partial fulfillment of
the requirements for
the Degree of
MASTER OF SCIENCE
May, 2005

MODELING PACKAGED HEAT PUMPS IN

A QUASI-STEADY STATE ENERGY

SIMULATION PROGRAM

Thesis Approved:

Dr. Daniel Fisher

Thesis Adviser

Dr. Jeffrey Spitler

Dr. Ronald Delahoussaye

Dr. A. Gordon Emslie

Dean of the Graduate College

ACKNOWLEDGEMENTS

This page is dedicated to everyone who has somehow laid a print in my life both directly involved in this research and those who stand by the sidelines cheering me on towards the end. First of all, thank you God for bringing me to form and giving me talents that are limited only by my own imagination. Dr. D.E. Fisher, you are the best advisor a graduate student could have, thank you for your generous support, optimistic attitude, guidance, and not to forget the Thanksgiving dinners. My committee members, Dr. J.D. Spitler and Dr. R.D. Delahoussaye for their constructive guidance and expertise.

Thank you Mum and Dad for your sacrifices to put me through college. My brother and his wife, Clement and Sue, and Yee Shyen for being the cheerleading squad. Calvin for guidance and valuable inputs; Shawn and Ben for helping with the experimental instrumentation; Chanvit for programming tips. Also a note of appreciation to all my colleagues; Xiaobing Liu, Dongyi Xiao, Haider, Muhammad, Wei Xiu, Xiao Wei, Brian Kastl, Arun Shenoy and Sankar for their friendships and the wonderful memories.

I would also like to express my gratitude to York International Unitary Product Group especially to Nathan Webber, Messrs C. Obosu and M. Chitti for providing the measured data and their expertise on air-to-air heat pumps. Special thanks also to ClimaterMaster especially to L.N. Nerurkar for providing the experimental data for water-to-air heat pumps. Last but not least, financial support from the U.S Department of Energy and advice from the EnergyPlus development team are gratefully acknowledged.

TABLE OF CONTENTS

Chapter *Page*

LIST OF TABLES

Table *Page*

LIST OF FIGURES

Figure *Page*

NOMENCLATURE

Symbols

BF	=	bypass factor
C_p	=	specific heat, J/(kg-K)
COP	=	coefficient of performance
dp	=	dew point temperature, °C
EIR	=	energy input ratio
FMF	=	flow modifying factor curve
h	=	enthalpy, J/kg
$h_{co}A_o$	=	load side external surface heat transfer coefficient, W/K
LHR	=	latent heat ratio
$\dot{m}_{air}$	=	air mass flow rate, kg/s
$\dot{m}_w$	=	water mass flow rate, kg/s
$\dot{m}_r$	=	refrigerant mass flow rate, kg/s
Mo	=	moisture holding capacity of the coil, kg
$N_{\max}$	=	heat pump cycling rate, cycles/hr
NTU	=	number of transfer units
P_c	=	condensing pressure, Pa
P_e	=	evaporating pressure, Pa
P_{dis}	=	discharge pressure, Pa
P_{suc}	=	suction pressure, Pa
$Power$	=	power consumption, W
PLR	=	part-load ratio
PLF	=	part-load fraction

SHR	=	sensible heat ratio
$t_{fandelay}$	=	fan delay time, s
t_{on}	=	duration of time the compressor is on, s
t_{off}	=	duration of time the compressor is off, s
t_{wet}	=	the ratio of the moisture holding capacity of the coil to the steady state latent capacity of the heat pump
t_0	=	time for condensate removal to begin, s
T_{db}	=	dry-bulb temperature, °C, °F or K
T_{wb}	=	wet-bulb temperature, °C, °F or K
TMF	=	temperature modifying factor curve
UA	=	heat transfer coefficient, W/K
W_{comp}	=	compressor work, W
Q_e	=	initial evaporation rate when the compressor off, W
Q_h	=	total heating capacity, W
Q_{lat}	=	latent capacity, W
Q_{sens}	=	sensible cooling capacity, W
Q_{source}	=	source side heat transfer rate, W
Q_{total}	=	total cooling capacity, W
X	=	runtime fraction
W_{loss}	=	compressor power losses due to mechanical and electrical losses, W
τ	=	heat pump time constant, s
γ	=	the ratio of the initial evaporation rate and steady-state latent capacity
ε	=	heat transfer effectiveness
w	=	humidity ratio, kg/kg

η	=	efficiency

1.0 Introduction

The rise in oil and energy prices has prompted the Department of Energy to increase research funding for renewable energy and increase the efficiency of unitary equipment systems. EnergyPlus, an hourly building simulation program funded by DOE, is one such endeavor that allows building and system designers to design better building envelops and unitary systems that are energy efficient and low in first cost.

1.1. Background

In hourly energy simulations, it is essential to accurately predict the performance of heat pumps over the range of full and part-load operating conditions. A number of heat pump models have been proposed by researchers over the years ranging from detailed deterministic models to simple curve-fit models. Detailed deterministic models are based on thermodynamic laws and heat transfer relations applied to individual components. The models generally require a lot of parameters or input data and require longer simulation times. On the other hand, simple curve-fit model treats the heat pump as a black box and the system performance is predicted using equations generated from the heat pump performance curve provided by the manufacturer's catalog.

However, the suitability of these models for incorporation into EnergyPlus has to be evaluated based on simulation run time, availability of data or required parameters, accuracy and stability of the models and ease of use. In short, the heat pump model

should be relatively easy to use, reasonably accurate and have a short simulation run time.

1.2. Objective

This research is focused on building upon previous heat pump models that have been developed by previous researchers in the form of validation, improvement, and implementation into EnergyPlus. From this research, the selection and implementation of heat pump models in EnergyPlus will be justified on the basis of models' accuracy, ease of use, and simulation run time.

Unitary heat pump models are discussed in Chapter 2 together with related models developed by researchers. The heat pump models implemented in EnergyPlus are steady state models. Since a properly size heat pump operates mostly at part-load conditions, the outputs for full load conditions need to be adjusted for part-load operation. Several methods developed by researchers, ranging from time-constant models to part-load fraction models are evaluated based on their adaptability to the EnergyPlus simulation environment. In addition, a part-load latent heat model transfer by Henderson and Rengarajan(1996) was incorporated in the water-air heat pump model to allow better prediction of the latent capacity at part-load condition.

The simulation environment for cycling unitary equipments in EnergyPlus is discussed in Chapter 3. The heat pump models modifications and implementation in EnergyPlus are described in Chapter 4. A curve-fit water-to-water heat pump model is developed based on the same approach used by Lash(1992) for the curve-fit water-to-air heat pump model.

The performance of the curve-fit air-to-air heat pump model in EnergyPlus is compared to a detailed deterministic model proposed by Iu et. al (2003) using experimental data obtained from the OSU test rig and the manufacturer. On the other hand, two water-to-air heat pump models were implemented in Energyplus: a parameter estimation based model by Jin (2002) and a curve-fit model based on Lash (1992). The two models are compared to experimental results obtained from the manufacturer in Chapter 5.2. In addition, the newly proposed curve-fit water-to-water heat pump is verified by comparison with the parameter estimation based water-to-water heat pump developed by Jin (2002)

At the end of this research project, EnergyPlus users will not only have a selection of heat pump models best suited to their needs but also have full confidence in the simulation results. Lastly, recommendations for future work and further validation of the models is proposed.

1.3. Scope

The scope of the research work is summarized and categorized based on the type of heat pump model. For air-to-air heat pump model, the main objective is to investigate the performance of EnergyPlus curve-fit model and the following tasks have been completed:

- Ran the OSU test facility and collected validation data for cooling mode.
- Conducted a preliminary study on the compressor shell heat loss.

- Modified the EnergyPlus curve-fit model to account for the effects of indoor dry-bulb temperature in heating mode.
- Validated the EnergyPlus curve-fit model with experimental data together with a detailed deterministic model by Iu et. al.(2003).
- Proposed a new curve-fit air-to-air heat pump model based on Lash (1992) approach.

For water-to-air heat pump model, the goal is to continue the work by previous researchers and implement the models into EnergyPlus simulation environment. The completed tasks are as follows:

- Implemented the parameter estimation based model by Jin (2002) into EnergyPlus.
- Modified Shenoy (2004) curve-fit model and finalized the implementation into EnergyPlus.
- Developed an Excel spreadsheet for generating parameters/coefficients for the curve-fit model and the parameter estimation based model.
- Modified the latent degradation model by Henderson and Rengarajan (1996) to include cycling fan operation mode. Conducted a parametric study of the model.
- Implemented the part-load fraction model and the latent degradation model for water-to-air heat pump model.
- Validated the curve-fit model and the parameter estimation based model using experimental measurements obtained from the manufacturer.
- Investigated the performance of both models beyond the catalog range.

For water-to-water heat pump model, the main objective is to develop and implement a new curve-fit model into EnergyPlus to accompany the parameter estimation based model which was implemented by Murugappan (2002). The completed works are as follows:

- Proposed a new curve-fit water-to-water heat pump model based on Lash (1992) approach and implemented the model into EnergyPlus.
- Developed an Excel spreadsheet for generating parameters/coefficients for the curve-fit model and the parameter estimation based model.
- Conducted a preliminary verification of the curve-fit model and compared its performance with the parameter estimation based model by Jin (2002).

2.0 Review of Heat Pump Models in the Literature

A number of heat pump models have been proposed by researchers over the years. These generally fall into two extremes: detailed deterministic models and simple curve-fit models. Detailed deterministic models are generally complicated models requiring numerous generally unavailable inputs. This makes them unfavorable to building simulation programs like EnergyPlus and DOE-2. In addition, it is generally accepted that simple curve-fit models tend to fail when operating beyond the catalog data. In recent years, parameter estimation based models have been developed by Oklahoma State University. These compares fairly well with detailed deterministic models while retaining the strength of the curve-fit model with easily accessible inputs.

2.1. Steady State Air-to-Air Heat Pump Models

2.1.1 EnergyPlus Model

The air-air heat pump model in EnergyPlus uses empirical functions for capacity and efficiency from DOE-2 (DOE 1982) in conjunction with the apparatus dew point (ADP)/bypass factor (BF) relations to determine the off-design performance (Henderson et. al 1992). The approach is analogous to the NTU-effectiveness calculations based on the sensible-only heat exchanger calculations extended to a cooling and dehumidifying coil.

The heat pump performance at off-design conditions is computed by adjusting the capacity and energy input ratio (inverse of COP) at rated conditions to the temperature modifying factor, TMF and flow fraction modifying factor, FMF. The TMF and FMF are non-dimensional factors or performance curves obtained from the heat pump catalog data. The TMF curves adjust the heat pump performance due to variation in air temperatures from the rated conditions. On the other hand, the FMF curves adjust for the performance effects of variation in air flow rate from the rated conditions.

For cooling mode, the rated condition (80˚F [26.7˚C] indoor dry bulb and 67˚F [19.4˚C] wet bulb; 95˚F [35.0˚C] outdoor dry bulb; 350~450 cfm/ton [0.047~0.06 m^3/s kW]) is essentially the ARI "A" Cooling Steady State Condition which is the standard rating conditions for air-source heat pumps. The TMF curves for total cooling capacity, $f_C\left(iwb, odb\right)$ and energy input ratio, $f_{EIR}\left(iwb, odb\right)$ are functions of the indoor wet-bulb temperature and outdoor dry-bulb temperature. Both of them are formulated in similar fashion as shown below.

$$f_C\left(iwb, odb\right) = \frac{C_C}{C_{C,rated}} = a_1 + a_2\left(iwb\right) + a_3\left(iwb\right)^2 + a_4\left(odb\right) + a_5\left(odb\right)^2 + a_6\left(iwb\right)\left(odb\right) \qquad (2.1)$$

$$f_{EIR}\left(iwb, odb\right) = \frac{EIR_C}{EIR_{C,rated}} = b_1 + b_2\left(iwb\right) + b_3\left(iwb\right)^2 + b_4\left(odb\right) + b_5\left(odb\right)^2 + b_6\left(iwb\right)\left(odb\right) \quad (2.2)$$

where

iwb = indoor wet-bulb temperature, ˚C

odb = outdoor dry-bulb temperature,˚C

EIR_C = cooling energy input ratio

$EIR_{C,rated}$ = rated cooling energy input ratio

C_C = total cooling capacity, W

$C_{C,rated}$ = rated total cooling capacity, W

To generate the TMF curves, data points at the rated air flow rate but at indoor air wet-bulb and outdoor air dry-bulb temperatures that vary from the rated conditions are selected from the manufacturer's catalog. The ratio of the respective total capacity to rated total capacity is calculated. Then, the coefficients for $f_C\left(iwb, odb\right)$ are calculated using the generalized least square method. The same approach is also used for calculating the coefficients for $f_{EIR}\left(iwb, odb\right)$.

The FMF curves are functions of the ratio of air flow rate to the rated air flow rate. The equations below show the FMF curves for the cooling capacity, $f_C\left(Q/Q_{rated}\right)$ and energy input ratio, $f_{EIR}\left(Q/Q_{rated}\right)$:

$$f_C\left(Q/Q_{rated}\right)=\frac{C_C}{C_{C,rated}}=c_1+c_2\left(Q/Q_{rated}\right)+c_3\left(Q/Q_{rated}\right)^2 \tag{2.3}$$

$$f_{EIR}\left(Q/Q_{rated}\right)=\frac{EIR_C}{EIR_{C,rated}}=d_1+d_2\left(Q/Q_{rated}\right)+d_3\left(Q/Q_{rated}\right)^2 \tag{2.4}$$

where:

Q = indoor air volumetric flow rate, m^3/s

Q_{rated} = rated indoor air volumetric flow rate, m^3/s

The FMF curves for the cooling capacity, $f_C\left(Q/Q_{rated}\right)$ and energy input ratio, $f_{EIR}\left(Q/Q_{rated}\right)$ can be obtained by plotting capacity ratios with their respective flow fractions in Excel. The data points selected from the catalog must be at rated indoor wet-bulb and outdoor dry-bulb temperatures but cover a range of indoor air flow rates. Using

the TMFs and FMFs, the cooling capacity and energy input ratio at rated conditions are adjusted for the off-rated conditions as follows:

$$C_C = C_{C,rated} \cdot f_C\left(iwb, odb\right) \cdot f_C\left(Q / Q_{rated}\right) \tag{2.5}$$

$$EIR_C = EIR_{C,rated} \cdot f_{EIR}\left(iwb, odb\right) \cdot f_{EIR}\left(Q / Q_{rated}\right) \tag{2.6}$$

In order to accurately predict the humidity level, the heat pump model must properly predict the split between sensible and latent capacity over a range of operating conditions. The sensible and latent fractions of the total capacity are determined by the apparatus dew point/bypass factor (ADP/BF) approach (Carrier et al. 1959). The approach is analogous to the NTU-effectiveness calculations used for sensible-only heat exchanger calculations extended to a cooling and dehumidifying coil. The rated total capacity and rated sensible heat transfer rate is used to determine the ratio of the change in the air humidity ratio to the change in the air-dry bulb temperature, known as *SlopeRated*.

$$SlopeRated = \left(\frac{w_{in} - w_{out}}{T_{db,in} - T_{db,out}} \right)_{rated} \tag{2.7}$$

where:

w_{in} = humidity ratio of air entering the cooling coil at rated conditions, kg/kg

w_{out} = humidity ratio of air exiting the cooling coil at rated conditions, kg/kg

$T_{db,in}$ = dry-bulb temperature of air entering the cooling coil at rated conditions, kg/kg

$T_{db,out}$ = dry-bulb temperature of air exiting the cooling coil at rated conditions, kg/kg

The apparatus dew point is the point on the saturation curve where the slope of the line between the point on the saturation curve and the inlet air conditions matches the *SlopeRated*. Once the apparatus dew point is found, the coil bypass factor at rated conditions BF_{rated} is calculated using the equation below:

$$BF_{rated} = \frac{h_{out,rated} - h_{ADP}}{h_{in,rated} - h_{ADP}} \qquad (2.8)$$

where:
$h_{out,rated}$ = enthalpy of air leaving the cooling coil at rated conditions, J/kg

$h_{in,rated}$ = enthalpy of air entering the cooling coil at rated conditions, J/kg

h_{ADP} = enthalpy of saturated air at the coil apparatus dew point, J/kg

For an air-to-refrigerant heat exchanger, the BF can be defined in terms of the number of transfer unit (NTU) as follows:

$$BF = 1 - e^{-NTU} \qquad (2.9)$$

where:
BF = bypass factor

NTU = number of transfer units

Equation (2.9) can be further extended and formulated in terms of the constant, a_o, and the indoor air flow rate, Q, as follows:

$$BF = 1 - e^{-\frac{UA}{\dot{m}_{air} C_p}} = 1 - e^{-\frac{a_o}{Q}} \qquad (2.10)$$

where:
UA = heat transfer coefficient, W/K

$\dot{m}_{air}$ = air mass flow rate, kg/s

C_p = air specific heat, J/(kg-K)

Q = indoor air volumetric flow rate, m^3/s

For a given coil geometry, the bypass factor is only a function of mass flow rate and the constant, a_o, which is determined from the rated conditions by rearranging Equation (2.10) to:

$$a_o = -\log_e\left(BF_{rated}\right) \cdot Q_{rated} \qquad (2.11)$$

where:
BF_{rated} = rated bypass factor

Q_{rated} = rated indoor air volumetric flow rate, m^3/s

Then the temperature and humidity of the air leaving the cooling coil are calculated with the ADP and BF approach shown below:

$$T_{exit} = BF \cdot T_{inlet} + (1 - BF) \cdot T_{ADP} \qquad (2.12)$$

$$w_{exit} = BF \cdot w_{inlet} + (1 - BF) \cdot w_{ADP} \qquad (2.13)$$

where:
w = absolute humidity, kg/kg

T = dry-bulb temperature, ˚C

inlet = evaporator inlet

exit = evaporator outlet

ADP = average saturated conditions at evaporator surface

For heating mode, the TMF curves for heating capacity and heating energy input ratio are functions of the indoor dry-bulb temperature and outdoor dry-bulb temperature.

The FMF curves are only functions of the ratio of the air flow rate to the rated flow rate. The rated conditions (70˚F [21.1˚C] indoor dry bulb and 60˚F [15.5˚C] indoor wet bulb; 47˚F [8.33˚C] outdoor dry bulb and 43˚F [6.11˚C] outdoor dry bulb; 350~450 cfm/ton [0.047~0.06 m3/s kW]) are the Standard Rating Conditions specified by ARI (2003). Both modifying factors and calculations for the heating capacity and heating energy input ratio are shown below.

$$C_H = C_{H,rated} \cdot f_H\left(idb, odb\right) \cdot f_H\left(Q / Q_{rated}\right) \tag{2.14}$$

$$EIR_H = EIR_{H,rated} \cdot f_{EIR}\left(idb, odb\right) \cdot f_{EIR}\left(Q / Q_{rated}\right) \tag{2.15}$$

idb = indoor dry-bulb temperature,˚C

odb = outdoor dry-bulb temperature,˚C

Q = indoor air volumetric flow rate, m^3/s

C_H = heat pump total heating capacity, W

EIR_H = heating energy input ratio

$$f_H\left(iwb, odb\right) = \frac{C_H}{C_{H,rated}} = e_1 + e_2\left(idb\right) + e_3\left(idb\right)^2 + e_4\left(odb\right) + e_5\left(odb\right)^2 + e_6\left(idb\right)\left(odb\right) \tag{2.16}$$

$$f_{EIR}\left(iwb, odb\right) = \frac{EIR_H}{EIR_{H,rated}} = \mathrm{f}_1 + \mathrm{f}_2\left(idb\right) + \mathrm{f}_3\left(idb\right)^2 + \mathrm{f}_4\left(odb\right) + \mathrm{f}_5\left(odb\right)^2 + \mathrm{f}_6\left(idb\right)\left(odb\right) \tag{2.17}$$

$$f_H\left(Q / Q_{rated}\right) = \frac{C_H}{C_{H,rated}} = g_1 + g_2\left(Q / Q_{rated}\right) + g_3\left(Q / Q_{rated}\right)^2 \tag{2.18}$$

$$f_{EIR}\left(Q/Q_{rated}\right)=\frac{EIR_H}{EIR_{H,rated}}=h_1+h_2\left(Q/Q_{rated}\right)+h_3\left(Q/Q_{rated}\right)^2 \quad (2.19)$$

EnergyPlus curve-fit air-to-air heat pump model requires 8 distinct curves to simulate the heat pump performance in both cooling and heating mode. The data points selected from the catalog data must meet the requirement of the respective curve which can be tedious. The main advantage however, is that this model requires very few data points. This could be a disadvantage as well since few data points meet the curve's requirement especially for the FMF curves which could lead to insensitivity of the model.

2.1.2 Detailed Deterministic Model by Iu et al.

The heat pump model proposed by Iu et al (2003) is a steady state multi-component based model that simulates the heat pump system as four main components, namely compressor, expansion device, and two heat exchangers (condenser and evaporator), as well as the distributor, and interconnecting lines. The model is capable of predicting the capacity and pressure drop effects of different circuit designs. The heat pump model uses different types of models ranging from semi-empirical to curve-fit equations to predict the heat transfer processes in each component

The compressor model uses two 10-coefficient polynomial equations from ARI (1999) to predict the refrigerant mass flow rate and the power consumption. The polynomial equations are generated from the compressor manufacturer's catalog. A semi-empirical equation from Arron and Domanski (1990) is used to model the short tube orifice, and the distributor pressure drop is obtained from the manufacturer's catalog data. The heat exchangers (condenser and evaporator) and interconnecting lines (i.e. discharge,

suction and liquid lines) are modeled using 1st principles approach, which means thermodynamic laws and heat transfer relations are used to predict the performance of the coil.

In short, the heat pump model is a detailed deterministic model that requires numerous physical inputs that are not available in the catalog data provided by the heat pump manufacturer. The model was primarily developed for advanced heat pump design and simulation. However, the model is not suitable for hourly energy simulation program due to long computational time and generally unavailable inputs. The model however serves as a benchmark for the verification of the EnergyPlus curve-fit air-to-air heat pump model.

2.2. Steady State Water-to-Air Heat Pump Models

2.2.1 Jin & Spitler Model

The water-air heat pump model developed by Jin(2002) is a parameter estimation based model which includes several unspecified parameters that are estimated from the heat pump catalog using a multi-variable optimization procedure. No additional data is required besides the heat pump catalog which makes this model attractive for building system designer and simulation users. In addition, the model retains the physically based representation of the heat pump compared to equation-fit models. Jin(2002) claims that this allows extrapolation beyond the catalog data without catastrophic failure compared to equation-fit models.

Besides that, Jin & Spitler (2002) claims that the parameter based model for water-water heat pump has relatively the same RMS error as detailed deterministic models and performs better than equation-fit models. However, they didn't make similar comparisons for their water-air heat pump model. The assumptions made in developing the model are as follows:

- The expansion process is isenthalpic.
- Expansion and compression in the compressor are isentropic processes with equal and constant isentropic exponents.
- The isentropic is exponent dependent on the refrigerant type, and the value is obtained from Bourdouxehe et al. (1994).
- No heat loss from the system (e.g. no heat loss from the compressor).

- Oil has negligible effects on the refrigerant properties and compressor operation
- The pressure drop at the discharge and suction valves are equal, constant and isenthalpic.

The heat pump model consists of four major components: compressor, evaporator, condenser and expansion device. Other components are neglected due to their comparatively small influence on the thermodynamic cycle or performance. The type and number of parameters depends on the operating mode, compressor type and source side fluid type. The parameters are estimated using a Nelder Mead Simplex routine converted to VBA(Visual Basic for Applications) from (Kuester and Mize 1973). A detailed description of the model is presented in Chapter 4.

2.2.2 Lash Model

Lash (1992) proposed an equation-fit model that uses five non-dimensional equations to predict the heat pump performance in cooling and heating mode. The heat pump performance is based on entering air temperatures, entering water temperatures and the inlet mass flow rate of water. The coefficients for the non-dimensional equations are obtained from the manufacturer's data using the generalized least squares method. The equations used to predict the heat pump performance in cooling and heating mode are shown below:

Cooling Mode:

$$\frac{Q_{total}}{Q_{total,ref}} = A1 + A2\left[\frac{T_{w,in}}{T_{ref}}\right] + A3\left[\frac{T_{ref}}{T_{wb}}\right]\left[\frac{\dot{m}_w}{\dot{m}_{w,ref}}\right] \quad (2.20)$$

$$\frac{Q_{sens}}{Q_{sens,ref}} = B1 + B2\left[\frac{T_{w,in}}{T_{ref}}\right] + B3\left[\frac{T_{ref}}{T_{wb}}\right]\left[\frac{\dot{m}_w}{\dot{m}_{w,ref}}\right] + B4\left[\frac{T_{ref}}{T_{db}}\right]\left[\frac{\dot{m}_w}{\dot{m}_{w,ref}}\right] \quad (2.21)$$

$$\frac{COP_c}{COP_{c,ref}} = C1 + C2\left[\frac{T_{w,in}}{T_{ref}}\right] + C3\left[\frac{T_{ref}}{T_{wb}}\right]\left[\frac{\dot{m}_w}{\dot{m}_{w,ref}}\right] \quad (2.22)$$

Heating Mode:

$$\frac{Q_h}{Q_{h,ref}} = D1 + D2\left[\frac{T_{w,in}}{T_{ref}}\right] + D3\left[\frac{T_{ref}}{T_{db}}\right]\left[\frac{\dot{m}_w}{\dot{m}_{w,ref}}\right] \quad (2.23)$$

$$\frac{COP_h}{COP_{h,ref}} = E1 + E2\left[\frac{T_{w,in}}{T_{ref}}\right] + E3\left[\frac{T_{ref}}{T_{db}}\right]\left[\frac{\dot{m}_w}{\dot{m}_{w,ref}}\right] \quad (2.24)$$

Where:

$A1$ - $E3$ = Equation fit coefficients for the cooling and heating mode

T_{ref} = 283K

$T_{w,in}$ = Entering water temperature, K

$\dot{m}_w$ = Mass flow rate of water through the heat pump

$\dot{m}_{w,ref}$ = Base mass flow rate of water through the heat pump

T_{db} = Entering air dry bulb temperature, K

T_{wb} = Entering air wet bulb temperature, K

Q_{total} = Total cooling capacity, W

$Q_{total,ref}$ = Reference total cooling capacity, W

Q_{sens} = Sensible cooling capacity, W

$Q_{sens,ref}$ = Reference sensible cooling capacity, W

Q_h = Total heating capacity, W

$Q_{h,ref}$ = Reference total heating capacity, W

COP_h = Heating coefficient of performance

$COP_{h,ref}$ = Reference heating coefficient of performance

COP_c = Cooling coefficient of performance

$COP_{c,ref}$ = Reference cooling coefficient of performance

The Lash (1992) equation fit model did not account for the effects of variable air flow rate on the capacities. Thus the model is insensitive to the variation of air flow rates from the base condition. However, Shenoy(2004) proposed the following equations to incorporate the effect of the air mass flow rate in the heat pump performance.

Cooling Mode:

$$\frac{Q_{total}}{Q_{total,ref}} = A1 + A2\left[\frac{T_{w,in}}{T_{ref}}\frac{\dot{m}_{air,ref}}{\dot{m}_{air}}\right] + A3\left[\frac{T_{ref}}{T_{wb}}\right]\left[\frac{\dot{m}_w}{\dot{m}_{w,ref}}\right] \tag{2.25}$$

$$\frac{Q_{sens}}{Q_{sens,ref}} = B1 + B2\left[\frac{T_{w,in}}{T_{ref}}\frac{\dot{m}_{air,ref}}{\dot{m}_{air}}\right] + B3\left[\frac{T_{ref}}{T_{wb}}\right]\left[\frac{\dot{m}_w}{\dot{m}_{w,ref}}\right] + B4\left[\frac{T_{ref}}{T_{db}}\right]\left[\frac{\dot{m}_w}{\dot{m}_{w,ref}}\right] \tag{2.26}$$

$$\frac{COP_c}{COP_{c,ref}} = C1 + C2\left[\frac{T_{w,in}}{T_{ref}}\frac{\dot{m}_{air,ref}}{\dot{m}_{air}}\right] + C3\left[\frac{T_{ref}}{T_{wb}}\right]\left[\frac{\dot{m}_w}{\dot{m}_{w,ref}}\right] \tag{2.27}$$

Heating Mode:

$$\frac{Q_h}{Q_{h,ref}} = D1 + D2\left[\frac{T_{w,in}}{T_{ref}}\frac{\dot{m}_{air,ref}}{\dot{m}_{air}}\right] + D3\left[\frac{T_{ref}}{T_{db}}\right]\left[\frac{\dot{m}_w}{\dot{m}_{w,ref}}\right] \tag{2.28}$$

$$\frac{COP_h}{COP_{h,ref}} = E1 + E2\left[\frac{T_{w,in}}{T_{ref}}\frac{\dot{m}_{air,ref}}{\dot{m}_{air}}\right] + E3\left[\frac{T_{ref}}{T_{db}}\right]\left[\frac{\dot{m}_w}{\dot{m}_{w,ref}}\right] \tag{2.29}$$

2.3. Heat Pump Cycling Models

On-off cycling is a major contributor to the degradation of performance in heat pumps. The U.S. Department of Energy (1979) proposed a test procedure for estimating the seasonal energy efficiency ratio (SEER) for air conditioners and heat pumps operating under cyclic conditions. Manufacturers are required by law to label the heat pump with SEER for heating and cooling mode. Researchers have acknowledged that on-off cycling of the heat pump to meet the cooling load has a detrimental effect on the heat pump performance. Work has been done to analyze the effect of percent on-time, cycling rate and thermostat control on transient sensible and latent load. Cycling models were evaluated for incorporation into the EnergyPlus steady-state heat pump models in order to predict the heat pump performance at part-load.

2.3.1 Time-Constant Models

Basically cycling models can be categorized as time-constant models and detailed models. Time-constant models are extensions of steady state models created by modeling the system performance using empirical functions. During startup, the system capacity or temperature across the indoor coil could be modeled as a first-order system (single time constant) which was done by Groff and Bullok (1979). The heat pump response at start up can be modeled as first-order whereby the instantaneous cycling capacity at time, t is as follows:

$$\dot{Q}_{cyc} = \dot{Q}_{ss}\left(1 - e^{-\frac{t}{\tau}}\right) \tag{2.30}$$

where:

$\dot{Q}_{ss}$ = steady-state or full-load capacity, W

$\dot{Q}_{cyc}$ = instantaneous cycling capacity at respective time, W

t = time after compressor is turned on, s

τ = heat pump time constant, s

O'Neal and Katipamula (1991) also claimed that the single-time constant model is adequate for simulating general cyclic performance of the heat pump even though it ignores the actual physical phenomena that occurs. Mulroy and Didion (1985) proposed a two-time constant model that allows estimation of the impact of refrigerant migration and thermal mass on cyclic performance.

$$\dot{Q}_{cyc} = \dot{Q}_{ss}\left(1 - e^{-\frac{t}{\tau 1}}\right)\left(1 + Ae^{-\frac{t}{\tau 2}}\right) \tag{2.31}$$

where

$\tau 1$ = first time constant, s

$\tau 2$ = second time constant, s

A = constant parameter

The first constant is to capture the capacity delay due to the mass of the heat exchanger. And the second constant is for the time delay to pump the refrigerant from the evaporator to the system. In addition, the two-time-constant model requires regressive curve fitting of the constants and is not explicitly derived from heat pump capacity like the single-time constant model. The two-time-constant is better at characterizing individual unit's dynamic performance.

2.3.2 Part-Load Fraction Model

At part-load conditions, steady state models require some sort of correlation to estimate the performance of the model. The part-load fraction (PLF) correlation takes into account the efficiency losses due to compressor cycling. Part-load ratio (PLR) is the ratio of the average heat pump's capacity at part-load to the full-load capacity as follows:

$$PLR = \frac{Part - Load\ \ Capacity}{Steady - State\ \ Capacity} \tag{2.32}$$

In EnergyPlus, the average heat pump part-load capacity is essentially the demand load of the heat pump for the respective time step. The steady-state capacity is the output of the heat pump model at full load. Part-load fraction (PLF) is defined as the ratio of the part-load energy efficiency ratio to the steady-state energy efficiency ratio as follows:

$$PLF = \frac{Part - Load\ \ EER}{Steady - State\ \ EER} \tag{2.33}$$

The energy efficiency ratio is the ratio of the heat pump capacity to the heat pump power consumption. Henderson and Rengarajan (1996) give a detailed theoretical derivation of the PLF equation which is shown below:

$$PLF_{new} = 1 - 4\tau N_{\max}(1 - PLR / PLF_{old})\left[1 - e^{\frac{-1}{4\tau N_{\max}(1-PLR/PLF_{old})}}\right] \tag{2.34}$$

The part-load fraction model requires two parameters: heat pump cycling rate (Nmax) and heat pump time constant (τ) to calculate for heat pump PLF from the PLR. Given PLR from the heat pump simulation and the two parameters, PLF_{new} is calculated using an initial guess of $PLF_{old} = 1$. For the second iteration the calculated PLF_{new} is used

as PLF_{old} and the iteration continues until convergence is achieved. Boone et. al. (1980) noted that with this model the PLF is overestimated at low loads for the following reasons:

- Power input due to crankcase heater, controls, fans in the off-period is large compared to the heating/cooling capacity.
- Heating/cooling capacity increases slowly when the compressor cycles on especially at low PLR, whereas the power input reaches steady state almost immediately.

Boone et. al. (1980) adjust the heat pump efficiency for the off-cycle power consumption using the fraction of on-cycle power use (pr) shown below:

$$\text{Adjusted PLF} = PLF' = \frac{PLR}{\left(\frac{PLR}{PLF} + \left(1 - \frac{PLR}{PLF}\right) pr\right)} \qquad (2.35)$$

The parameters required to calculate the adjusted PLF are based on field tests and experiments. Henderson et al. (1999) categorize the parameters with respect to the heat pump condition and recommends some values for use in DOE-2.

Condition	Cycling Rate, Nmax	Time Constant, τ	Fraction of on-cycle power use,pr
Poor Heat Pump	3	60	0.03
Typical Heat Pump	2.5	60	0.01
Good Heat Pump	3	30	0.01

Table 2.1: Recommended Part-Load Fraction Parameters by DOE-2, Henderson et al. (1999)

Instead of iterating for PLF from PLR as described in Equation (2.34), the part-load fraction model is incorporated in DOE-2 and EnergyPlus as a curve-fit equation. Using the parameters recommended in Table 2.1, the adjusted PLF is calculated beforehand as a

function of the PLR using Equation (2.34) and Equation (2.35). The relationships between the adjusted PLF and PLR for the three heat pump conditions are then curve-fitted and represented by the following equations:

$$PLF' = a + b\left(PLR\right) + c\left(PLR\right)^2 + d\left(PLR\right)^3 \qquad (2.36)$$

Only the coefficients: a,b,c and d are provided to the user based on the heat pump conditions. Although this method is less computationally expensive, the user is required to generate the curve if the conditions/parameters are different from what is listed in Table 2.1.

After calculating the adjusted PLF from the PLR, the run-time fraction, X can be calculated from the equation below:

$$X = \frac{PLR}{PLF'} = \frac{t_{on}}{t_{cycle}} \qquad (2.37)$$

where:

X = compressor runtime fraction

t_{on} = compressor on-time (duration of on-time), s

t_{cycle} = compressor cycle-time (duration of one cycle: on-time and off-time), s

Mathematical derivation of the run-time fraction is shown by Henderson and Rengarajan (1996). The run-time fraction is essentially the percent on-time which is the ratio of the on-time to the cycle time.

The part-load ratio and runtime fraction are used to adjust the steady state heat pump model's capacity and power consumption for part-load conditions. Unlike the heat pump capacity, the power consumption of the heat pump reaches steady-state almost instantaneously after the heat pump is turned on. Thus the heat pump power input is

adjusted based on the run-time fraction and the heat pump capacity is adjusted based on the part-load ratio as follows:

$$Q_{part-load} = Q_{ss} \times PLR \tag{2.38}$$

$$Power_{part-load} = Power_{ss} \times X \tag{2.39}$$

2.3.3 Part-Load Fraction Model by Katipamula and O'Neal (1992)

Katipamula and O'Neal (1992) conducted a series of tests by varying variables that influence the PLF of the heat pump in cooling mode. The tests were conducted according to the standard heat pump test procedure, and the functional relationship of each independent variable (fraction on-time, indoor dew-point, cycling rate, indoor dry-bulb temperatures, and outdoor dry-bulb temperature) with the dependent variable (PLF) was evaluated. From the study, they found that the indoor dry-bulb temperature and outdoor dry-bulb temperature had no influence on the PLF thus they are omitted. The final expression of their model is shown below:

$$PLF = \alpha_0 + \alpha_1 \left(1 - \exp(-k/\tau)\right) + \alpha_2 dp + \alpha_3 N \max \tag{2.40}$$

where

k = heat pump on-time, s

τ = heat pump time constant, s

dp = dew point temperature, °C

$N_{\max}$ = heat pump cycling rate, cycles/hr

Katipamula and O'Neal (1992) concluded that the fraction on-time affected the PLF the most while the dew point temperature and cycling rates are not very significant. The model requires several selected tests at various off-design conditions in order to determine the functional relationship of the PLF with the fraction on-time, dew point temperature and cycling rate.

2.3.4 Henderson and Rengarajan Model

The part-load fraction models discussed in Section 2.3.2 and Section 2.3.3 do not account for re-evaporation of moisture from the cooling coil back into the air stream when the compressor is shut off. Henderson and Rengarajan (1996) proposed a model based on the single-time constant model to predict latent capacity at part-load condition with constant fan operation. The model can be applied both to air-air heat pumps and water-air heat pumps but the model requires measured field data which are not available from the catalog or the manufacturer.

The model predicts the latent heat ratio (LHR) at part-load conditions as a function of the run-time fraction (X). The model requires parameters at rated conditions such as the maximum cycling rate of the thermostat ($N_{\max}$), the heat pump time constant (τ), the ratio of the initial evaporation rate to the steady-state latent capacity (γ), and the ratio of the moisture holding capacity of the coil to the steady state latent capacity of the heat pump (t_{wet}). The assumptions made in developing the model are as follows;

- The model assumes that the cooling coil can only hold an amount of water, (Mo). Additional condensate will drains from the coil once the maximum amount, Mo, has been reached.
- Condensate removal begins once (Mo) is reached. The hysteresis effect due to previous wetting, surface tension, and a dirty coil is negligible.
- The time constant for the total, sensible and latent capacity at start-up is the same.

The assumptions enable the model to be used for calculating the net latent capacity at quasi-steady cyclic conditions. Since the process of moisture evaporation from the deactivated coil is complex, they proposed three simplified evaporation models which are referred to as exponential decay, linear decay and constant evaporation. The advantage of this model is that it can be applied to any kind of system simulation model as long as the parameters, run-time fraction (X) and the latent heat ratio at steady-state conditions are available. The latent degradation model is described in more detail in Chapter 4.3.

3.0 Simulation of Cycling Equipment in a Quasi-Steady State Simulation Environment

This chapter describes the EnergyPlus simulation environment and the methodology employed in solving the simulation state variables at the inlet and outlet of each component. The zone/air loop interaction is investigated mainly focusing on the unitary equipment simulation manager.

3.1. Overview of the EnergyPlus Quasi-Steady State Simulation Methodology

EnergyPlus is an integrated simulation environment whereby the major parts, zone, system and plant are solved simultaneously based on fundamental heat balance principles. In EnergyPlus (2004), interactions between zones, system and plant are achieved by fluid loop models which calculate the simulation state variables at the inlet and outlet of each component.

The simultaneous solution of the zones, systems and plant is controlled by an integrated solution manager which relies on successive substitution iteration using the Gauss-Seidel philosophy of continuous updating. The integrated solution manager will drive the zone cooling demand, system supply capacity and plant capacity to convergence given the zone thermostat set point. EnergyPlus yields more realistic and accurate simulation results compared to building simulation programs such as BLAST(Building Loads Analysis and System Thermodynamics) or DOE-2, which use the sequential

simulation method with no feedback from one part of the simulation to another. For the sequential simulation method, the zone cooling demand is fed to the air handling systems, but the response from the system is not used to update the zone conditions. This can lead to nonphysical results.

3.1.1 Successive Substitution with Lagging

The zone and system integration uses a shortened simulation time step, typically between 0.1 and 0.25 hours and the IBLAST's time-marching method by Taylor et. al. (1990, 1991) with the zone conditions lagged by one time step. The error associated with this approach depends on the time step, with shorter time steps resulting in higher accuracy but longer computation time. Zone air capacity was introduced into the heat balance to allow the maximum increase in the time step without jeopardizing stability. The resulting method called "lagging with zone capacitance" allows the dynamic processes in the zone to be captured more precisely compared to the sequential programs that use time steps of one hour.

3.1.2 Ideal Controls

In real buildings, the thermostat serves as the basic control for most systems by taking samples of the air temperature and sending signals to the control unit. For unitary equipment in EnergyPlus, the temperature predictor-corrector serves as the thermostat and control unit and is responsible for controlling the air system to meet the desired zone temperature. Real controllers sample the zone conditions at shorter intervals than the

characteristic response time of the zone system. This results in a well controlled slowly oscillating zone temperature. However, the simulation model can only sample the zone conditions based on the system's variable adaptive time step described further in Section 3.1.3.

The zone load is used as a starting point to place a demand on the air system. The system simulation determines the actual supply capability, and the zone temperature is adjusted according to the system response.

Heat pump models in EnergyPlus have two types of fan operating modes which are cycling fan (AUTO) and continuous fan. For continuous fan mode, the supply air temperature is a continuous function of the zone temperature. The fan is kept running at constant spend and the zone temperature is kept within the desired range by switching the compressor on and off. The fraction of the time step that the compressor is turned on is known as the run-time fraction. For cycling fan(AUTO) mode, both supply air temperature and supply air volume are continuous functions of the zone temperature. Although the fan operates at constant speed, the intermittent fan acts as a variable volume system by adjusting the air flow rate based on the heat pump part-load ratio, PLR.

Zone humidity is also an important factor that should be simulated to achieve desirable thermal comfort. A methodology similar to the temperature predictor-corrector is used to simulate the humidity of the zone. The idea is to predict the moisture load from the scheduled latent loads, zone infiltration and outside air. Then, system components with moisture control such as cooling coils, dehumidifiers, and humidifiers will try to meet the predicted moisture load and provide feedback from the system to update the zone conditions. This process is repeated until convergence is achieved.

3.1.3 Variable Time Step

Initially, developers of IBLAST used a fixed time step of 0.25 hours to update the zone temperatures, but instabilities occurred after integration of the central plant simulation. Very short time steps were required to keep the simulation stable and eventually the simulation became too computationally expensive. An adaptive variable time step was proposed to maintain the stability of the simulation when the zone conditions are changing rapidly and speed up the computation when the conditions are fairly consistent.

EnergyPlus adopted the two time step approach from IBLAST. For stability reasons, a variable adaptive time step determined by the program is used for updating the zone temperature and system response. However, the adaptive variable time step approach could not be applied easily to the surface heat transfer calculations. Thus the contributions to the zone loads from the surface heat transfer, internal gains, and infiltration are updated at a default or user specified time step that is constant. This approach yields simulation stability and accuracy while keeping computation time at a minimum.

3.2. Simulation of Unitary Equipment in EnergyPlus

Unitary system models including the air-air heat pump and water-air heat pump implemented in EnergyPlus are steady state models. However, the heat pump will operate mostly at part-load by cycling on and off to keep the zone temperature at the thermostat set point. The output of the model will represent the actual performance of the unitary

equipment at full load. Thus cycling models described in Chapter 2 must be used to predict the performance of the heat pump at part-load. The cycling models used in EnergyPlus is the part-load fraction model and the latent degradation model by Henderson and Rengarajan (1996).

3.2.1 Zone/Air Loop Interactions

The air loop simulation can be divided into the air primary loop and zone equipment. The supply side or air primary loop is defined by the section starting from the node after the return streams from the zone are combined until just before the air streams are branched off to individual zone as shown in Figure 3.1. The demand side or zone equipment is the rest of the zone/air loop which includes everything from the point where the duct is split to serve various zones to the point where the return ducts are mixed to a single return duct.

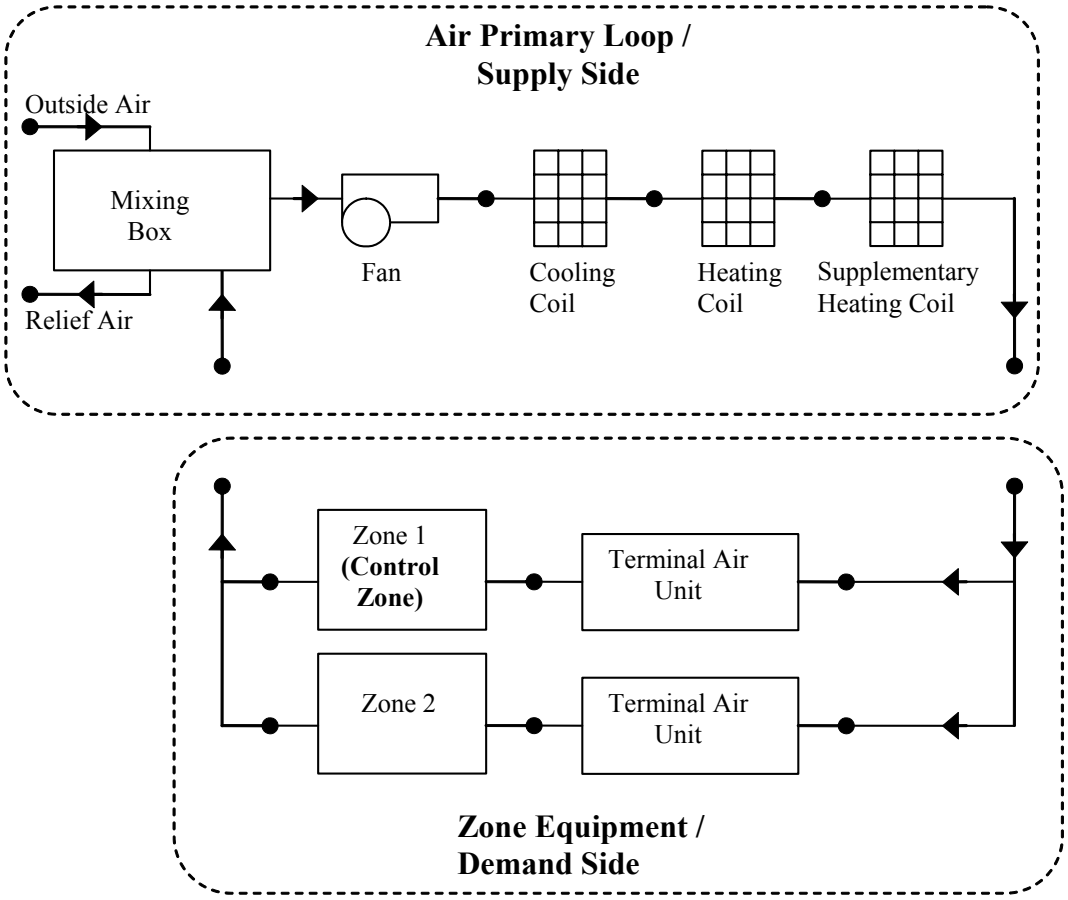

Figure 3.1: Zone Equipment/Air Primary Loop Interaction

According to EnergyPlus(2004), the air loop simulation uses an iterative method to solve the algebraic energy and mass balance equations combined with the steady state component models. The zone simulation and air handling system simulation are integrated by calling the system simulation from the zone air heat balance to determine the system respond to the zone load. During each simulation time step of the air primary loop, the zone temperatures and humidity ratios are held constant. The simulation of the air primary loop iterates until the zone load is met or system capacity is exceeded. Then the zone temperatures and humidity ratios are corrected based on the simulation results of

the primary air system. The full air loop simulation is managed by 2 managers: *ManageAirLoops* (simulates the primary air systems or supply side) and *ManageZoneEquipment* (simulates the zone equipments or demand side).

ManageAirLoops manages the primary air system side or supply side which includes the mixing box, fan and coils. The subroutine *SimAirLoops* does the actual simulation of the primary air systems and tries to converge on the zone load served by the systems. More details on the iterative procedure is discussed in Section 3.2.2

ManageZoneEquipment simulates all the equipments directly connected to the zone. Initially, the supply air plenum and zone splitters are simulated based on the primary air system outlet conditions. Then each air terminal unit modulates its air flow rate in order to satisfy its zone load. Air outlet conditions and flow rates from the zone are passed to the mixer and eventually back to the return air node which is the inlet of the primary air system.

The direct air unit model may be used to describe the simple system configuration typical of residential unitary equipment based systems. The direct air unit allows the primary air system to supply air directly to the zone without any zone level control or tempering. The direct air unit requires specification of the zone inlet node which acts as both the zone inlet node and the outlet node of the zone splitter. For instance, the water-to-air heat pump unit acquires the zone load demanded by the "control zone" and modulates the air flow rate and capacity to meet the load required. The heating or cooling capacity delivered by the heat pump is distributed to all the zones by the direct air units serving each of the zones.

3.2.2 Unitary Equipment Simulation Manager

HVACFurnace is a subroutine under *SimAirLoops* which manages the simulation of air-to-air and water-to-air heat pumps. The EnergyPlus air-to-air and water-to-air heat pump models are "virtual components" that consists of an ON-OFF fan, a heating coil, a cooling coil, and a gas or electric supplemental heating coil.

A single heat pump may be configured to serve multiple zones as shown in Figure 3.1, with one thermostat located in the "control zone". One of the parameters required is the fraction of the total system volumetric airflow that is supplied to the control zone. The heat pump cooling or heating load is determined by the control zone cooling load and the fraction of the total system volumetric airflow that is supplied to the control zone:

$$Heat\ Pump\ Cooling\ Load = \frac{Control\ Zone\ Cooling\ Load}{Control\ Zone\ Air\ Flow\ Fraction} \quad (3.1)$$

The heat pump model is capable of simulating two fan operating modes: cycling fan (AUTO) and continuous fan. In cycling fan mode, the fan cycles on and off together with the compressor. The fan heat contributes to the sensible heat balance of the air primary systems. The algorithm for the heat pump simulation in cooling mode is listed as follows:

1. In cooling mode, the heating coil and the supplementary heating coil are turned OFF, and the coil inlet conditions are passed to the outlet nodes. The sensible capacity of the cooling coil is determined using two steps. First the full load output of the heat pump is calculated as shown in Equation (3.2). Then a simulation is performed with the compressor OFF and the fan on as shown in Equation (3.3).

$$FullCoolOutput = \left(\dot{m}_{air}\right)\left(h_{out,full\ load} - h_{control\ zone}\right)_{HR\ \min} \quad (3.2)$$

$$NoCoolOutput = \left(\dot{m}_{air}\right)\left(h_{out,coil\ off} - h_{control\ zone}\right)_{HR\ \min} \quad (3.3)$$

where:

$\dot{m}_{air}$ = air mass flow rate kg/s

$h_{out,coil\ off}$ = enthalpy of the air exiting the heat pump at full-load conditions, J/kg

$h_{out,coil\ off}$ = enthalpy of the air exiting the heat pump with cooling coil OFF, J/kg

$HR_{\min}$ = enthalpy evaluated at the minimum humidity ratio of the heat pump exiting air which is constant

The cooling coil sensible capacity is calculated as:

$$HPCoilSensCapacity = FullCoolOutput - NoCoolOutput \quad (3.4)$$

2. Determine the part-load ratio, PLR or the heat pump,

$$PLR = \frac{\left(HeatPumpCoolingLoad - NoCoolOutput\right)}{HPCoilSensCapacity} \quad (3.5)$$

3. Based on the PLR, calculate the part-load fraction and the runtime fraction using the part-load fraction model discussed in Section 2.3.2.
4. Simulate the cooling coil again using the calculated PLR and runtime fraction. The heat pump model is a steady state model thus the cooling coil output is at full load conditions. The PLR and runtime fraction is used to adjust the heat pump outputs to part-load conditions based on the operating mode of the fan. For AUTO fan, the heat pump design air flow rate is multiplied by the PLR to determine the average air flow rate for the entire time step. The cooling coil outlet conditions

such as the enthalpy and humidity ratio are not adjusted and represent the full-load values. For continuous fan, the outlet air flow rate is kept constant at the design air flow rate, while the other cooling coil outlet conditions are calculated as the "average" conditions over the simulation time step. The outlet conditions are averaged using the PLR as follows,

$$h_{outlet} = (PLR)\,h_{outlet,\,full\ load} + (1 - PLR)\,h_{inlet} \qquad (3.6)$$

$$w_{outlet} = (PLR)\,w_{outlet,\,full\ load} + (1 - PLR)\,w_{inlet} \qquad (3.7)$$

5. For AUTO fan mode, the part-load performance of the cooling coil and fan is non-linear thus iterations are required until the heat pump output matches the required cooling load. The PLR is adjusted accordingly and if the heat pump capacity is unable to meet the required load, PLR is set to 1 with the heat pump running at full load. For continuous fan mode, the fan heat remains constant since the air flow rate is constant at the design air flow rate. Thus the calculated *FullCoolOutput* and *NoCoolOutput* in Step 1 are constant. No iteration is required for continuous fan mode since the PLR is also constant.

For heating mode, the algorithm for the heat pump simulation is similar to the cooling mode. The only difference is the remaining heating load will be passed to the supplementary heating coil when the heat pump heating coil can not meet the zone demand.

4.0 Implementation of Heat Pump Models in EnergyPlus

The heat pump models that have been implemented in EnergyPlus consist of curve-fit and parameter estimation models. The model developer and documentation for each heat pump models is shown in Table 4.1.

Heat Pump Model	Developer	Implemented into E+ by	Current Reference for Model Implemetation
Air-to-Air			
Curve-Fit Model	Adopted from DOE 2	Buhl & Shirey	EnergyPlus(2004)
Water-to-Air			
Curve-Fit Model	Lash (1992)	Shenoy(2004) & Tang	Shenoy(2004)
Parameter Based Model	Jin (2002)	Fisher and Tang	EnergyPlus(2004)
Water-to-Water			
Curve-Fit Model	Tang	Tang	N/A
Parameter Based Model	Jin (2002)	Murugappan (2002)	EnergyPlus(2004)

Table 4.1: Summary of Heat Pump Models in EnergyPlus

In this research project, the heat pump models that have been developed by previous researchers have been modified and implemented in EnergyPlus. The models are chosen for their robustness and generally available parameters. In addition to that, these models are further validated using measured data from the OSU laboratories and from heat pump manufacturers. This chapter gives a brief summary of the models with modifications. A curve-fit water-to-water heat pump model is also proposed based on the same approach used in the curve-fit water-to-air heat pump by Lash (1992).

4.1. Curve-Fit Water to Air Heat Pump Model

The curve-fit water-air heat pump model is based on Lash (1992) and Shenoy (2004). However, further analysis of the model for several different heat pumps shows that the model has some problem capturing the heat pump performance for heating and cooling mode. This section describes the modifications of the model and changes to the implementation procedure into EnergyPlus as previously explained in Shenoy (2004).

4.1.1 Modification of Lash (1992) and Shenoy (2004)

The water-air heat pump model was proposed by Lash (1992) and later improved by Shenoy (2004) to include variable air flow rate. Using Equation 2.25-2.29 and the Generalized Least Squares method, the proposed model is tested for 1-ton, 2-ton, 3-ton and 5-ton heat pump for both cooling and heating mode. The model is evaluated for a range of heat pump capacities to evaluate the robustness of the model.

For cooling mode, 54 data points are obtained from the manufacturer catalog data with entering water temperatures of 30°F to 110°F, two sets of air flow rates, entering air dry-bulb temperature of 80°F and an entering air wet-bulb temperature of 67°F. The data points are then extended to 810 points for a range of entering air dry-bulb and wet-bulb temperature using the correction factors provided in the catalog. As mentioned in Appendix B of Jin (2002), some points in the dataset are invalid because the relative humidity of the exiting air exceeds 100%. The relative humidity of the exiting air is calculated from the inlet air conditions, latent capacity and sensible capacity indicated in the catalog. These data points are not included in the coefficients computation; data sets with no latent capacity are also excluded. As a result, the number of data points used to

generate the coefficients for cooling mode varies for different heat pumps. The percentage error of the calculated performance compared to the catalog data is shown in the table below:

	Cooling			
	1-ton	2-ton	3-ton	6-ton
Number of Data Points	466	510	348	468
Total Capacity RMS error (%)	10.40	10.27	9.31	9.26
Sensible Capacity RMS error (%)	8.99	10.80	8.10	8.99
Heat Rejection RMS error (%)	7.03	6.49	6.17	6.75
Total Power Input RMS error (%)	28.52	31.65	26.48	26.09

Table 4.2: Comparison of Cooling Catalog Data and Simulation Results for Curve-Fit Water-to-Air Heat Pump Model by Shenoy(2004): Eq 2.25-2.27

Table 4.2 shows that there is no significant trend of deterioration in performance as the model is used to simulate a range of capacities. However, the model does a poor job of simulating the power consumption with percentage RMS error of more than 25%.

For heating mode, 44 data points are obtained from the catalog data for entering water temperatures of 30°F to 110°F, two sets of air flow rates and an entering air dry-bulb temperature of 80°F. The data points are then extended to 252 data points to account for variation of entering air dry-bulb temperature using the correction factors provided by the manufacturer. The simulation results using the generated coefficients are compared with the catalog data and the results are shown below in Table 4.3:

	Heating			
	1-ton	2-ton	3-ton	6-ton
Number of Data Points	252	252	252	252
Heating Capacity RMS error (%)	24.61	21.48	20.56	21.31
Heat Absorption RMS error (%)	36.14	29.30	28.36	30.95
Total Power Input RMS error (%)	9.42	11.40	11.53	11.15

Table 4.3: Comparison of Heating Catalog Data and Simulation Results for Curve-Fit Water-to-Air Heat Pump Model by Shenoy(2004): Eq 2.28-2.29

As shown, the model did a poor job simulating the heating capacity and the heat absorption or source side heat transfer rate of the heat pump. The heating capacities have RMS errors of more than 20%, and the heat absorption results have RMS errors of more than 28%. However, the accuracy of the model seems to be consistent and insensitive to the variation of the heat pump capacity.

Table 4.2 and Table 4.3 show that the model requires improvement to achieve simulation results with percentage RMS errors of at less than 10%. It is noted that heating capacity and heat absorption are a strong function of the water inlet temperature and a weak function of the air flow rate. Combining the water inlet temperature and the air flow rate together under a single coefficient, D2 and E2 will result in coefficients that are unable to capture the change in heat pump performance with respect to the change in the inlet water temperature.

Thus Equation 2.25 - 2.29 is modified by including an additional term in each equation which results in the equations below:

Cooling Mode:

$$\frac{Q_{total}}{Q_{total,ref}} = A1 + A2\left[\frac{T_{w,in}}{T_{ref}}\right] + A3\left[\frac{T_{ref}}{T_{wb}}\right]\left[\frac{\dot{m}_w}{\dot{m}_{w,ref}}\right] + A4\left[\frac{\dot{m}_{air,ref}}{\dot{m}_{air}}\right] \tag{4.1}$$

$$\frac{Q_{sens}}{Q_{sens,ref}} = B1 + B2\left[\frac{T_{w,in}}{T_{ref}}\right] + B3\left[\frac{T_{ref}}{T_{wb}}\right]\left[\frac{\dot{m}_w}{\dot{m}_{w,ref}}\right] + B4\left[\frac{T_{ref}}{T_{db}}\right]\left[\frac{\dot{m}_w}{\dot{m}_{w,ref}}\right] + B5\left[\frac{\dot{m}_{air,ref}}{\dot{m}_{air}}\right] \tag{4.2}$$

$$\frac{COP_c}{COP_{c,ref}} = C1 + C2\left[\frac{T_{w,in}}{T_{ref}}\right] + C3\left[\frac{T_{ref}}{T_{wb}}\right]\left[\frac{\dot{m}_w}{\dot{m}_{w,ref}}\right] + C4\left[\frac{\dot{m}_{air,ref}}{\dot{m}_{air}}\right] \tag{4.3}$$

Heating Mode:

$$\frac{Q_h}{Q_{h,ref}} = D1 + D2\left[\frac{T_{w,in}}{T_{ref}}\right] + D3\left[\frac{T_{ref}}{T_{db}}\right]\left[\frac{\dot{m}_w}{\dot{m}_{w,ref}}\right] + D4\left[\frac{\dot{m}_{air,ref}}{\dot{m}_{air}}\right] \quad (4.4)$$

$$\frac{COP_h}{COP_{h,ref}} = E1 + E2\left[\frac{T_{w,in}}{T_{ref}}\right] + E3\left[\frac{T_{ref}}{T_{db}}\right]\left[\frac{\dot{m}_w}{\dot{m}_{w,ref}}\right] + E4\left[\frac{\dot{m}_{air,ref}}{\dot{m}_{air}}\right] \quad (4.5)$$

The equations above are implemented into the model and it is simulated for the same data points. The simulations results for the heating and cooling mode are shown in Table 4.4 and Table 4.5:

	Cooling			
	1-ton	**2-ton**	**3-ton**	**6-ton**
Number of Data Points	466	510	348	468
Total Cooling RMS error (%)	5.70	5.50	5.03	5.77
Sensible Cooling RMS error (%)	8.81	9.76	8.09	8.77
Heat Rejection RMS error (%)	9.16	6.82	5.86	6.60
Total Power Input RMS error (%)	28.34	20.74	17.06	14.70

Table 4.4: Comparison of Cooling Catalog Data and Simulation Results for Curve-Fit Water-to-Air Heat Pump Model Version 1: Eq 4.1-4.3

	Heating			
	1-ton	**2-ton**	**3-ton**	**6-ton**
Number of Data Points	252	252	252	252
Heating Capacity RMS error (%)	1.71	1.25	1.12	1.24
Heat Absorption RMS error (%)	7.17	7.67	6.23	7.97
Total Power Input RMS error (%)	8.90	8.86	8.51	8.98

Table 4.5: Comparison of Heating Catalog Data and Simulation Results for Curve-Fit Water-to-Air Heat Pump Model Version 1: Eq 4.4-4.5

Comparing Table 4.2 and Table 4.4, the percentage RMS error for the sensible capacity improved to about 5% from 10% while there is no significant improvement to the total cooling capacity, heat rejection and the power consumption. However, there is a huge improvement for the heating capacity and heat absorption for the heating mode by comparing Table 4.3 and Table 4.5. Error for heating capacity dropped from over 20% to

about 1% while the heat absorption dropped from about 30% to around 7%. No significant improvement is observed for the power consumption.

Table 4.4 and Table 4.5 show that the model is still unable to simulate the compressor power well especially for cooling mode. In order to calculate the power consumption, the product of the calculated COP and calculated capacity has to be taken as shown in the equation below:

$$W_{calculated} = COP_{calculated} \times Capacity_{calculated} \qquad (4.6)$$

This procedure allows propagation of error from the capacity to the power consumption. In order to prevent the propagation of error, a new equation is proposed as a substitute for Equation 4.3 and 4.5 by fitting the coefficients directly to the heat pump power consumption.

Since most heat pump catalog data gives the air and water volumetric flow rate instead of the mass flow rate, the air mass flow rate and water mass flow rate are converted to volumetric flow rate for convenience. In addition, it also prevents the discrepancies in the fluid property routines employed in the Coefficient Calculator Program and EnergyPlus.

In addition, the source side heat transfer rate or heat rejection for cooling mode is calculated in Table 4.2, Table 4.3, Table 4.4 and Table 4.5 by adding the total power consumption and the load side heat transfer rate. The heat pump manufacturer assumed that there are no losses as reflected in the catalog data. As a result, addition of the power input and the load side heat transfer rate always equal to the source side heat transfer rate

for cooling mode. A new set of equations for simulating the source side heat transfer curve is proposed to account for the compressor shell loss. Most researchers assume that the compressor shell loss is about 10% of the compressor power input.

By observing the heat pump catalog and correction factors, the source side heat transfer rate is a function of the water inlet temperature, inlet wet bulb temperature, and load side and source side mass flow rates. Thus the formulation of the source side heat transfer rate equation is similar to the total cooling and heating capacity which are influenced by the same variables. With more experience in the governing equations and the numerical solver, it is possible to formulate all the equations in a simpler and standard form. For maximum capability in capturing the heat pump performance curve, one coefficient is assigned to each variable which reduces the error drastically based on observation. The equations below shows the reformulation of the entire set of governing equations in its final form;

Cooling Mode:

$$\frac{Q_{total}}{Q_{total,ref}} = A1 + A2\left[\frac{T_{wb}}{T_{ref}}\right] + A3\left[\frac{T_{w,in}}{T_{ref}}\right] + A4\left[\frac{\dot{V}_{air}}{\dot{V}_{air,ref}}\right] + A5\left[\frac{\dot{V}_{w}}{\dot{V}_{w,ref}}\right] \tag{4.7}$$

$$\frac{Q_{sens}}{Q_{sens,ref}} = B1 + B2\left[\frac{T_{db}}{T_{ref}}\right] + B3\left[\frac{T_{wb}}{T_{ref}}\right] + B4\left[\frac{T_{w,in}}{T_{ref}}\right] + B5\left[\frac{\dot{V}_{air}}{\dot{V}_{air,ref}}\right] + B5\left[\frac{\dot{V}_{w}}{\dot{V}_{w,ref}}\right] \tag{4.8}$$

$$\frac{Power_{c}}{Power_{c,ref}} = C1 + C2\left[\frac{T_{wb}}{T_{ref}}\right] + C3\left[\frac{T_{w,in}}{T_{ref}}\right] + C4\left[\frac{\dot{V}_{air}}{\dot{V}_{air,ref}}\right] + C5\left[\frac{\dot{V}_{w}}{\dot{V}_{w,ref}}\right] \tag{4.9}$$

$$\frac{Q_{source,c}}{Q_{source,c,ref}} = D1 + D2\left[\frac{T_{wb}}{T_{ref}}\right] + D3\left[\frac{T_{w,in}}{T_{ref}}\right] + D4\left[\frac{\dot{V}_{air}}{\dot{V}_{air,ref}}\right] + D5\left[\frac{\dot{V}_{w}}{\dot{V}_{w,ref}}\right] \tag{4.10}$$

Heating Mode:

$$\frac{Q_h}{Q_{h,ref}} = E1 + E2\left[\frac{T_{db}}{T_{ref}}\right] + E3\left[\frac{T_{w,in}}{T_{ref}}\right] + E4\left[\frac{\dot{V}_{air}}{\dot{V}_{air,ref}}\right] + E5\left[\frac{\dot{V}_w}{\dot{V}_{w,ref}}\right] \quad (4.11)$$

$$\frac{Power_h}{Power_{h,ref}} = F1 + F2\left[\frac{T_{db}}{T_{ref}}\right] + F3\left[\frac{T_{w,in}}{T_{ref}}\right] + F4\left[\frac{\dot{V}_{air}}{\dot{V}_{air,ref}}\right] + F5\left[\frac{\dot{V}_w}{\dot{V}_{w,ref}}\right] \quad (4.12)$$

$$\frac{Q_{source,c}}{Q_{source,c,ref}} = G1 + G2\left[\frac{T_{db}}{T_{ref}}\right] + G3\left[\frac{T_{w,in}}{T_{ref}}\right] + G4\left[\frac{\dot{V}_{air}}{\dot{V}_{air,ref}}\right] + G5\left[\frac{\dot{V}_w}{\dot{V}_{w,ref}}\right] \quad (4.13)$$

Using the same data points, Equation 4.7-4.10 are used to simulate the heat pump for cooling mode and Equation 4.11- 4.13 for heating mode. The results are shown in Table 4.6 and Table 4.7 below:

	Cooling			
	1-ton	**2-ton**	**3-ton**	**6-ton**
Number of Data Points	466	510	348	468
Total Cooling RMS error (%)	3.12	2.76	2.68	2.72
Sensible Cooling RMS error (%)	4.46	5.13	4.49	4.25
Heat Rejection RMS error (%)	2.22	2.37	2.19	2.19
Total Power Input RMS error (%)	5.68	4.16	1.86	2.97

Table 4.6: Comparison of Cooling Catalog Data and Simulation Results for Curve-Fit Water-to-Air Heat Pump Model Version 2: Eq 4.7-4.10

	Heating			
	1-ton	**2-ton**	**3-ton**	**6-ton**
Number of Data Points	252	252	252	252
Heating Capacity RMS error (%)	1.60	1.59	0.84	1.02
Heat Absorption RMS error (%)	2.50	2.24	1.61	1.59
Total Power Input RMS error (%)	0.83	1.28	1.47	0.91

Table 4.7: Comparison of Heating Catalog Data and Simulation Results for Curve-Fit Water-to-Air Heat Pump Model Version 2: Eq 4.11-4.13

Table 4.6 and Table 4.7 show that increasing the number of coefficients improved the model accuracy for both heating and cooling mode with RMS error of less than 6%. The governing equations have a general form whereby the inlet conditions are divided by the rated inlet conditions. This form results in each term having a uniform value of about 1.0. Thus the coefficient for the inlet variable indirectly shows the sensitivity of calculated output to the respective inlet variable. The coefficient for the inlet variable will have a negative sign if the inlet variable is inversely proportional to the calculated output.

4.1.2 Catalog Data Points

Unlike the parameter estimation based model, the curve-fit model uses matrix functions to calculate the coefficients. The "knowns" and "unknowns" are formulated in matrix form and solved using the generalized least square method as described by Shenoy (2004). Thus the number of data points required is essentially based on the number of coefficients. For example, the minimum number of data points for cooling mode is 6 because there are 6 coefficients required in calculating the sensible cooling capacity (Equation 4.8). The general mathematical rule of requiring n equations to solve for n unknowns applies to this model. The equations are essentially the data points obtained from the catalog data.

In order for the generalized least square method to work properly, the data points obtained from the catalog data should vary all model variables. For instance, the inlet air flow rate should not be fixed at a certain flow rate. Using fixed inlet air flow rate will cause the model to be insensitive to the variation of air flow and might even cause problem in calculating the coefficients. The generalized least square method uses matrix transpose, inverse and multiplication to calculate the coefficients thus one might

encounter a scenario of "division by zero" or huge errors if the inlet conditions are fixed. This problem is a major drawback to the model where the catalog data does not have varying inlet conditions. The failure of the generalized least square method is illustrated in Appendix F.

However, a quick check on the following heat pump manufacturer's catalog data; Addison, ClimateMaster, Trane, and Florida Heat Pump(FHP), only FHP does not publish heat pump performance data at varying air and water flow rates on their website. Software is available on the FHP website which could be used to generate the heat pump performance at different inlet conditions. The other heat pump manufacturers provide corrections factors to adjust for either the air temperatures or flow rates which will give the heat pump performance variables at varying inlet conditions. In short, the catalog data points used for the coefficient generator should have varying inlet conditions and one should expect the model not to perform as expected if the inlet conditions are fixed.

4.1.3 Model Implementation in EnergyPlus

Implementation of the curve-fit water-to-air heat pump model in EnergyPlus is generally similar to Shenoy (2004). The only changes to the model are the governing equations and the required performance coefficients. In addition, the proposed source side curve was not implemented in EnergyPlus because simulating the source side heat transfer rate individually would cause the heat balance equations to be out of balance which is discomforting to some users. Figure 4.1 below shows the performance coefficients, inputs and outputs of the model:

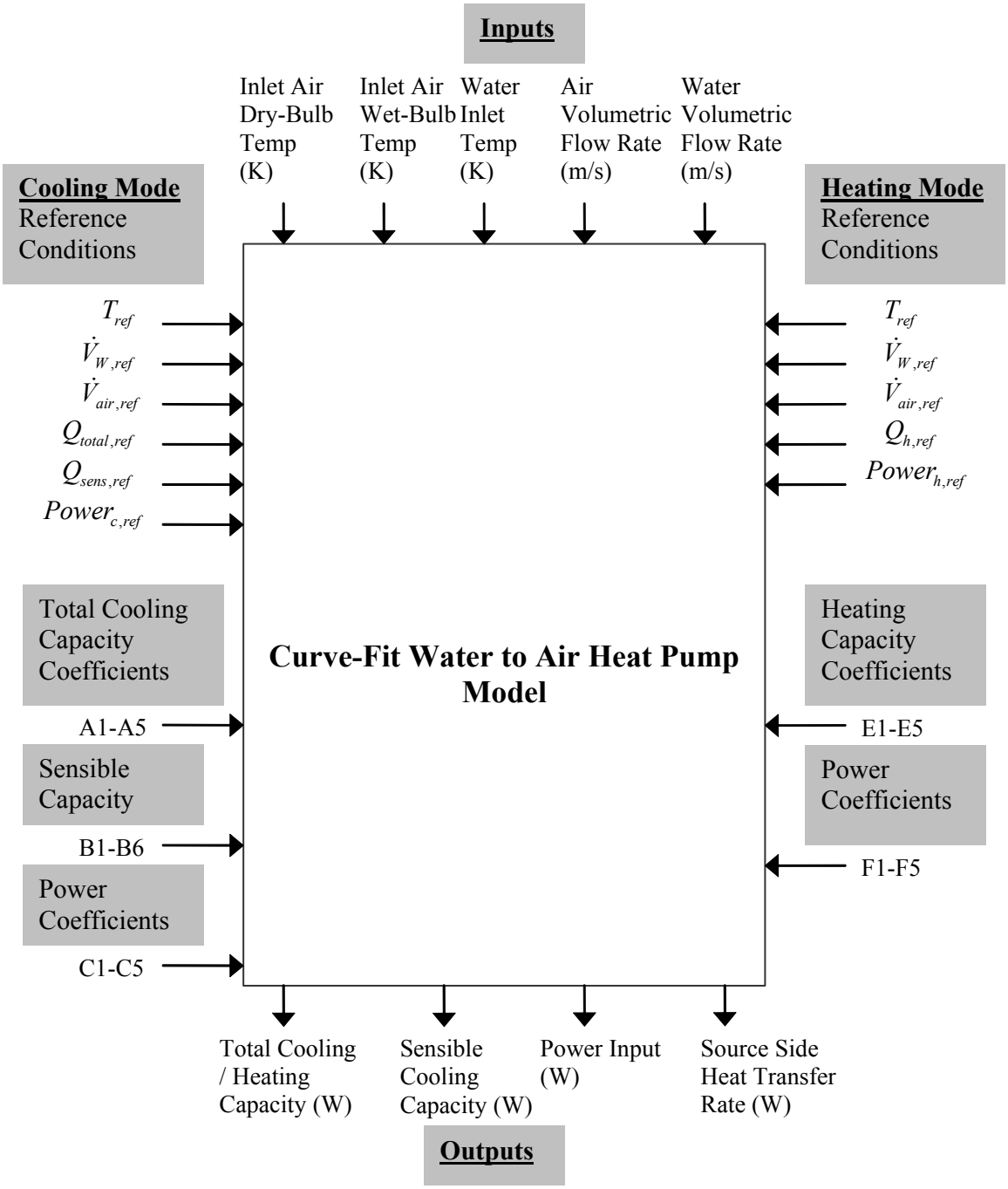

Figure 4.1: Information Flow Chart for Curve-Fit Water-to-Air Heat Pump Model

As described earlier in Chapter 3, the Furnace Module will call the heat pump model to simulate the performance of the heat pump at the zone sensible demand and the

corresponding compressor runtime fraction. The figure below shows the flow diagram of the curve-fit water-to-air heat pump model.

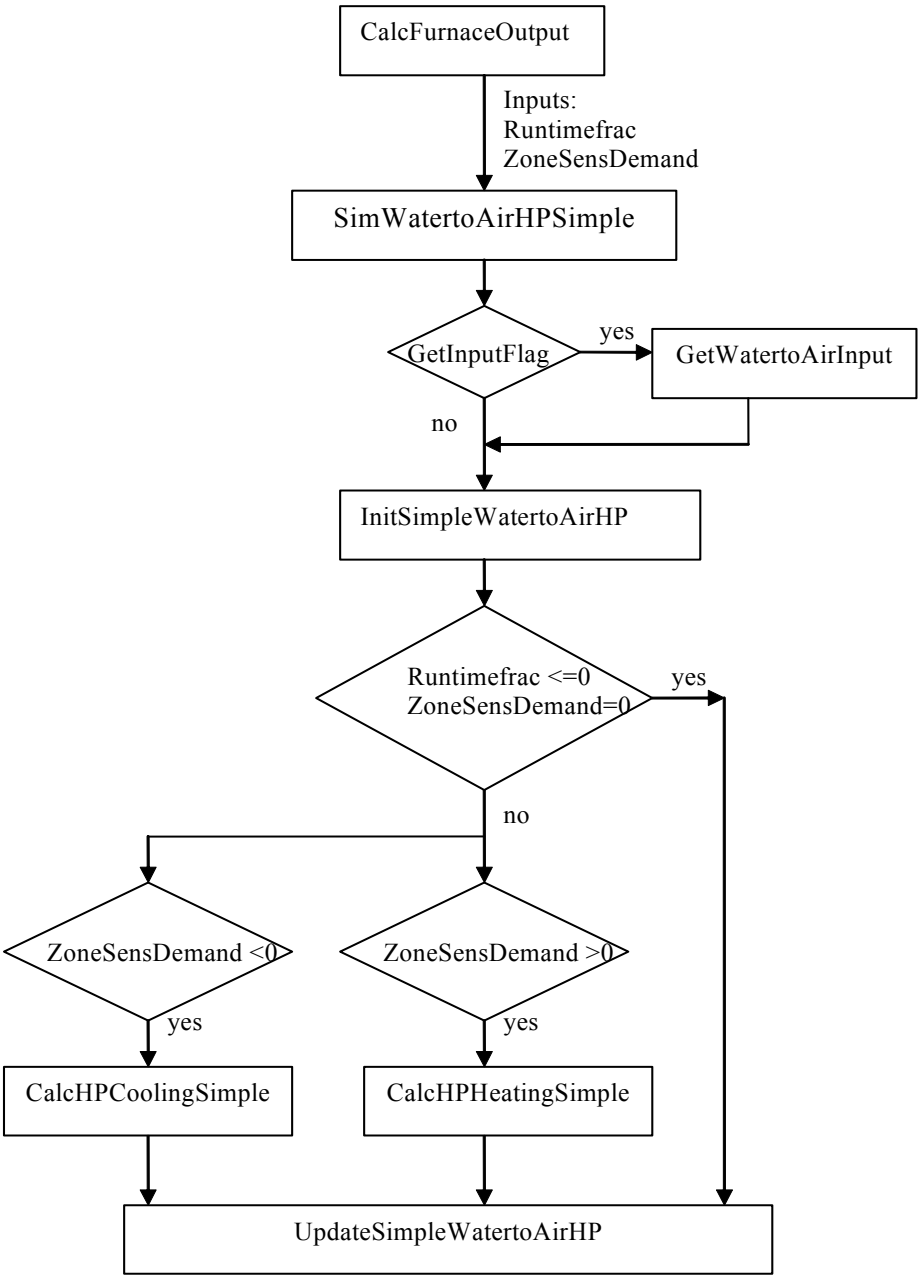

Figure 4.2: Flow Diagram for Curve-Fit Water-to-Air Heat Pump Model

In addition, the latent degradation model by Henderson and Rengarajan (1996) is incorporated to simulate the latent and sensible capacity of the heat pump at part-load conditions. Refer to Chapter 4.3 for details on interaction between the heat pump cooling coil subroutine or CalcHPCoolingSimple and the latent degradation model. For the sake of brevity, more details on the input data file structure (IDF), input data dictionary (IDD), and output reports can be obtained from the EnergyPlus website.

4.2. Parameter Estimation Based Water-to-Air Heat Pump Model

The Parameter Estimation Based Water-Air Heat Pump Model was developed by Jin (2002). The model is capable of simulating performance of heat pump under heating and cooling mode and the usage antifreeze as the source side fluid. The table below shows the comparison for the requirements to implement curve-fit and parameter estimation heat pump models in EnergyPlus:

Curve-Fit Model	**Parameter Estimation Model**
Requires coefficients generated using Generalized Least Square Method. Does not require refrigerant property routines. No successive substitution method is required.	Requires 8-10 parameters depending on the compressor type and source side fluid. Requires refrigerant property routines Successive substitution method is required to drive the model to convergence.

4.2.1 Model Development

This section gives a brief outline of the model which is described in detail by Jin (2002). Generally, the heat pump is modeled as 4 major components: the compressor, expansion device, evaporator and condenser. The thermodynamics process that might occur in the refrigerant lines, accumulator and etc. are ignored due to their small contribution. The diagram below shows the configuration of the water-air heat pump in cooling mode.

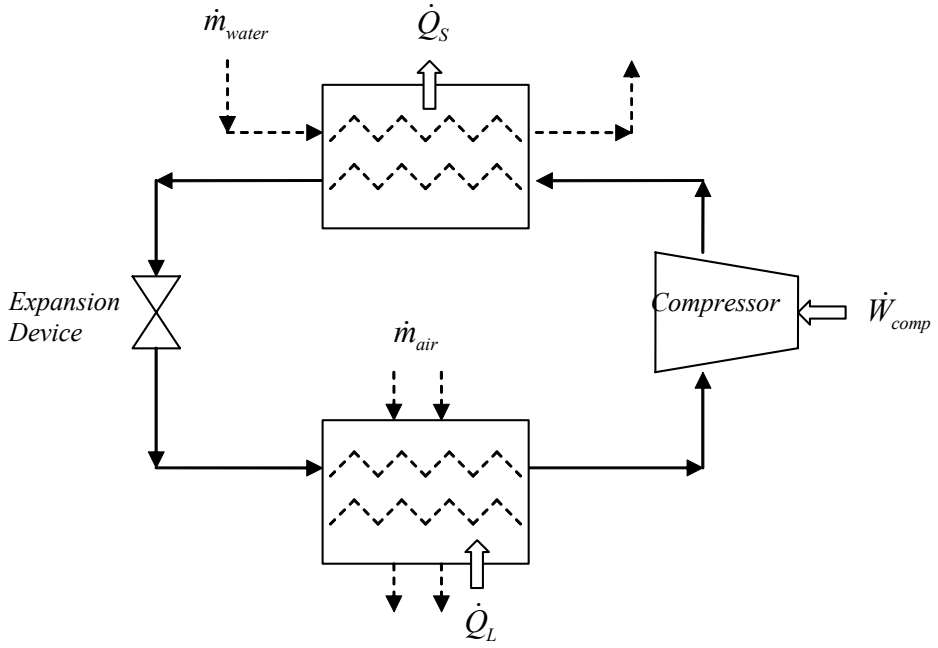

Figure 4.3: Water-Air Heat Pump Configuration

The heat pump model is capable of handling reciprocating, scroll and rotary compressors. The refrigerant mass flow rate for each compressor is computed as shown in Equation 4.14-4.16. The work done by each compressor is modeled as shown in Equation 4.17-4.18.

Reciprocating:

$$\dot{m}_r = \frac{PD}{v_{suc}}\left[1 + C_1 - C_1\left(\frac{P_{dis}}{P_{suc}}\right)^{1/\gamma}\right] \tag{4.14}$$

Rotary:

$$\dot{m}_r = \frac{\dot{V}_d}{v_{suc}} \tag{4.15}$$

Scroll:

$$\dot{m}_r = \frac{\dot{V}_r}{v_{suc}} - C_2\frac{P_c}{P_e} \tag{4.16}$$

where:

$\dot{m}_r$ = refrigerant mass flow rate, kg/s

PD = piston displacement, m^3/s

v_{suc} = specific volume at suction state, m^3/kg

C_1 = clearance factor

P_{dis} = discharge pressure, Pa

P_{suc} = suction pressure, Pa

γ = isentropic exponent

$\dot{V}_r$ = the refrigerant volume flow rate at the beginning of the compression, m^3/s

C_2 = coefficient to define the relationship between pressure ratio and leakage rate

P_c = condensing pressure, Pa

P_e = evaporating pressure, Pa

$\dot{V}_d$ = displacement of rolling piston compressor, m^3/s

Reciprocating and Rotary:

$$\dot{W}_t = \frac{\gamma}{\gamma - 1} \dot{m}_r P_{suc} v_{suc} \left[\left(\frac{P_{dis}}{P_{suc}} \right)^{\frac{\gamma - 1}{\gamma}} - 1 \right] \tag{4.17}$$

Scroll:

$$W_t = \frac{\gamma}{\gamma - 1} P_e \dot{V}_r \left[\frac{\gamma - 1}{\gamma} \frac{\left(\frac{P_c}{P_e} \right)}{v_i} + \frac{1}{\gamma} v_i^{\gamma - 1} - 1 \right] \tag{4.18}$$

where:

$\dot{W}_t$ = theoretical power, W

γ = isentropic exponent

$\dot{m}_r$ = refrigerant mass flow rate, kg/s

P_{suc} = suction pressure, Pa

v_{suc} = specific volume at suction state, m^3/kg

P_{dis} = discharge pressure, Pa

$\dot{V}_r$ = the refrigerant volume flow rate at the beginning of the compression, m^3/s

P_c = condensing pressure, Pa

P_e = evaporating pressure, Pa

v_i = 'built-in' volume ratio

A simple linear representation is used to estimate the actual required power input to the compressor by taking account of the efficiency of the compressor and electro-mechanical power loss shown in the following equation:

$$\dot{W} = \frac{\dot{W}_t}{\eta} + \dot{W}_{loss} \tag{4.19}$$

where $\dot{W}$ is the compressor power input, η is the efficiency of the compressor and $\dot{W}_{loss}$ is the constant part of the electro-mechanical power losses.

The source side heat exchangers in both heating and cooling mode, as well as the load side heat exchanger in heating mode are identified as sensible heat exchangers. Sensible heat exchangers only have phase change on the refrigerant side. Sensible heat exchanger is modeled as a counter-flow heat exchanger with negligible pressure drop and the thermal effectiveness is as calculated follows:

$$\varepsilon = 1 - e^{-NTU} \tag{4.20}$$

$$NTU = \frac{UA}{\dot{m}_F C_{pF}} \tag{4.21}$$

where

ε = heat transfer effectiveness

NTU = number of transfer units

UA = heat transfer coefficient, W/K

$\dot{m}_F$ = water mass flow rate or air mass flow rate in case of heating mode, kg/s

C_{pF} = water or air specific heat, J/(kg-K)

Under extreme operating conditions, anti-freeze is added to the water loop to prevent it from freezing. Addition of the antifreeze changes the heat transfer coefficients and hence the performance of the heat pump. The overall heat transfer coefficient for the mixture can be computed as follows:

$$(UA)_{total\_antifreeze} = \frac{1}{\frac{C_3 \dot{V}^{-0.8}}{DF} + C_2} \tag{4.22}$$

where

$\dot{V}$ = fluid volumetric flow rate, m^3/s

DF = degradation factor

$C_3 \dot{V}^{-0.8}$ = estimated coolant side resistance, K/W

C_2 = estimated resistance due to refrigerant to tube wall convection, tube wall conduction and fouling, K/W

The coefficients C_2 and C_3 is estimated from the catalog data that uses pure water as the working fluid. Thus the performance of the heat pump with various percentage of antifreeze can be evaluated once the coefficients C_2 and C_3 are known and the degradation factor, DF can calculated as follows:

$$DF = \frac{h_{antifreeze}}{h_{water}} = \left(\frac{\mu_{antifreeze}}{\mu_{water}}\right)^{-0.47} \left(\frac{\rho_{antifreeze}}{\rho_{water}}\right)^{0.8} \left(\frac{C_{p,antifreeze}}{C_{p,water}}\right)^{0.33} \left(\frac{k_{antifreeze}}{k_{water}}\right)^{0.67} \tag{4.23}$$

In cooling mode, the load side heat exchanger is modeled as a direct expansion cooling coil. The coil is assumed to be completely wet or completely dry. The total

cooling capacity is calculated by the 'enthalpy method' developed by McElgin and Wiley (1940). The total heat transfer for the completely wet coil is,

$$\dot{Q}_{wet} = \varepsilon_{wet} \dot{m}_{air} \left(i_{a,i} - i_{s,e} \right) \tag{4.24}$$

The heat transfer effectiveness, ε_{wet} based on the enthalpy potential method is as follows:

$$\varepsilon_{wet} = \frac{i_{a,i} - i_{a,o}}{i_{a,i} - i_{s,e}} \tag{4.25}$$

where:

$$\varepsilon_{wet} = 1 - e^{(-NTU_{wet})} \tag{4.26}$$

$i_{a,i}$ = enthalpy of moist air at inlet state, J/kg

$i_{a,o}$ = enthalpy of moist air at outlet state, J/kg

$i_{s,e}$ = enthalpy of moist air at evaporating temperature, J/kg

The overall number of transfer units, NTU_{wet}, is based on the outside and inside surface heat transfer coefficient as following:

$$NTU_{wet} = \frac{\left(\frac{1}{h_{c,o} A_o} + \frac{C_{ps}}{C_{pa} \left(UA \right)_i} \right)}{\left(\dot{m}_{air} C_{pa} \right)} \tag{4.27}$$

where:

C_{ps} is the specific heat of saturated air defined by: $C_{ps} = \left(\frac{dh_s}{dT} \right)_{T=T_e}$

$h_{c,o}A_o$ = external surface heat transfer coefficient, W/K

$(UA)_i$ = inside surface heat transfer coefficient, W/K

$\dot{m}_{air}$ = air mass flow rate, kg/s

C_{pa} = air specific heat, J/(kg-K)

The number of transfer units can be simplified by grouping the inside and outside heat transfer coefficients as an overall heat transfer coefficient, $(UA)_{tot}$.

$$NTU_{wet} = \frac{(UA)_{tot}}{(\dot{m}_{air} C_{pa})} \tag{4.28}$$

Equation 4.20-4.26 is used to calculate the total heat transfer, and a method is required to split the total heat transfer into the sensible and latent heat transfers. The effective surface temperature, $T_{s,e}$, based on the analysis of dehumidifying coils in ASHRAE Handbook of HVAC Systems and Equipment (ASHRAE 2000) is used to determine the sensible heat transfer rate of the cooling coil. The enthalpy of the saturated air is as follows:

$$i_{s,s,e} = i_{a,i} - \frac{i_{a,i} - i_{a,o}}{1 - e^{\left(-\frac{h_{c,o} A_o}{m_a C_{pa}}\right)}} \tag{4.29}$$

The effective surface temperature, $T_{s,e}$, is calculated iteratively from the corresponding enthalpy of saturated air, $i_{s,s,e}$. After computing the effective surface temperature, the sensible heat transfer rate can be computed using the following equation:

$$\dot{Q}_{sen} = \left(1 - e^{\left(\frac{h_{c,o} A_o}{m_{air} C_{pa}}\right)}\right) \dot{m}_{air} C_{pa} \left(T_{a,i} - T_{s,e}\right) \tag{4.30}$$

4.2.2 Parameter Estimation Procedure

The heat pump model requires distinct parameters based on the operating mode, compressor type and the type of fluid. The general parameters required in cooling mode are shown below:

UA_{tot} = load side total heat transfer coefficient, W/K

$h_{co}A_o$ = load side external surface heat transfer coefficient, W/K

ΔT_{sh} = superheat temperature at the evaporator outlet, ˚C

W_{loss} = compressor power losses due to mechanical and electrical losses, W

η = compressor's efficiency, dimensionless

The parameters required by the respective compressor models are as follows:

Reciprocating Compressor:

PD = compressor piston displacement, m^3/s

ΔP = compressor suction/discharge pressure drop, Pascal

C_1 = compressor clearance factor, dimensionless

Rotary Compressor:

PD = compressor piston displacement, m^3/s

ΔP = compressor suction/discharge pressure drop, Pascal

Scroll Compressor:

$\dot{V}_r$ = refrigerant volume flow rate at the beginning of the compression, m^3/s

v_i = built-in-volume ratio, dimensionless

C_2 = leak rate coefficient the relationship between pressure ratio and leakage rate, dimensionless

As shown in Equation 4.22, additional parameters are required to calculate the source side heat transfer coefficient for use of an antifreeze mixture as the source side fluid. The parameters needed for water and antifreeze are as follows:

Pure water:

UA_s = source side heat transfer coefficient, W/K

Mixture of antifreeze and water:

C_1 = source side heat transfer resistance1

C_2 = source side heat transfer resistance2, K/W

All the parameters are required in cooling and heating mode except for the load side exterior heat transfer coefficient, $h_{co}A_o$. The load side external heat transfer coefficient, $h_{co}A_o$, is only required in cooling mode to determine the sensible heat and latent heat for the dehumidifying cooling coil. The load side exterior heat transfer coefficient, $h_{co}A_o$, can be estimated separately using the golden search minimum method to find the optimal values that gives the lowest sum of squares of relative errors for both sensible and latent heat.

$$SSE = \sum_{i=1}^{N}\left[\left(\frac{\left(\dot{Q}_{sens,cat}\right)_i - \left(\dot{Q}_{sens}\right)_i}{\left(\dot{Q}_{sens,cat}\right)_i}\right)^2 + \left(\frac{\left(\dot{Q}_{lat,cat}\right)_i - \left(\dot{Q}_{lat}\right)_i}{\left(\dot{Q}_{lat,cat}\right)_i}\right)^2\right] \le err \qquad (4.31)$$

where

err = tolerance error

$\dot{Q}_{sens,cat}$ = catalog sensible capacity, W

$\dot{Q}_{sens}$ = calculated sensible capacity, W

$\dot{Q}_{lat,cat}$ = catalog latent capacity, W

$\dot{Q}_{lat}$ = calculated latent capacity, W

The procedure for estimating the load side exterior heat transfer coefficient is outline in the flow diagram below:

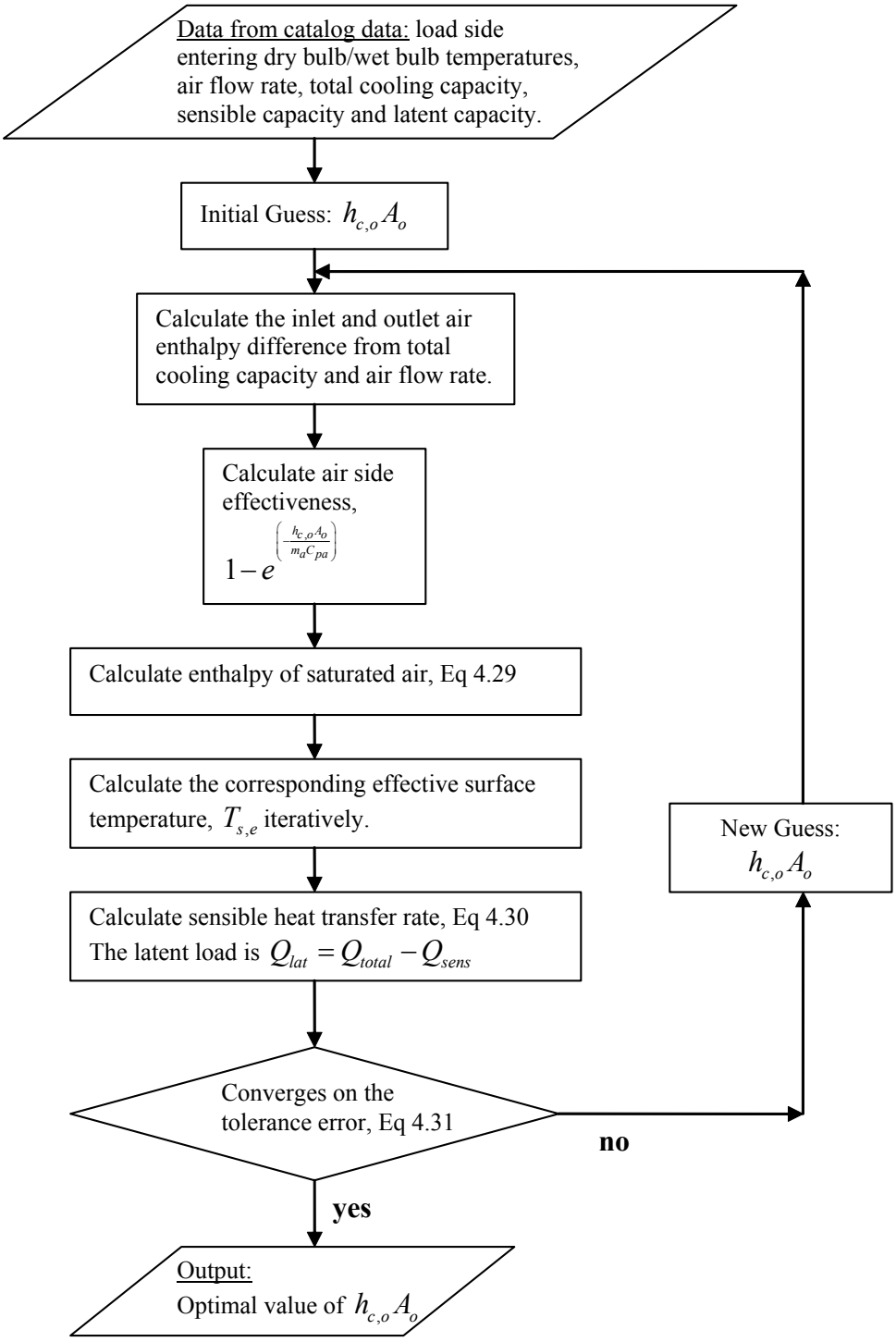

Figure 4.4: Flow Diagram for Estimating the Load Side Exterior Heat Transfer Coefficient

For the case of reciprocating compressor with pure water as the source side fluid, the rest of the parameters UA_s, UA_{tot}, ΔT_{sh}, W_{loss}, η, PD, ΔP and C_1 are searched for the optimal values to converge on the heat transfers and compressor power. Nelder Mead Simplex is used to estimate the parameters that will give the minimum value of the following objective function.

$$SSE_2 = \sum_{i=1}^{N}\left[\left(\frac{\left(\dot{W}_{cat}\right)_i - \left(\dot{W}\right)_i}{\left(\dot{W}_{cat}\right)_i}\right)^2 + \left(\frac{\left(\dot{Q}_{L,cat}\right)_i - \left(\dot{Q}_L\right)_i}{\left(\dot{Q}_{L,cat}\right)_i}\right)^2 + \left(\frac{\left(\dot{Q}_{S,cat}\right)_i - \left(\dot{Q}_S\right)_i}{\left(\dot{Q}_{S,cat}\right)_i}\right)^2\right] \quad (4.32)$$

where:

$\dot{W}_{cat}$ = catalog compressor power consumption, W

$\dot{W}$ = calculated compressor power consumption, W

$\dot{Q}_{L,cat}$ = catalog load side heat transfer rate, W

$\dot{Q}_L$ = calculated load side heat transfer rate W

$\dot{Q}_{S,cat}$ = catalog source side heat transfer rate W

$\dot{Q}_S$ = calculated source side heat transfer rate W

The parameter estimation procedure is outlined in the following flow diagram,

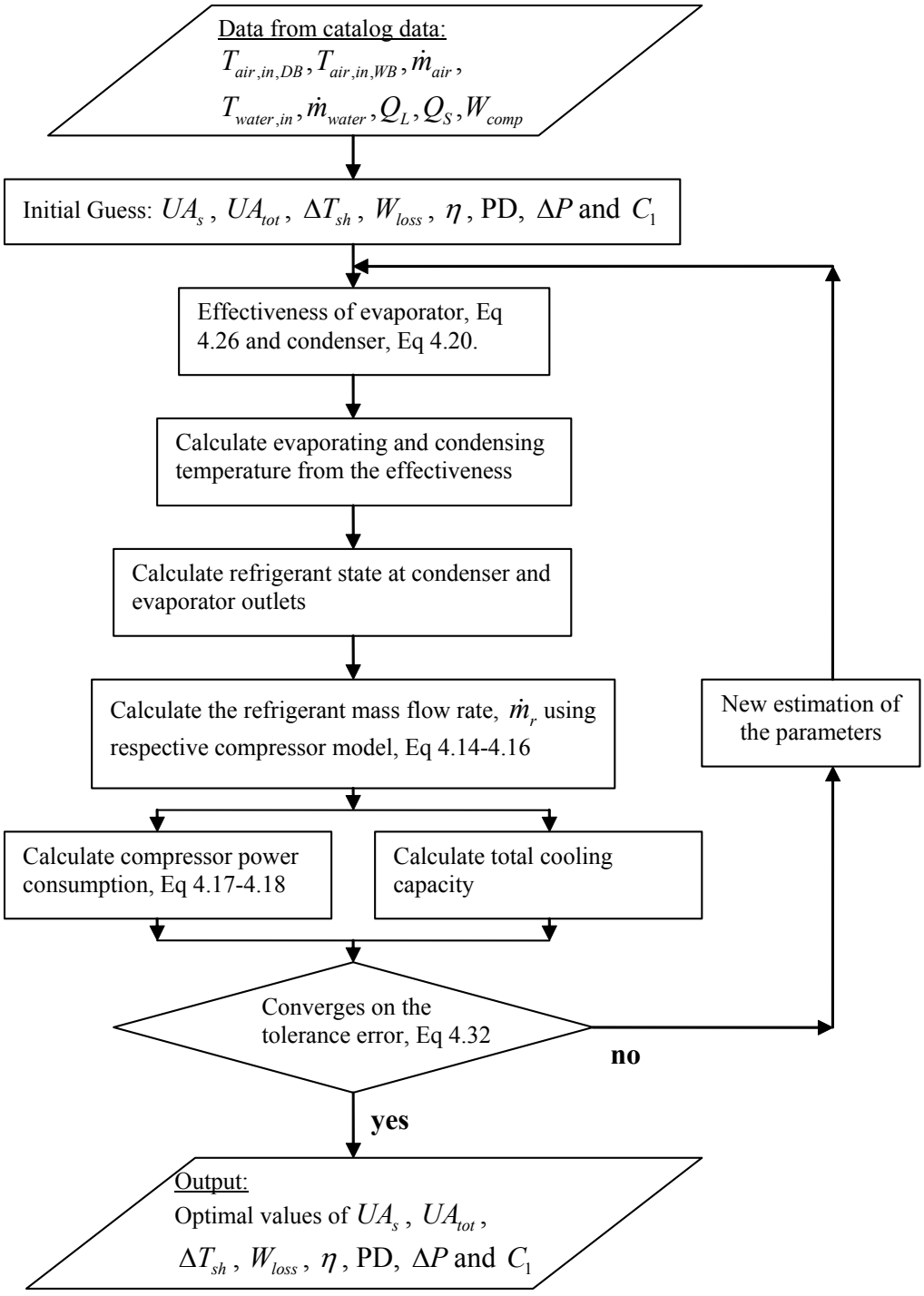

Figure 4.5: Flow Diagram for Parameter Estimation Program

4.2.3 Model Implementation

The two objective functions described earlier are combined into a single program that uses the parameters generated to solve for the heat transfer rates and compressor power given the inlet conditions. The program requires two nested iterative loops to solve for the load side heat transfer rate and the source side heat transfer rate using the successive substitution method. Figure 4.6 shows the inputs, outputs and the parameters required by the heat pump model. The algorithm for the model is shown in Figure 4.7.

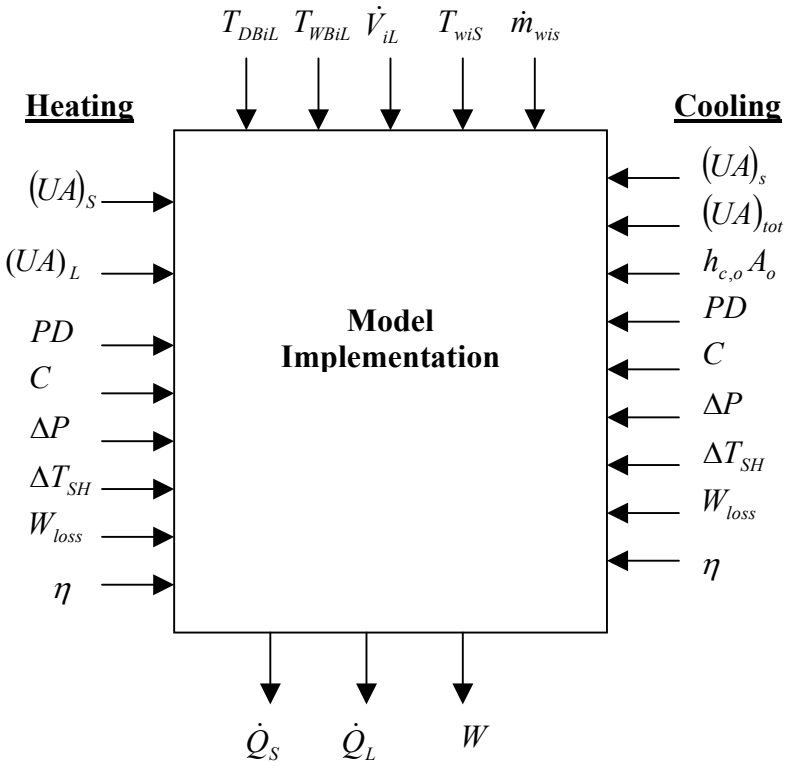

Figure 4.6: Information Flow Chart for Parameter Estimation Based Water-to-Air Heat Pump Model

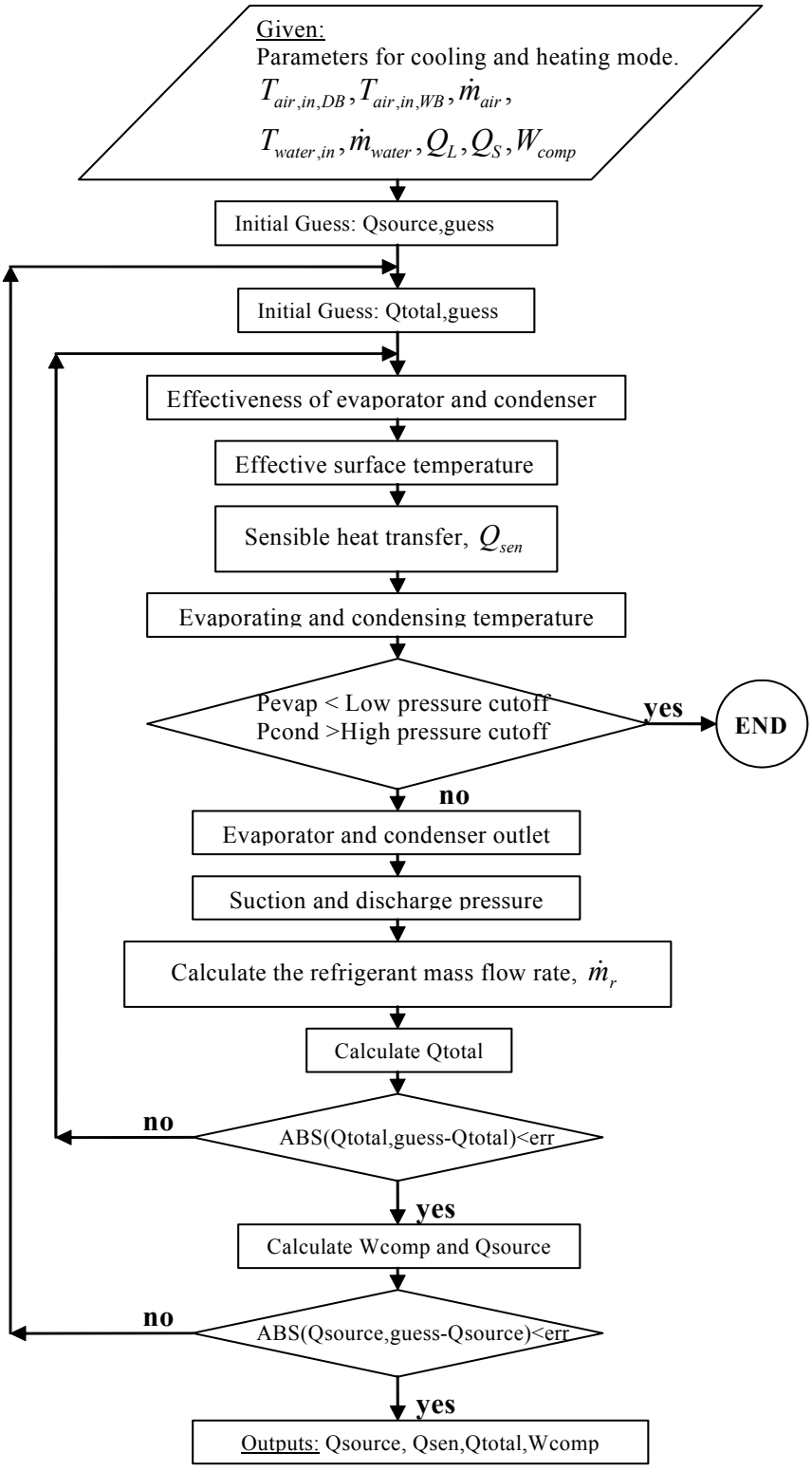

Figure 4.7: Flow Diagram for Parameter Estimation Based Water-to-Air Heat Pump Model, Jin(2002)

High pressure cutoff and low pressure cutoff is the maximum allowable condenser pressure and minimum allowable evaporator pressure. These two parameters are required to increase the robustness of the program for extreme operating conditions. EnergyPlus uses successive substitution with lagging to converge on the system, zone and plant. The inlet flow rates and inlet temperatures to the heat pump model vary every iteration until convergence is achieved. Thus the heat pump model might attempt to use physically unrealistic values which will results in unrealistic results or errors in the refrigerant properties. Physical heat pumps in the industry also possess this safety measure to protect the heat pump from overly high or low operating pressure. If the maximum allowable condenser pressure or minimum allowable evaporator pressure is exceeded, the heat pump model will be shut off and the outlet conditions will be set equal to the inlet conditions.

4.2.4 Accounting for Fan Heat

The cooling capacity and heating capacity reported in the catalog data includes the contribution of heat from the indoor fan. Note that the total power input in the catalog data includes the fan power, W_{fan} and compressor power, W_{comp}. The manufacturers conduct the experiment in an enclosed chamber and assume no heat loss from the packaged heat pump. The heat balance equation reflected in the catalog data are as follows:

Cooling Capacity:

$$\left(Q_{TotalCool,coil} - Q_{fan,heat}\right) = Q_{source} - \left(W_{comp} + W_{fan}\right)$$

Heating Capacity:

$$\left(Q_{Heat,coil} + Q_{fan,heat}\right) = Q_{source} + \left(W_{comp} + W_{fan}\right)$$

All the fan power input, W_{fan} will eventually be converted to heat, $Q_{fan,heat}$ and reflected in the load side heat transfer rate. In reality, some fan and compressor shell energy will be lost to the environment. The compressor shell heat loss is about 10% of the compressor power input based on experiments conducted by other researchers and here at OSU. However, the amount of fan heat lost to the environment is usually negligible since the fan is mounted in the air stream. The manufacturers' experimental data balance of within 5% for the rating conditions.

Unfortunately, the fan power consumption is not reported in the manufacturer catalog data. This causes a problem for the parameter estimation based model because the model can only take account of the coil heat transfer. Besides that, the model can only model the compressor power input but the manufacturers provide the total power input which includes both the compressor and the fan power. Given the lack of information, contribution from the fan is included in the parameter calculation. Thus the model outputs reflect contributions from the fan in both the coil capacity and power consumption. The model works reasonably well but the model tends to show insensitivity in the power calculation beyond the catalog data range as discussed in Section 5.2.3.

4.3. Part-Load Latent Degradation Model

Khatar et al. (1985) investigated the effect of fan cycling on air conditioner latent load. They found that 19% of the moisture accumulated during the compressor “ON” cycle is re-evaporated back to the air stream during the compressor “OFF” cycle. In addition, they found that at low run time fractions, the moisture removal rate for fan “AUTO” mode is 2.5 times higher than for fan “CONTINUOUS” mode. However, at high run time fraction, the moisture removal for both fan modes is about the same. The table below shows the advantages and disadvantages of both fan control modes.

	Fan "ON" mode	Fan "AUTO" mode
Comfort	Air flow rate remains the same, provides some degree of comfort.	False thermostat reading due to pockets of warm air.
Fan Power	More fan power consumption.	Less fan power consumption.
Moisture Removal	During compressor "off" cycle, moisture from cooling coil and drain pan re-evaporate back to zone. Oversized system with high compressor cycling rate would cause humidity problem.	Moisture drains out. Oversized system with high compressor cycling rate would cause humidity problem.
Humidity Control	Harder to mantain. Condensed water evaporates back to air stream. Thermostat set to lower temperature to elminate extra humidity leads to more energy consumption.	Easier to mantain. Amount of condensed water re-evaporating back to air stream is minimal.
Sensible Cooling	Provides cooling when compressor cycles off. But more compressor work to bring the coil temperature back down when it cycles on.	No cooling or air flow when compressor cycles off.
Air Infiltration	Indoor air fan induced air infiltration.	Indoor air fan induced air infiltration is reduced.
Sound	Fan noise on all the time.	Fan noise switching on and off. May be disturbing.

Table 4.8: Comparison of Fan Mode Operating Mode

4.3.1 Model Development

In order to account for the moisture that is re-evaporated back into the air stream, Henderson and Rengarajan(1996) proposed a part-load latent degradation model for continuous fan mode. The model assumes that the cooling coil can only hold a certain amount of water and additional condensate will drain out once the maximum amount has been exceeded without any hysteresis effects from previous wetting, surface tension and surface dirt. Besides that, the latent capacity, total capacity and sensible capacity take the same amount of time to reach steady state, and thus havethe same time constant based on the single time constant model described in Section 2.3.1.

Figure 4.8 shows the phenomena of the moisture building up in the coil when the compressor turned on. The latent capacity response of the coil can be modeled by the single time constant method discussed in Section 2.3.1. The latent capacity at time, t is as follows:

$$Q_L(t) = Q_L\left(1 - e^{\frac{t}{\tau}}\right) \qquad (4.35)$$

where:

$Q_L(t)$ = latent capacity at t time, W

Q_L = steady-state latent capacity, W

τ = heat pump time constant, s

After the moisture had exceeded the maximum moisture holding capacity of the coil, M_o, condensates starts to drain from the coil. All the latent capacity of the coil from time t_0 onwards is considered to be useful. When the compressor cycle off, the moisture that is held in the coil, M_o is evaporated back into the air stream. If the off-time of the

compressor is long, the amount of moisture evaporated back into the air stream is equal to M_o.

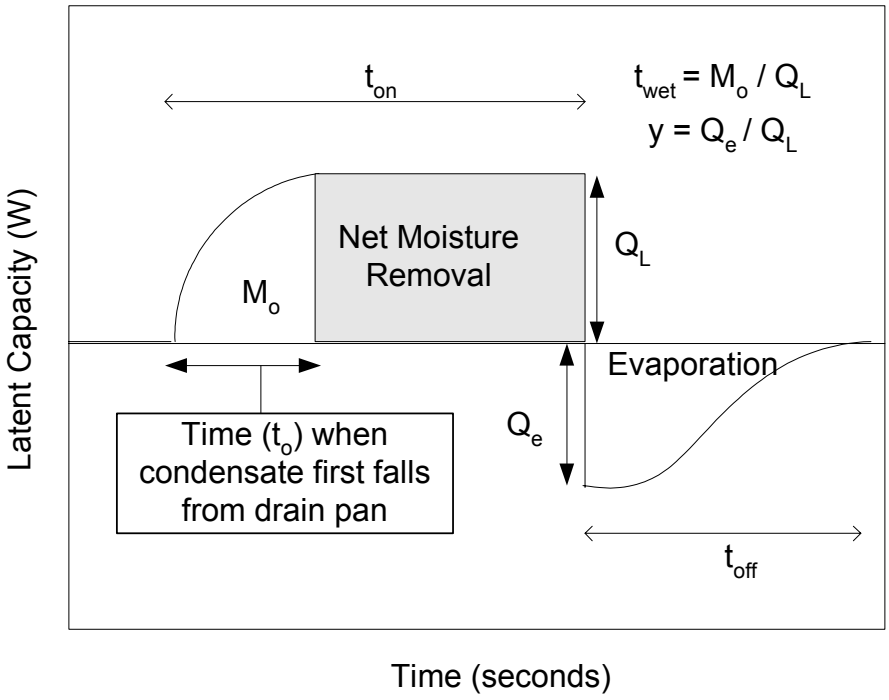

Figure 4.8: Concept of Moisture Buildup and Evaporation on Coil

Symbols used in Figure 4.8:

t_{on} = duration of time the compressor is on, s

t_{off} = duration of time the compressor is off, s

Q_L = steady-state latent capacity, W

Q_e = initial evaporation rate after compressor shut off, W

M_o = maximum moisture holding capacity of the coil, J

t_0 = time when condensate first falls from the drain pan, s

t_{wet} = the ratio of the moisture holding capacity of the coil, M_o to the steady-state latent capacity, Q_L, s

γ = the ratio of the initial evaporation rate, Q_e to the steady state latent capacity, Q_L

The model calculates the time t_0 to estimate the amount of useful moisture removal or effective latent capacity. The model uses two non-dimensionalized parameters t_{wet} and γ. Henderson and Rengarajan (1996) believe that the values for both parameters are similar for a large class of cooling coils with the same coil geometry and features. Henderson et.al (2003) conducted several test for different coil geometry at the nominal conditions of ASHRAE Test A conditions. From their study, they found that the mass of moisture retained in the coil is mostly a function of the coil surface geometry with some secondary dependence on the entering dew point and face velocity. On the other hand, the moisture evaporation rate during the off-cycle is function of the wet-bulb depression or the difference between the wet-bulb and dry-bulb temperatures of the entering air as follows:

$$Q_e = Q_{e,rated} \frac{(DB - WB)}{(DB_{rated} - WB_{rated})} \tag{4.36}$$

where:

Q_e = initial evaporation rate after compressor shut off, W

$Q_{e,rated}$ = initial evaporation rate after compressor shut off at nominal conditions, W

DB = inlet air dry-bulb temperature, °C

WB = inlet air wet-bulb temperature, °C

DB_{rated} = rated inlet air dry-bulb temperature, 26.7°C

WB_{rated} = rated inlet air wet-bulb temperature, 19.4°C

Since the parameters are similar for the same coil geometry, the parameters can be calculated by adjusting the parameters γ_{rated} and $t_{wet,rated}$ at the nominal conditions to the respective inlet air conditions as following:

$$t_{wet} = t_{wet,rated} \frac{Q_{L,rated}}{Q_L(DB,WB)} \tag{4.37}$$

$$\gamma = \gamma_{rated} \frac{(DB - WB)}{(DB_{rated} - WB_{rated})} \frac{Q_{L,rated}}{Q_L(DB,WB)} \tag{4.38}$$

where:

γ_{rated} = parameter γ at nominal conditions

$t_{wet,rated}$ = parameter t_{wet} at nominal conditions, s

$Q_{L,rated}$ = steady-state latent capacity at nominal conditions, W

$Q_L(DB,WB)$ = steady-state latent capacity at actual operating conditions, W

Three possible evaporation models were proposed which are exponential decay, linear decay, and constant evaporation. Henderson and Rengarajan (1996) suggested that the linear decay model appears to be the most physically realistic during the off cycle and also results in "middle of the road" performance. Based on recommendations by the researchers, the linear decay evaporation model shown in Figure 4.9 was selected for EnergyPlus.

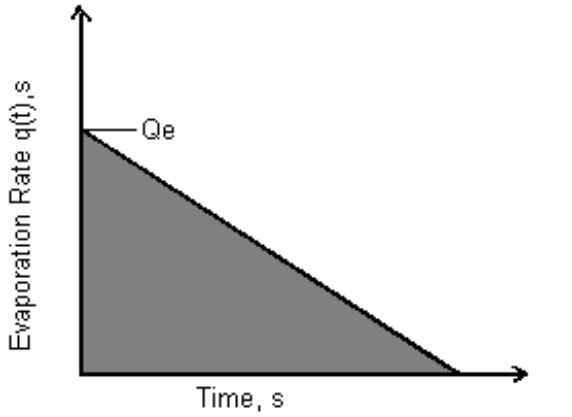

Figure 4.9: Linear Decay Evaporation Model

The linear decay evaporation model assumes that the wetted surface area decreases with the amount of water left on the coil. The evaporation rate, $q(t)$ at time, t is shown below:

$$q(t) = Q_e - \left(\frac{Q_e^{\,2}}{2M_o} \right) t \qquad (4.39)$$

where:

$q(t)$ = evaporation rate at time, t , W

The amount of moisture evaporated from the coil, $M(t)$ can be calculated by taking the integral of the evaporation rate, $q(t)$ as following;

$$M(t) = \int_0^t q(t)\, dt = Q_e t - \left(\frac{Q_e^{\,2}}{4M_o} \right) t^2, \; t \le \frac{M_o}{Q_e} \qquad (4.40)$$

The maximum moisture holding capacity of the coil, M_o before condensate removal begins at time, $t = t_0$, is equal to the amount of moisture remaining in the coil

when the compressor is first activated, M_i and the addition of moisture to the coil from time, $t = 0$ to $t = t_0$. The amount of moisture added to the coil from time, $t = 0$ to $t = t_0$ can be calculated by taking the integral of the heat pump latent capacity response given in Equation (4.35). Equation (4.41a) and Equation (4.41b) below shows the derivation of the maximum moisture holding capacity of the coil, M_o.

$$M_o = M_i + \int_0^{t_o} Q_L \left(1 - e^{\frac{t}{\tau}}\right) dt \tag{4.41a}$$

$$M_o = M_i + Q_L \left(t_o + \tau \left(e^{-\frac{t_o}{\tau}} - 1\right)\right) \tag{4.41b}$$

where:

M_i = amount of moisture remaining in the coil when the compressor is first activated, J

t_0 = time when condensate first falls from the drain pan, s

The amount of moisture remaining in the coil when the compressor is first activated, M_i is calculated by deducting the amount of moisture evaporated from the coil during the off-cycle, $M\left(t_{off}\right)$ from the maximum moisture holding capacity of the coil, M_o. The amount of moisture evaporated from the coil back into the air stream can be calculated from Equation (4.40). Equation (4.42a) and Equation (4.42b) below shows the derivation for the amount of moisture remaining in the coil when the compressor is first activated, M_i

$$M_i = M_o - M\left(t_{off}\right) \tag{4.42a}$$

$$M_i = M_o - Q_e t_{off} + \left(\frac{Q_e^{\,2}}{4M_o}\right) t_{off}^{\,2},\ t_{off} \le \frac{M_o}{Q_e} \tag{4.42b}$$

$M\left(t_{off}\right)$ = amount of moisture evaporated from the coil during the off-cycle, J

t_{off} = duration of time the compressor is off, s

The duration of the compressor on-time, t_{on} and off-time, t_{off} can be calculated from the heat pump cycling rate, $N_{\max}$ and the run-time fraction, X. The part-load fraction model discussed in Section 2.3.2 is employed to calculate the run-time fraction, X. Parameters $N_{\max}$ and τ can be obtained from the recommended values in Table 2.1. The compressor on-time, t_{on} and off-time, t_{off} are calculated as follows:

$$t_{on} = \frac{1}{4N_{\max}\left(1-X\right)} \tag{4.43}$$

$$t_{off} = \frac{1}{4N_{\max}\left(X\right)} \tag{4.44}$$

where:

t_{on} = duration of time the compressor is on, s

t_{off} = duration of time the compressor is off, s

$N_{\max}$ = heat pump cycling rates, cycles/s

X = compressor run-time fraction

By equating Equation (4.41b) and Equation (4.42b), M_i and M_o are eliminated and the value t_o can be computed as follows:

$$t_o^{\,j+1} = \frac{1}{Q_L}\left(Q_e t_{off} - \frac{Q_e^{\,2}}{4M_o} t_{off}^{\,2}\right) - \tau\left(e^{-\frac{t_o^{\,j}}{\tau}} - 1\right),\ t_{off} \le \frac{2M_o}{Q_e} \tag{4.45}$$

The time when condensate removal starts is at t_0 and it is determined by successive substitution, where ${t_0}^j$ is used to calculate ${t_0}^{j+1}$. Substituting the two non-dimensionalized parameters t_{wet} and γ into Equation (4.45) resulting in Equation (4.46)

$$ {t_0}^{j+1} = \gamma t_{off} - \left\{ \frac{\gamma^2}{4t_{wet}} \right\} {t_{off}}^2 - \tau \left(e^{-\frac{{t_0}^j}{\tau}} - 1 \right), \quad t_{off} \le \frac{2t_{wet}}{\gamma^2} \tag{4.46} $$

By knowing t_0, the net amount of moisture removal for each cycle indicated by the shaded area in Figure 4.8 is given below:

$$ q_L = Q_L \left(t_{on} - t_0 \right) \tag{4.47} $$

where:

q_L = net amount of moisture removal for each cycle, J

Q_L = steady-state latent capacity, W

t_{on} = duration of time the compressor is on, s

t_0 = time for condensate removal to begin, s

The equation above only applies for $t_{on} > t_0$ or the net latent capacity is zero. With the assumption that the time constant (τ) is similar for total, latent and sensible capacity, the integrated total capacity for each on-cycle is given by:

$$ q_T = \int_0^{t_{on}} Q_S \left(1 - e^{-\frac{t}{\tau}} \right) dt + \int_0^{t_{on}} Q_L \left(1 - e^{-\frac{t}{\tau}} \right) dt \tag{4.48a} $$

$$ q_T = \left(Q_S + Q_L \right) \left(t_{on} + \tau \left(e^{-\frac{t_{on}}{\tau}} - 1 \right) \right) \tag{4.48b} $$

where:

q_L = integrated total capacity for each on-cycle, J

Q_L = steady-state latent capacity, W

Q_S = steady-state sensible capacity, W

Thus rearranging Equation(4.45) and Equation(4.48b), the latent heat ratio for each cycle can be determined as following:

$$LHR_{eff} = \frac{q_L}{q_T} = \left\{ \frac{Q_L}{Q_L + Q_S} \right\} \frac{\left| t_{on} - t_0 \right|^+}{\left(t_{on} + \tau \left(e^{-\frac{t_{on}}{\tau}} - 1 \right) \right)} \tag{4.49a}$$

$$\frac{LHR_{eff}}{LHR_{ss}} = \frac{\left| t_{on} - t_0 \right|^+}{\left(t_{on} + \tau \left(e^{-\frac{t_{on}}{\tau}} - 1 \right) \right)} \tag{4.49b}$$

where:

LHR_{eff} = effective latent heat ratio due to cycling

LHR_{ss} = steady-state latent heat ratio

$\left| t_{on} - t_0 \right|^+$ indicates that the equation is only valid if $t_{on} > t_0$. For cases where $t_{on} < t_0$, the effective latent heat ratio at part-load is equal to zero because the amount of moisture in the coil did not reach the maximum moisture holding capacity of the coil, M_o thus no moisture is drained from the coil. From their sensitivity analysis, the LHR function is affected the most by t_{wet} and $N_{\max}$. The effect of γ is reduced at lower runtime fraction because the evaporation is completed before the end of the off cycle. The heat pump time constant, τ has little effect on the LHR function.

4.3.2 Modification of Part-Load Latent Degradation Model for Cycling Fan

For cycling fan operation or fan "AUTO" mode, the heat pump control has a built in delay time for the evaporator fan to shut off after the compressor cycles off. Fan time delay is preprogrammed into the heat pump control to save energy by extracting sensible heat from the cool coil after the compressor has shut off. Although fan delay allows more sensible heat transfer, it is at the expense of the fan power and latent heat transfer. The built in time delay for the fan can usually be obtained from the heat pump manual. For example, the fan time delay for the 3-ton York heat pump in the OSU laboratory is 60 secs.

The model proposed by Henderson and Rengarajan (1996) is based on continuous fan operation with evaporation of moisture from the coil taking place for the entire compressor off cycle period, t_{off}. The amount of moisture that evaporates from the coil back to the air stream is calculated by taking the integral of the evaporation rate over the entire off-time, t_{off} shown in Equation (4.40).

For cycling fan operation or fan AUTO mode, EnergyPlus assumes that there is no evaporation of the moisture back to air stream, thus $LHR_{eff} = LHR_{ss}$. This can be a source of error since moisture is evaporated back to the air stream both by natural convection during the entire heat pump off cycle period and forced convection during the fan time delay period. In cycling fan operation, forced evaporation from the coil can be accounted for by applying the fan delay time, $t_{fandelay}$ to the model proposed by Henderson and Rengarajan (1996).

By assuming that there is no evaporation of moisture from the coil by natural convection, the amount of moisture evaporated back to the air stream is calculated by taking the integral of the evaporation rate over the fan delay time, $t_{fandelay}$.

$$\int_0^{t_{fandelay}} q(t)dt = M\left(t_{fandelay}\right) \qquad (4.50)$$

The steps required to calculate the LHR ratio is similar to Henderson and Rengarajan (1996) with the exception that off-time, t_{off} in all the equations is replaced the fan delay time, $t_{fandelay}$. Equation (4.46), which calculates the time when condensate removal starts is altered to the following form:

$$t_0^{\,j+1} = \gamma t_{fandelay} - \left\{\frac{\gamma^2}{4t_{wet}}\right\} t_{fandelay}^{\,2} - \tau\left(e^{-\frac{t_0^{\,j}}{\tau}} - 1\right), \quad t_{fandelay} \le \frac{2t_{wet}}{\gamma^2} \qquad (4.51)$$

Using the $t_{fandelay}$ instead of t_{off}, will results in a smaller value of t_0, thus the net amount of moisture removed from the coil will be more as shown in Equation (4.47). With the increase in the latent heat ratio, the effective sensible heat ratio will be less for AUTO fan mode compared to constant fan operation.

4.3.3 Model Implementation

The model requires parameters such as the heat pump maximum cycling rate, ($N_{\max}$), the heat pump time constant,(τ), the ratio of the initial evaporation rate and the steady-state latent capacity at rated conditions,(γ_{rated}), the ratio of the moisture holding capacity of the coil to the steady state latent capacity at rated conditions ($t_{wet,rated}$) and the

fan delay time, ($t_{fandelay}$). The calculation process for the Latent Degradation Model is summarized below:

1. First, the part-load fraction model discussed in Section 2.3.2 is used to calculate the runtime fraction, X based on the heat pump part-load ratio.
2. Run the heat pump simulation at rated conditions (26.7°C dry-bulb, 19.4°C wet-bulb) to obtain $Q_{L,rated}$. Then run the heat pump simulation again with the actual operating conditions to obtain Q_L and LHR_{ss}.
3. Calculate the compressor off cycle period, t_{off} and on cycle period, t_{on} using the heat pump cycling rate, $N_{\max}$ and runtime fraction, X as shown in Equation (4.43) and Equation (4.44).
4. Adjust the parameters γ_{rated} and $t_{wet,rated}$ according to the inlet dry-bulb and wet-bulb temperatures using Equation (4.37) and Equation (4.38).
5. Calculate the time when condensate removal starts, t_0 from Equation (4.46) or Equation (4.51) depending on the fan operation mode using successive substitution method.
6. Use Equation (4.49b) to calculate the ratio of cyclic latent heat ratio to the steady-state heat ratio, $\frac{LHR_{eff}}{LHR_{ss}}$.
7. Calculate the effective sensible heat ratio, SHR_{eff} by adjusting the steady-state sensible heat ratio, SHR_{ss} as following:

$$SHR_{eff} = 1.0 - LHR_{ss}\frac{LHR_{eff}}{LHR_{ss}} \quad (4.30)$$

The flow diagram in Figure 4.10 summarizes the parameters, inputs and outputs of the model. Figure 4.11 shows the interaction between the water-to-air heat pump model and the latent degradation model:

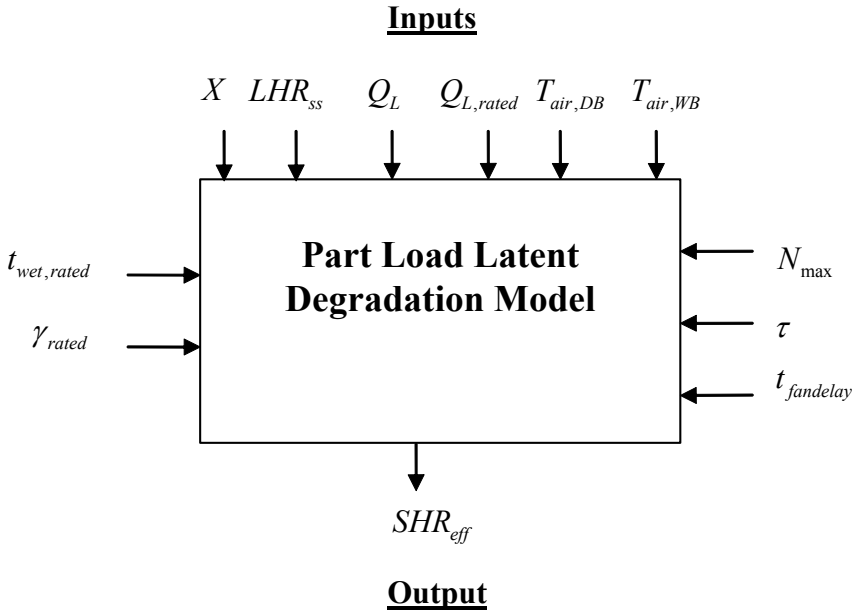

Figure 4.10: Information Flow Chart for Latent Degradation Model

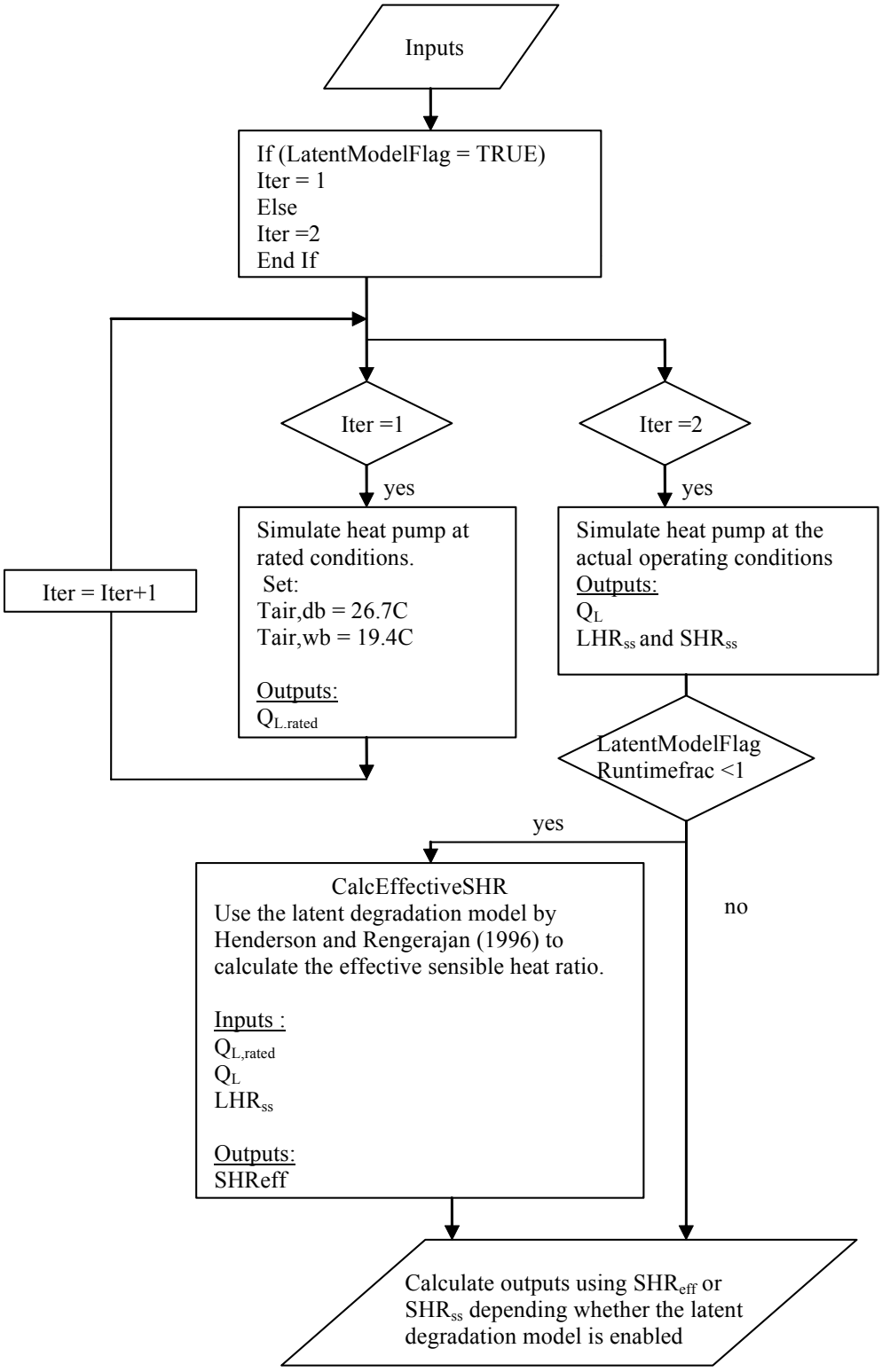

Figure 4.11: Interaction of the Latent Degradation Model with Water to Air Heat Pump Cooling Coil Subroutine

4.3.4 Model Sensitivity Analysis

The latent degradation model calculates the sensible heat ratio as a function of the runtime fraction, X. The model requires five parameters: $N_{\max}, \tau, \gamma, t_{wet}$ and $t_{fandelay}$. The base case parameters used for the model sensitivity analysis are shown in Table 4.9.

Parameter	Value
Evaporation Model	Linear Decay
$N_{\max}$	2.5 cycles/hr
τ	60s
Fraction of on-cycle power use,pr	0.01
γ	0.6
t_{wet}	1200s
$t_{fandelay}$	60s

Table 4.9: Base Parameter Values for Model Sensitivity Analysis

The linear decay evaporation proposed by Henderson and Rengarajan (1996) is used and the heat pump is assumed to be a "typical" heat pump using the parameters recommended by Henderson et al. (1999) as shown in Table 2.1. The base value for parameter t_{wet} is assumed to be 1200 seconds based on the study by Henderson et al. (2003). Note that the base parameter values are different from the values used by Henderson and Rengarajan (1996) in their model sensitivity analysis.

For continuous fan mode, Figure 4.12 shows that the parameter t_{wet} has a small effect on the LHR ratios at higher runtime fractions. A higher t_{wet} results in lower LHR ratios which is significant at lower runtime fractions. Higher t_{wet} simply means that it takes longer to reach the maximum moisture holding capacity of the coil before draining of the condensates begins. This results in less effective moisture removal. At runtime

fractions of less than 0.3, the latent capacity of the coil is zero because all of the moisture that condenses on the coil is evaporated back into the air stream.

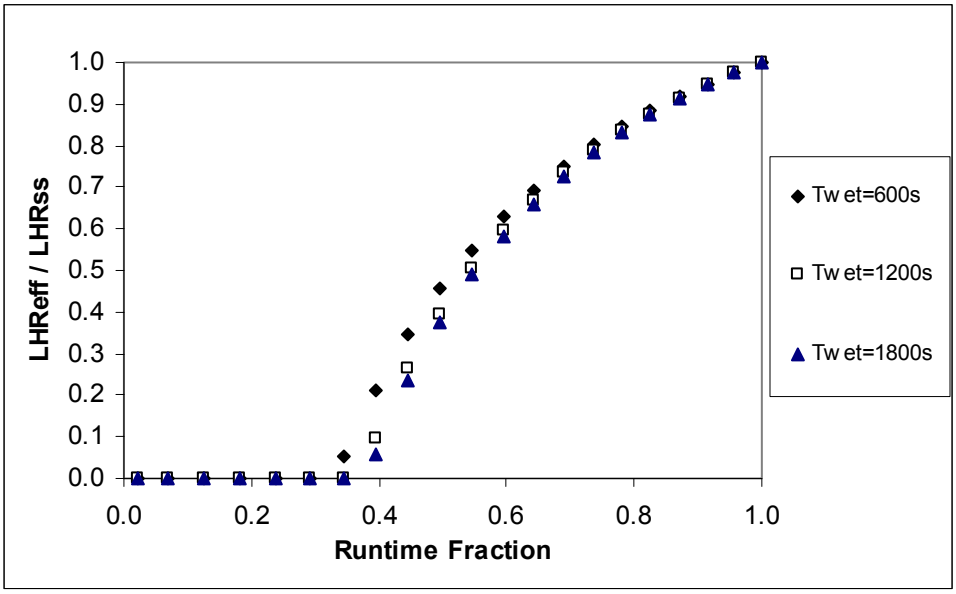

Figure 4.12: Sensitivity of Part-Load Latent Degradation Model to t_{wet} for Continuous Fan

For cycling fan mode, Figure 4.13 shows that t_{wet} does not have a significant effect on LHR ratios. The dominate parameter is t_{off} or $t_{fandelay}$ for cycling fan mode. Regardless of the runtime fraction, the off-cycle period of the heat pump is fixed at 60s by the fan time delay, $t_{fandelay}$ which only allows evaporation of moisture back to the air stream for a small period of time.

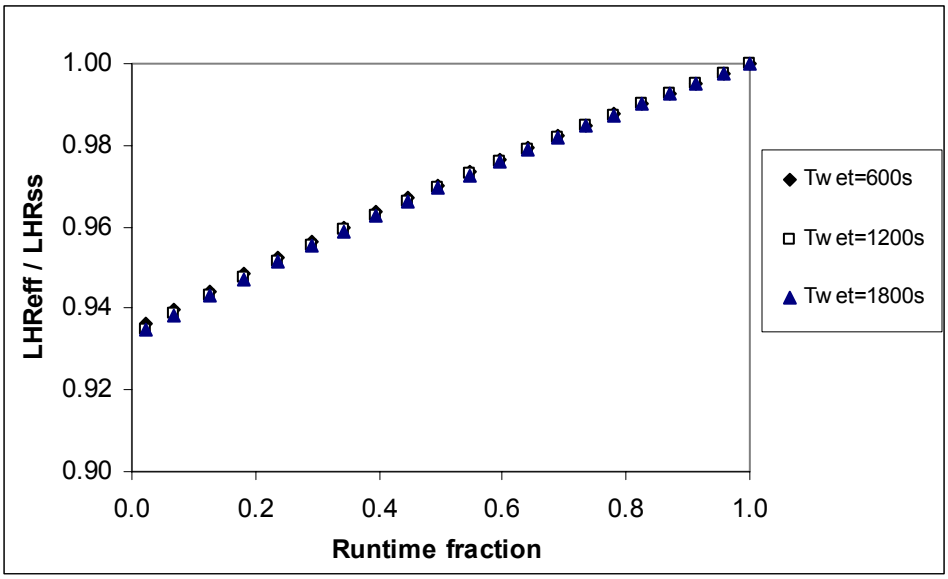

Figure 4.13: Sensitivity of Part-Load Latent Degradation Model to t_{wet} for Cycling Fan

The effect of the fan time delay, $t_{fandelay}$ is shown in Figure 4.14. For cycling fan mode, longer $t_{fandelay}$ allows more extraction of sensible heat from the coil but at the expense of a reduction in moisture removal. Figure 4.14 shows that $t_{fandelay}$ of 30s allow no re-evaporation of moisture from the coil and the latent capacity at part-load conditions is equal to the latent capacity at steady state conditions. By using the model, an economic analysis can be easily done to determine the optimal value of $t_{fandelay}$ for the heat pump control.

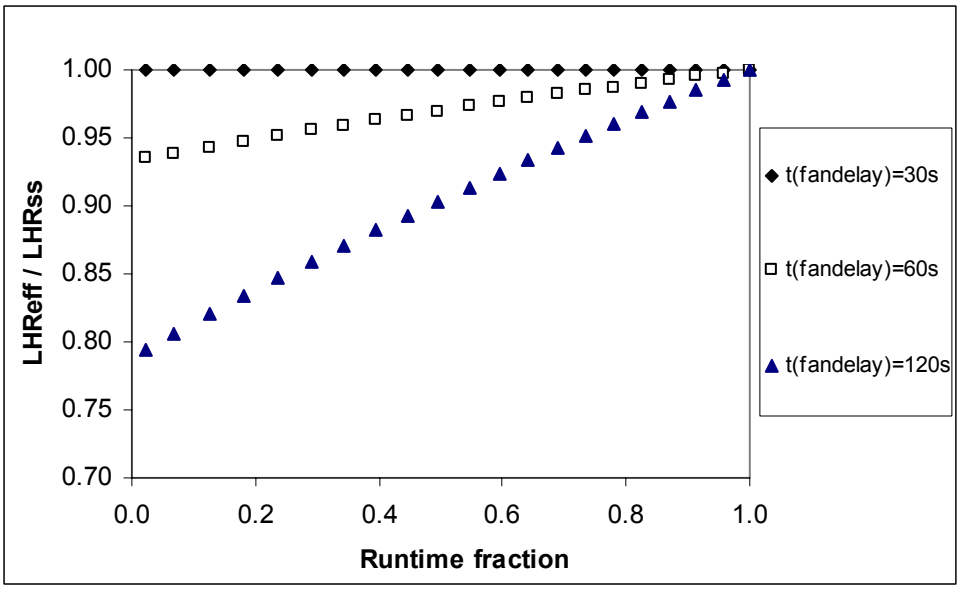

Figure 4.14: Sensitivity of Part-Load Latent Degradation Model to $t_{fandelay}$ for Cycling Fan

For continuous and cycling fan modes, Figure 4.15 and Figure 4.16 both show that γ has a significant impact on the latent capacity of the heat pump at part-load conditions. The parameter γ is the ratio of the initial evaporation rate to the steady state latent capacity. Higher initial evaporation rate allows more moisture being evaporated back to the air stream for a given off-cycle period, t_{off}.

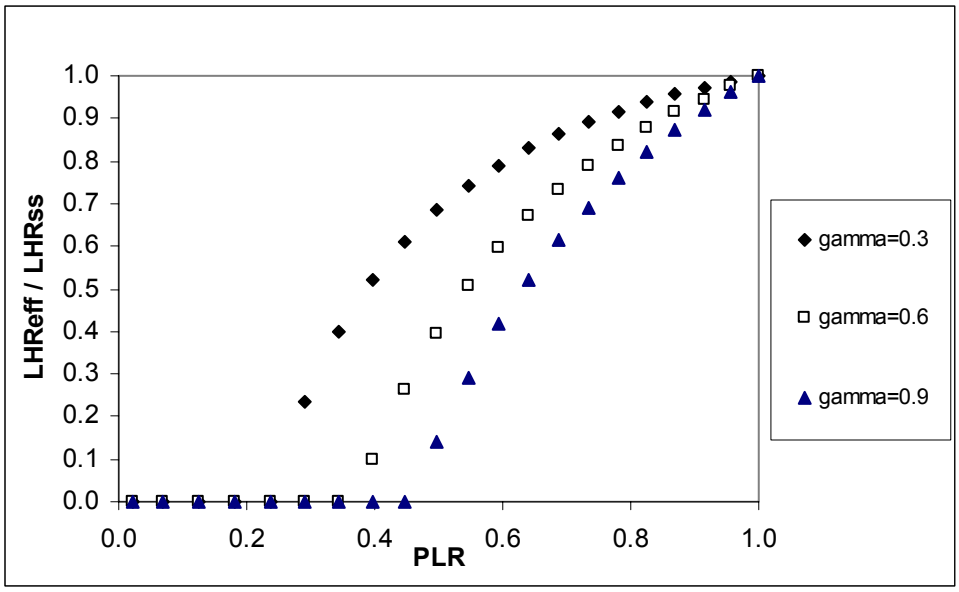

Figure 4.15: Sensitivity of Part-Load Latent Degradation Model to γ for Continuous Fan

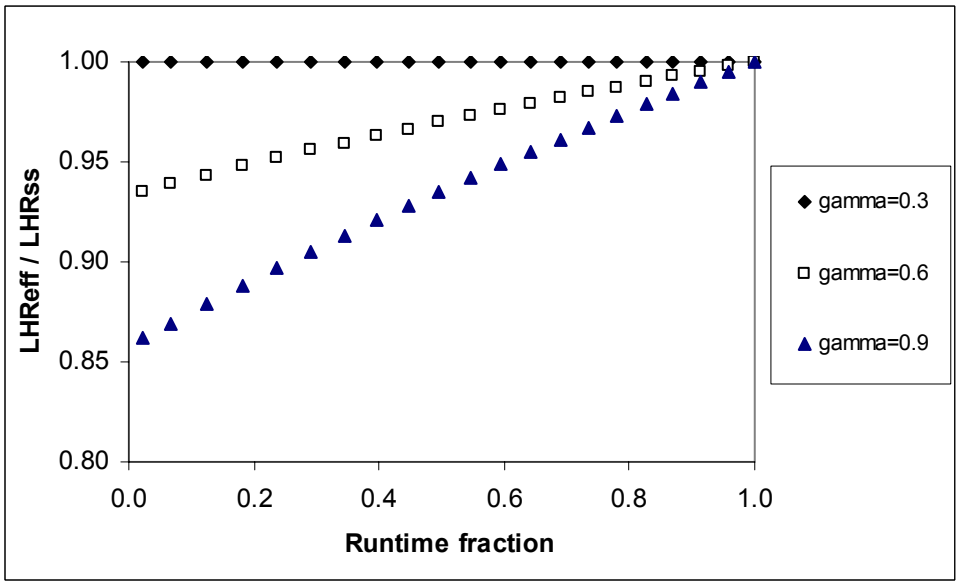

Figure 4.16: Sensitivity of Part-Load Latent Degradation Model to γ for Cycling Fan

4.4. Curve-Fit Water-Water Heat Pump Model

As shown in Table 4.1, no curve-fit model for water-water heat pump has been developed. The current model implemented in EnergyPlus is the parameter estimation based model developed by Jin (2002). A simple water-to-water curve-fit model that is similar to the simple water-to-air curve-fit model will be a useful addition to the EnergyPlus heat pump models. The curve-fit model will allow users to conduct a quick simulation of the water-to-water heat pump without the drawbacks associated with the more computationally expensive parameter estimation based model.

4.4.1 Model Development

The same methodology used to develop the curve-fit water-to-air heat pump is employed in developing this model. The methodology involved using the generalized least square method to generate a set of performance coefficients from the catalog data at indicated reference conditions. Then the respective coefficients and indicated reference conditions are used in the model to simulate the heat pump performance.

The water-to-water heat pump model should be less complex than the water-to-air heat pump model since no sensible and latent load split is required. The variables that influenced the water-to-water heat pump performance are load side inlet water temperature, source side inlet temperature, source side water flow rate and load side water flow rate. The governing equations are formulated in an organized fashion whereby the heat pump input variables are divided by the reference values. The governing equations for the cooling and heating mode are as following:

Cooling Mode:

$$\frac{Q_c}{Q_{c,ref}} = A1 + A2\left[\frac{T_{L,in}}{T_{ref}}\right] + A3\left[\frac{T_{S,in}}{T_{ref}}\right] + A4\left[\frac{\dot{V}_L}{\dot{V}_{L,ref}}\right] + A5\left[\frac{\dot{V}_S}{\dot{V}_{S,ref}}\right] \tag{4.7}$$

$$\frac{Power_c}{Power_{c,ref}} = B1 + B2\left[\frac{T_{L,in}}{T_{ref}}\right] + B3\left[\frac{T_{S,in}}{T_{ref}}\right] + B4\left[\frac{\dot{V}_L}{\dot{V}_{L,ref}}\right] + B5\left[\frac{\dot{V}_S}{\dot{V}_{S,ref}}\right] \tag{4.9}$$

$$\frac{Q_{source,c}}{Q_{source,c,ref}} = C1 + C2\left[\frac{T_{L,in}}{T_{ref}}\right] + C3\left[\frac{T_{S,in}}{T_{ref}}\right] + C4\left[\frac{\dot{V}_L}{\dot{V}_{L,ref}}\right] + C5\left[\frac{\dot{V}_S}{\dot{V}_{S,ref}}\right] \tag{4.10}$$

Heating Mode:

$$\frac{Q_h}{Q_{h,ref}} = D1 + D2\left[\frac{T_{L,in}}{T_{ref}}\right] + D3\left[\frac{T_{S,in}}{T_{ref}}\right] + D4\left[\frac{\dot{V}_L}{\dot{V}_{L,ref}}\right] + D5\left[\frac{\dot{V}_S}{\dot{V}_{S,ref}}\right] \tag{4.11}$$

$$\frac{Power_h}{Power_{h,ref}} = E1 + E2\left[\frac{T_{L,in}}{T_{ref}}\right] + E3\left[\frac{T_{S,in}}{T_{ref}}\right] + E4\left[\frac{\dot{V}_L}{\dot{V}_{L,ref}}\right] + E5\left[\frac{\dot{V}_S}{\dot{V}_{S,ref}}\right] \tag{4.12}$$

$$\frac{Q_{source,c}}{Q_{source,c,ref}} = F1 + F2\left[\frac{T_{L,in}}{T_{ref}}\right] + F3\left[\frac{T_{S,in}}{T_{ref}}\right] + F4\left[\frac{\dot{V}_L}{\dot{V}_{L,ref}}\right] + F5\left[\frac{\dot{V}_S}{\dot{V}_{S,ref}}\right] \tag{4.13}$$

The reference conditions indicated in the governing equations are important issues that need to be considered carefully. The reference conditions used when generating the performance coefficients must be the same as the reference conditions used later in the model. The reference temperature T_{ref} is fixed at 283K. Temperature unit of Kelvin is used instead of Celsius to keep the ratio of the water inlet temperature and reference temperature positive value should the water inlet temperature drop below the freezing point. For cooling mode, the reference conditions; reference load side volumetric flow rate, $\dot{V}_{L,ref}$,reference source side volumetric flow rate, $\dot{V}_{S,ref}$, reference power input, $Power_{c,ref}$ and reference source side heat transfer rate, $Q_{source,c,ref}$ are the conditions

when the heat pump is operating at the highest cooling capacity or reference cooling capacity, $Q_{c,ref}$ indicated in the manufacturer's catalog. The same procedure is repeated for the heating mode but note that the reference conditions might differ from the reference conditions specified for the cooling mode.

An information flow chart showing the inputs, reference conditions, performance coefficients and outputs are shown in the figure below:

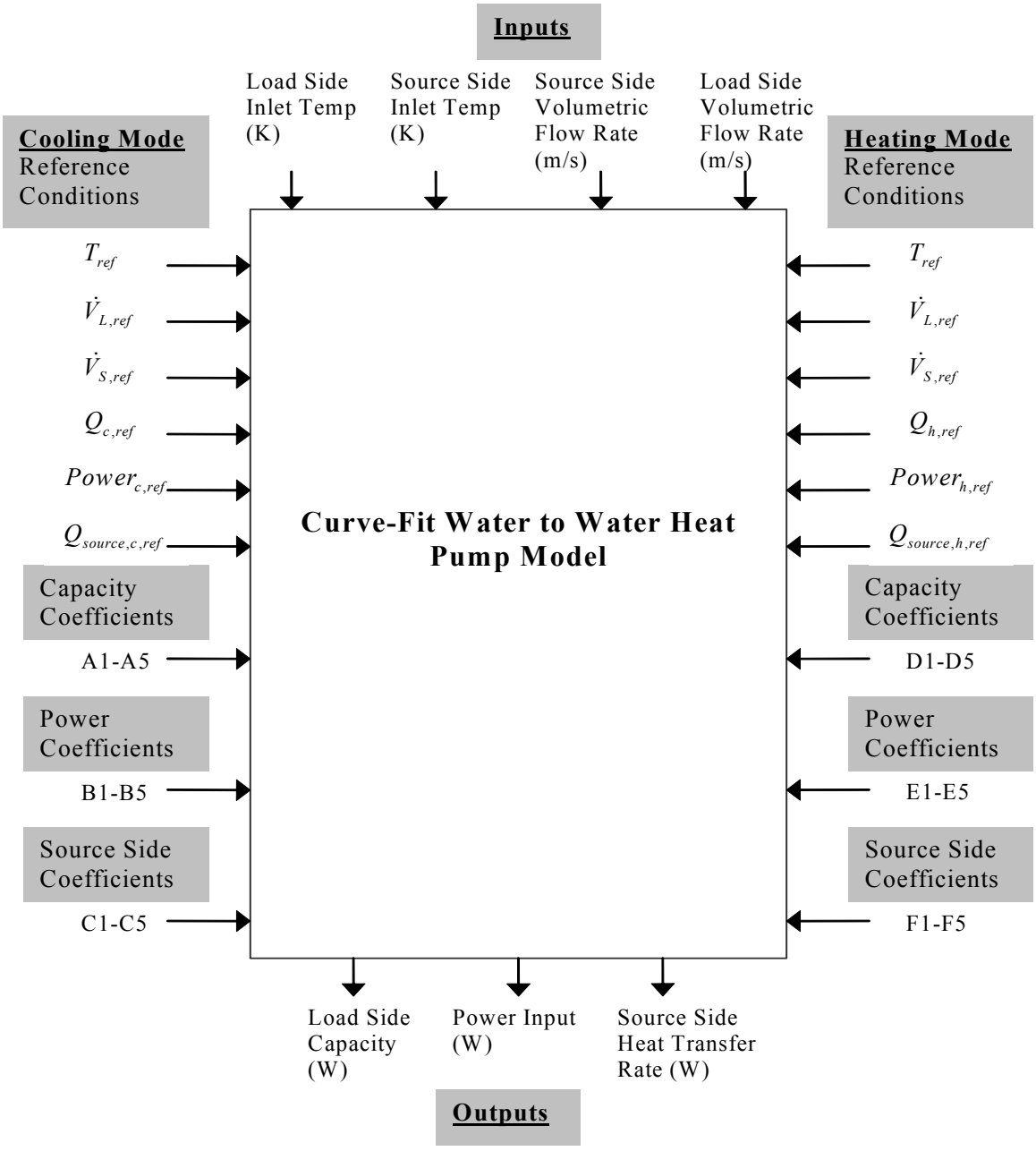

Figure 4.17: Information Flow Chart for Water-Water Heat Pump Simple

4.4.2 Model Implementation into EnergyPlus

The model implementation procedure in EnergyPlus is identical to the implementation of the parameter estimation based water-to-water heat pump by Muraggapan (2002). Assuming no losses, the source side heat transfer rate for cooling and heating mode is calculated as following;

$$Q_{source,c} = Q_c + Power_c \qquad (4.14)$$

$$Q_{source,h} = Q_h - Power_h \qquad (4.15)$$

Although there will be losses in reality, this approach is chosen so that the heat balance equation will always balanced out nicely which is also analogous to the catalog data. As mentioned earlier, the "balanced" heat balance equation will give a sense of assurance to the user that the heat pump model is working "properly". For research purposes, it is certainly more advisable to simulate the source side heat transfer rate using another curve which will yield higher accuracy and more flexibility as well.

The control strategy for the heat pump model is adopted from Muraggapan (2002) which uses the "cycle time control logic". This strategy keeps the heat pump from short-cycling whereby the heat pump will stay on or off for the specified cycle time after switching states. The control logic is identical to the operation of a physical heat pump whereby the heat pump does not switch between on and off instantly. Refer to Muraggapan (2002) for the further details on the control strategy and implementation procedure.

5.0 Validation of the Heat Pump Models

The EnergyPlus air-to-air and water-to-air heat pump models are validated using measured data from the OSU test loop and the manufacturer's test facility. For the water-to-water heat pump models, the proposed curve-fit model is verified by comparison with the parameter estimation based model developed by Jin (2002). The approach of this study is to use the models as would any EnergyPlus user without any information other than heat pump catalog data. Descriptions of the procedure used to generate the coefficients and parameters for each model are shown in Appendix A, B, C and D. The uncertainties associated with each model are investigated and quantified.

5.1. Steady-State Air-to-Air Heat Pump Model Validation

The EnergyPlus curve-fit air-to-air heat pump is validated using experimental data and compared to the detailed deterministic model by Iu et.al (2003). The experimental data for the cooling mode is obtained from the OSU heat pump test loop described in Weber (2003). Due to the limitations of the test rig, the experimental data for heating mode is obtained from the manufacturer's testing facility.

5.1.1 The Experimental Facility

The unitary heat pump installed in the OSU test loop has a capacity of 3-tons with R-22 as the working refrigerant. The unit has a scroll compressor and a short tube orifice as the expansion device. The ambient air on the condenser side is controlled with variable

capacity (up to 12KW) forced air heaters. The condenser side is partially enclosed to provide some control of the condenser inlet conditions. The air loop on the evaporator side is controlled using a variable electric heating coil (up to 15 KW), a humidifier, a constant centrifugal booster fan, and an elliptic nozzle for flow measurement. The air flow rate is adjusted by changing the fan pulley. Figure 5.1 shows the test rig with the locations of the temperature and pressure sensors.

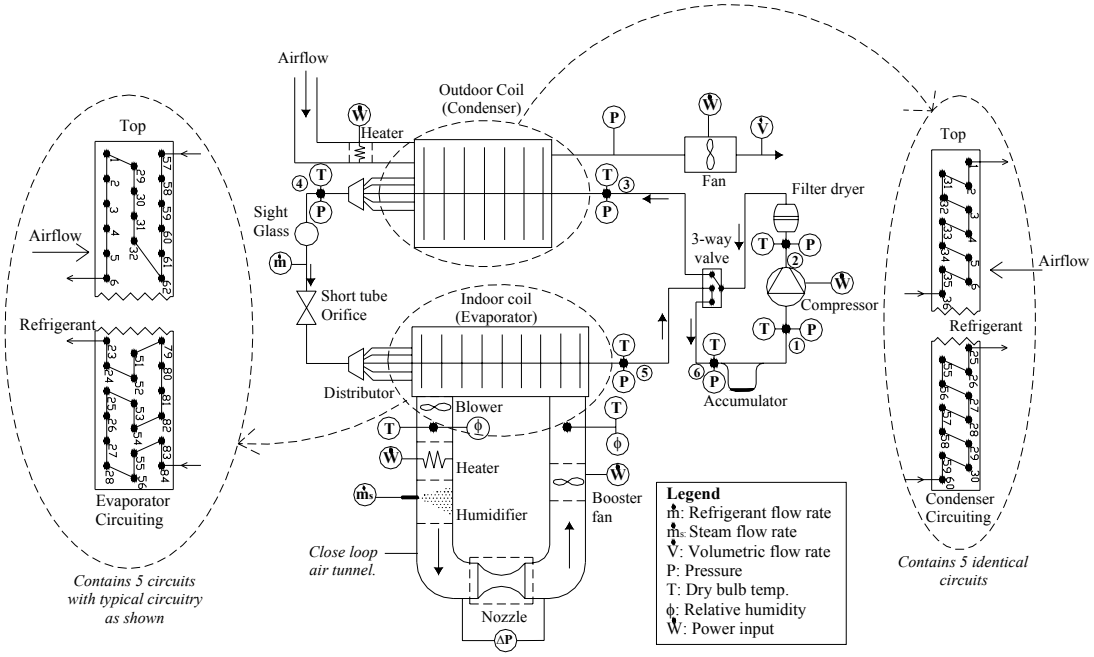

Figure 5.1: Schematic of the Test Loop, Iu et.al (2003) (Used with permission)

The uncertainties in the measurements are shown in Figure 5.2. Weber (2003) provides a detailed description of the instrumentation. The uncertainty for the evaporator and condenser capacities is calculated as $\pm 5\%$. The calculated compressor power uncertainty is $\pm 0.4\%$.

Location	Measurement	Instrument	Uncertainty
Refrigerant side	Temperature	T-type thermocouples	±0.1 °C
	Pressure	Pressure transducers	±4.5 kPa
	Mass flow rate	Coriolis flow meter	±0.5 $kg.hr^{-1}$
Indoor air side	Dry bulb temperature	T-type thermocouples	±0.1 °C
	Relative humidity	Solid state humidity sensor	±2% RH
	Volumetric flow rate	Nozzle and pressure transducer	±2 $m^3.min^{-1}$
Outdoor air side	Dry bulb temperature	T-type thermocouples	±0.1 °C
	Volumetric flow rate	Hot wire velocity transducer	±0.3 $m^3.min^{-1}$
Electric side	Current	Current transducer	±0.1 A
	Voltage	Voltage transducer	±0.8 VAC

Figure 5.2: Uncertainty for Measuring Device

5.1.2 Experimental Procedure

The ARI standard 210/240 (2003) was used as the guideline for the experimental procedure and test matrix. Due to the hardware limitation of the testing facility, the heating mode experimental data was obtained from the manufacturer's test rooms. The "A" Cooling Steady State, "B" Cooling Steady State, and Maximum Operating Condition test were conducted on this OSU rig. "A" Cooling Steady State was used as the baseline test with the following conditions:

- outdoor coil inlet air temperature of 35°C(95°F) dry bulb
- indoor coil inlet air temperatures of 26.7°C(80°F) dry bulb and 19.4°C(80°F) wet bulb (52% relative humidity)
- indoor coil air volumetric flow rate of 34 m^3min^{-1} (1200 CFM)
- outdoor coil air volumetric flow rate of 48.8 m^3min^{-1} (1700 CFM)

The heat pump performance is evaluated over a range of evaporator inlet air temperatures, condenser inlet air temperatures, and evaporator air flow rates. For each test, one parameter is varied from the baseline conditions and the heat pump performance at steady-state is evaluated. The test matrix for the cooling mode is shown in Figure 5.3:

Test	Description	Outdoor Coil Air Inlet Temp,°C (°F)	Indoor Coil Air Inlet Temp,°C (°F)	Indoor Coil Air Flow Rate, m^3/min (CFM)
1	Variation of outdoor temperature	27.7[C] (82)	26.7 (80)	35 (1200)
2		31.3 (88)		
3		35.0[A] (95)		
4		40.5 (105)		
5		46.2[B] (115)		
6	Variation of indoor temperature	35.0 (95)	20.7 (69)	35 (1200)
7			22.7 (73)	
8			24.7 (76)	
9			26.7[A] (80)	
10			28.7 (84)	
11	Variation of indoor air flow rate	35.0 (95)	26.7 (80)	22 (760)
12				27 (950)
13				31 (1090)
14				35[A] (1200)
15				38 (1330)

A -ARI "A" Cooling Steady State; B - ARI maximum operating conditions;
C - ARI "C" Cooling Steady State.

Figure 5.3: Experimental Test Matrix for Validation of Air-Air Heat Pump Models

5.1.3 Experimental Validation Results

Performance of two air-to-air heat pump models; the EnergyPlus curve-fit model and the detailed deterministic model by Iu et.al (2003) has been compared with measured experimental data. The accuracy of the curve-fit model is affected by two uncertainties: errors in the catalog data, and the model's ability to match the catalog data exactly. As mentioned by previous researchers and Jin (2002) and Shenoy(2004), the full set of catalog data is typically extrapolated from a small number of experimental points by the manufacturer. The errors are then indirectly propagated to the curve-fit model which uses the catalog data to generate the coefficients. In order to quantify the error associated with the two uncertainties, the data from the catalog is included in the figures. Data from the catalog was interpolated to match the experiment's boundary conditions. A few points are

omitted because the experimental boundary conditions are beyond the catalog data range. Appendix A shows the procedure for generating the coefficients for the EnergyPlus curve-fit air-to-air heat pump model. The performance of both heat pump models in cooling mode is shown in Figure 5.4 to Figure 5.6.

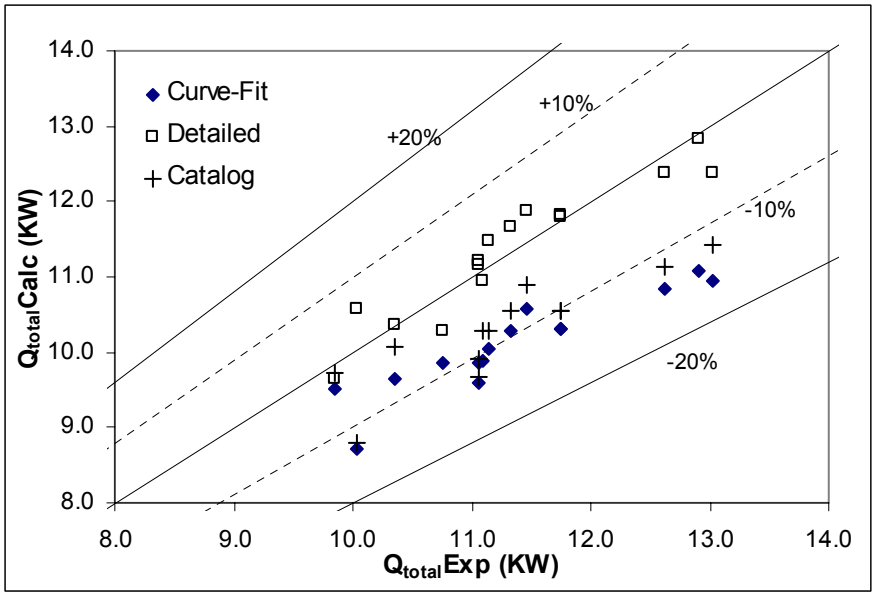

Figure 5.4: Validation of Curve-Fit Model and Detailed Model for Total Cooling Capacity (Cooling Mode)

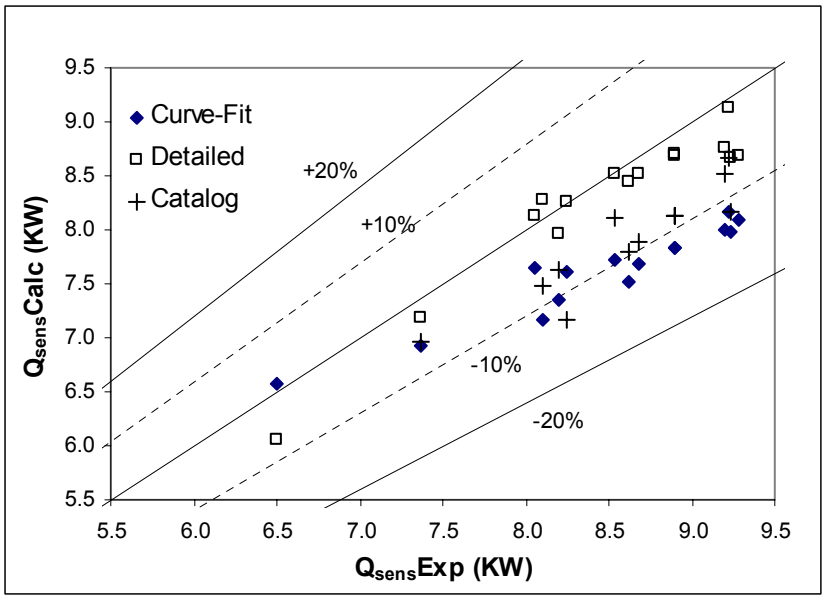

Figure 5.5: Validation of Curve-Fit Model and Detailed Model for Sensible Cooling Capacity (Cooling Mode)

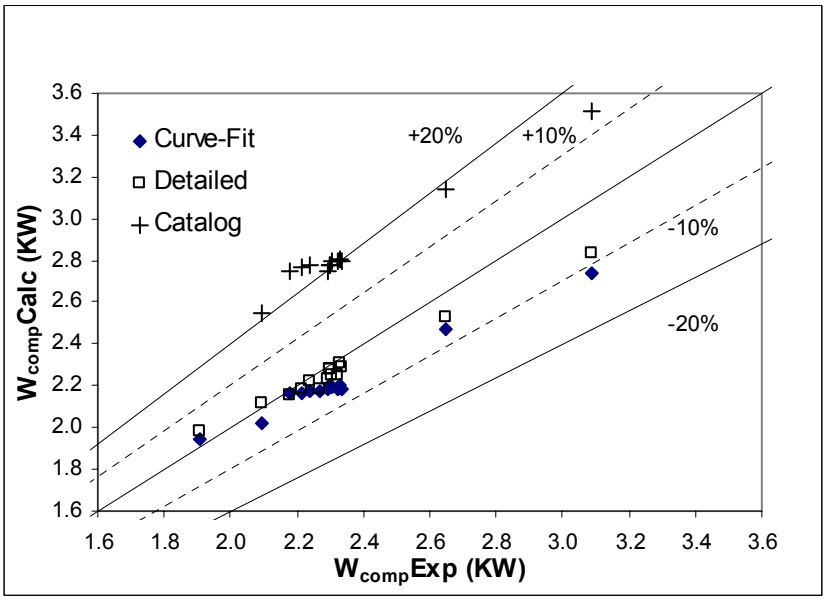

Figure 5.6: Validation of Curve-Fit Model and Detailed Model for Compressor Power (Cooling Mode)

In addition, Figure 5.7 and Figure 5.8 show the heat pump performance in heating mode.

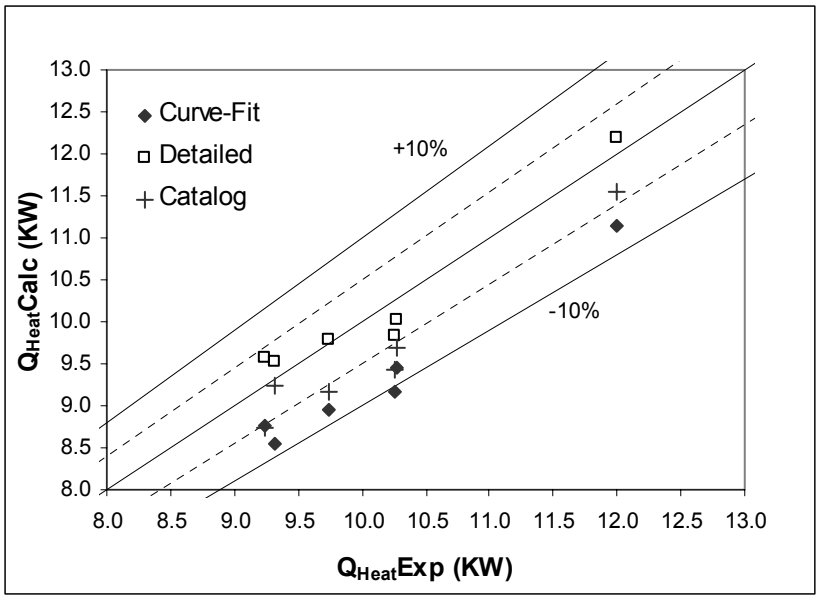

Figure 5.7: Validation of Curve-Fit Model and Detailed Model for Heating Capacity (Heating Mode)

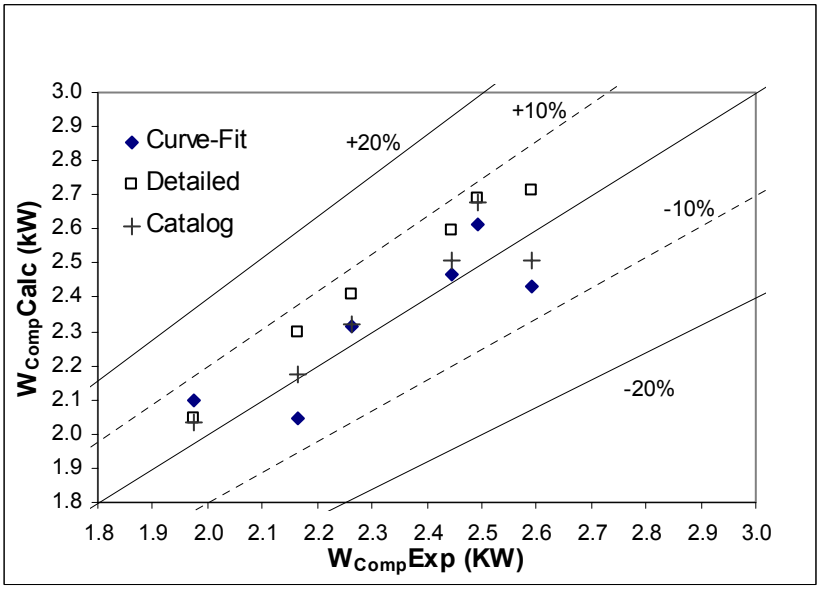

Figure 5.8: Validation of Curve-Fit Model and Detailed Model for Compressor Power (Heating Mode)

	%RMS error	
	Curve-Fit Model	Detailed Model
Total Cooling Capacity	11.29	2.76
Sensible Capacity	10.57	3.54
Cooling Compressor Power	5.22	3.21
Heating Capacity	8.02	2.67
Heating Compressor Power	4.77	5.96

Table 5.1: Percentage RMS error for Curve-Fit Model and Detailed Model

Table 5.1 summarizes the percentage RMS error for the detailed model and the curve-fit model in cooling and heating mode. The detailed deterministic model has a very high accuracy with RMS error of less than 6%. The experimental data for cooling mode is from the OSU test rig with 208VAC while the rating tests run by the manufacturer are at 230VAC. According the catalog data, the heat pump can operate on both line voltages 208/230 at frequency of 60Hz. The line voltage for OSU test rig is estimated to be 208 based on spot checks of the voltage readings which fall within the range of 203V to 210V.

An empirical correction factor of $\dot{W}_{208V} \cong \frac{\dot{W}_{230V}}{1.25}$ calculated by Iu et. al(2003) is used to correct for compressor power. The empirical correction factor is calculated by comparing the experimental data from the manufacturer and OSU test rig. Refer to Appendix A.3 for the adjustments made to the EnergyPlus outputs. In addition, the refrigerant charge used in the OSU test rig was 9.5 pounds while the manufacturer used 9 pounds. However, the effect is compensated for by the longer liquid line used to connect the refrigerant flow meter in the OSU test rig.

Due to different test configurations, Figure 5.4 and Figure 5.5 show that both the total and sensible capacities indicated in the catalog data are lower than the OSU experimental data. Thus the curve-fit model underestimated the measured total and sensible capacities, but the results are very close to the catalog data with an error of about 5%. The capacities shown in the catalog data are less than the measured data because the manufacturer conducted the rating test at higher voltage thus the compressor power is higher. With a higher compressor power, the condenser operating pressure is higher, thus resulting in a lower change in enthalpy on the evaporator side. Figure 5.6 shows that the compressor power for the curve-fit model closely matches the experimental results because the power correction factor was applied.

On the other hand, the curve-fit model performed better in heating mode than in cooling mode with reasonable a overall RMS error of less than 8%. This is attributed to the fact that both the catalog data and the measured data are from the manufacturer's test facility. For heating mode, the curve-fit model closely matches the catalog data with an error of about 5% as shown in Figure 5.7 and Figure 5.8. The differences between the catalog data and the measured data vary between 3% to 8% for both heating capacity and compressor power.

5.1.4 Investigation of Compressor Shell Heat Loss

In addition to the standard testing procedure, several tests are conducted to estimate the compressor shell heat loss that is neglected by the heat pump manufacturer when generating the catalog data. From this study, a better understanding is gained of the fraction of power supplied to the compressor that is lost to the surrounding. In brief, the experimental procedure is as follows;

1. Conduct the usual steady-state test for an uninsulated compressor under cooling mode using one of the conditions shown in Figure 5.3. Estimate the heat loss due to the refrigerant line and compressor shell,

$$Q_{Loss}(Uninsulated) = Q_{LineLoss} + Q_{ShellLoss} = Q_{EVP,1} + W_{COMP,1} - Q_{COND,1} \qquad (5.2)$$

2. Turn off the heat pump and allow the compressor to cool off. Then insulate the compressor with two layers of 1 inch insulation batt and conduct the experiment under the same operating conditions as Step 1. The heat loss from the compressor is assumed to be negligible. Find the refrigerant line loss as following;

$$Q_{Loss}(Insulated) = Q_{LineLoss} = Q_{EVP,2} + W_{COMP,2} - Q_{COND,2} \qquad (5.3)$$

3. Assuming that the refrigerant line loss is the same for the two experiments, the percentage of compressor shell heat loss is computed as following;

$$Q_{ShellLoss} = Q_{Loss}(Uninsulated) - Q_{Loss}(Insulated) \qquad (5.4)$$

$$\text{Percentage Shell Loss} = \frac{Q_{ShellLoss}}{0.5\left(W_{COMP,1} + W_{COMP,2}\right)} \times 100\% \qquad (5.5)$$

where:

$Q_{LineLoss}$ = refrigerant line loss, W

$Q_{ShellLoss}$ = compressor shell loss, W

Q_{EVP} = evaporator heat transfer rate, W

Q_{COND} = condenser heat transfer rate, W

W_{COMP} = compressor power, W

The compressor shell heat loss is evaluated for several operating conditions; TCND82, TCND88, TCND95, CFM1090, CFM1200, and CFM1330. The notation, TCND82, indicates that the condenser inlet air dry-bulb temperature is set at 82°F and the rest of the parameters are at the baseline conditions. Note that TCND95 and CFM1200 are the baseline conditions and have the same inlet conditions. The result of the study is shown in Figure 5.9.

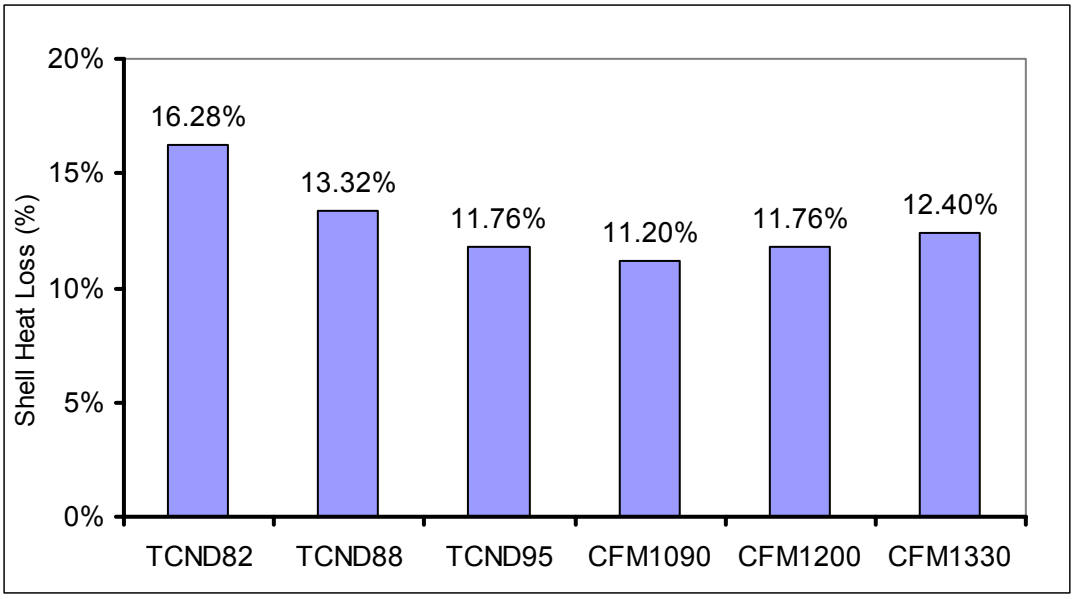

Figure 5.9: Percentage of Compressor Shell Heat Loss in Cooling Mode

The amount of heat loss by convection from the compressor shell depends on the temperature difference between shell exterior surface temperature and the air outlet temperature of the outdoor coil, assuming that the convection coefficient remains constant.

$$Q_{conv} = hA_{shell}\left(T_{shell} - T_{air,out,ODC}\right)$$

One thermocouple is placed at the top and another at the lower side of the compressor shell and the overall temperature of the shell is the average of the two thermocouple readings. Figure 5.10 shows the percentage of shell heat loss for TCND82, TCND88 and TCND95 decreases as the condenser inlet air increases. This is due to the decrease in the temperature difference between the compressor shell and the outlet air temperature of the outdoor coil in addition to the increase in the compressor power as shown in Figure 5.10.

	Tshell-Tao,ODC (F)	QShellLoss(KW)	Wcomp (KW)	%ShellHeatLoss
TCND82	18.69	0.320	1.97	16.28%
TCND88	16.04	0.286	2.15	13.32%
TCND95	16.01	0.279	2.38	11.76%
CFM1090	13.26	0.265	2.36	11.20%
CFM1200	15.43	0.279	2.38	11.76%
CFM1340	15.10	0.296	2.39	12.40%

Figure 5.10: Analysis of Compressor Shell Heat Loss

For CFM1090,CFM1200, and CFM1330, the percentage of compressor shell heat loss is fairly constant at about 11-12%. The assumption that the compressor shell loss is directly proportional to the temperature difference between the shell and outlet air temperature of the outdoor coil is valid except for CFM1330. The procedure used to calculate the compressor heat loss is susceptible to the uncertainty in the condenser, evaporator and compressor power measurements. A more detailed study and research is required to confirm the assumptions made in this study.

5.1.5 Summary of Air-to-Air Heat Pump Validation

The EnergyPlus curve-fit air-to-air heat pump model is able to match the catalog data with an error of about 5%. The curve-fit model is able to capture the heat pump performance adequately with an RMS error of 4%-12%. More than half of the error

is due to the difference between the catalog data and the measured data. It is expected that the curve-fit model would perform better if the experimental data could be used to generate the curves. Unfortunately, the number of experimental data is not sufficient to do so. One particular drawback of the model is that it requires two curves to calculate the heat pump outputs which is the temperature modifying factor(TMF) and flow fraction modifying factor(FMF). In addition to the difficulty of generating two curves and propagation of errors from both curves, the data points need to be selected from the catalog as shown in Appendix A. For example, the data points used for generating the FMF curve must have the same inlet dry-bulb and wet-bulb temperatures at rated conditions with varying air flow rate. Another curve-fit air-air heat pump model based on the Lash(1992) approach was proposed in Appendix E whereby only one curve is required to simulate one output. The suggested model is expected to perform better than the currently available air-to-air curve-fit model. Finally, the compressor shell heat loss is about 11%-16% of the total compressor power input based on six tests conducted in this study. This indicates the manufacturer's assumption of zero compressor loss introduces significant error in the catalog data.

5.2. Steady-State Water-to-Air Heat Pump Model Validation

This section consists of further validation of the Jin (2002) parameter estimation based water-to-air heat pump model and the modified curve-fit water-to-air heat pump model originally developed by Lash (1992). Parameter/coefficient generators are used to generate the parameters for both models using catalog data provided by the manufacturer. This section also discusses the findings regarding the uncertainty of using the models in the EnergyPlus simulation environment. The uncertainties in the heat pump models can be categorized as following:

1. Uncertainty in the catalog data: As mentioned in Jin (2002), the ARI standard allowable tolerance is $\pm 5\%$ for the rating conditions, further extrapolation of the experimental data will increase the error in the catalog data.
2. Uncertainty in the model: This is the uncertainty due to the heat pump models not being able to match the catalog data exactly.
3. Computational uncertainty due to refrigerant properties and truncation error: The refrigerant property routines used to generate the parameters are different from the refrigerant property routines in EnergyPlus. The parameter estimator uses empirical functions adopted from HVACSIM+ while EnergyPlus uses a "table-lookup" method using refrigerant properties generated from REFPROP 6.0 by NIST. Incorporating the EnergyPlus "table-lookup" method in the VBA parameter estimator tool requires a Dynamic Link Library(DLL) which is not easily accessible for debugging purposes. In addition, Jin's model uses successive

substitution to converge on the load side and source side heat transfer rates. Truncation error would also introduce discrepancies between the parameter generator and, the EnergyPlus outputs. The convergence tolerance set for EnergyPlus is also much lower than the parameter estimator to reduce the simulation time.

The models are validated using 23 cooling experimental data points and 16 heating experimental data points from the manufacturer's testing facility. A 3-ton heat pump with a three-speed PSC fan was tested.

5.2.1 Experimental Validation Results for Cooling Mode

The parameters and coefficients for the heat pump models are generated from the catalog data, as discussed in Appendix B. Table 5.2 shows the difference between the parameter/coefficient generator outputs and the catalog data

	%RMS error	
	Curve-Fit Model	**PE-Based Model**
Number of Data Points	348	348
Total Cooling Capacity	2.68	6.61
Sensible Capacity	4.49	5.90
Heat Rejection	2.19	5.50
Power Input (Cooling)	1.86	4.05

Table 5.2: Parameter/Coefficient Generator Outputs Compared with Catalog Data (Cooling)

The model that provides a better match with the catalog data will generally have lower error when compared to the experimental data since the experimental data was used by the manufacturer to generate the catalog data. The performance of both models

in the EnergyPlus simulation environment compared to the experimental data is shown in Table 5.3.

	%RMS error	
	Curve-Fit Model	PE-Based Model
Total Cooling Capacity	5.51	4.04
Sensible Capacity	11.85	7.58
Heat Rejection	4.14	6.27
Power Input (Cooling)	2.25	4.17

Table 5.3: Comparison of Water-to-Air Heat Pump Models using Catalog Data with Experimental Measurements (Cooling)

Table 5.2 shows that the curve-fit model does a better job of fitting a large number of the data points. This is due to the fact that the curve-fit model has more coefficients than the parameter estimation model and is less constrained by the form of the equations. Table 5.3 shows that when the comparison is limited to experimental data which is likely to cover extreme operating conditions, the parameter estimation model does a significantly better job of matching the data. This suggests that the physical form of the parameter estimation model is useful in damping the effect of the outliers in the catalog data set.

Figure 5.11 to Figure 5.14 illustrate both the discrepancies between the measured and extrapolated catalog data and the usefulness of the parameter estimation model in damping the effects on non-physical catalog data points. Figure 5.12 shows that though the curve-fit model did an excellent job of fitting the catalog data, the physically constrained parameter estimation model did a better job of matching the actual experimental data. This trend is also shown by the total capacity(Figure 5.11) and to a lesser extent by the heat rejection rate(Figure 5.14).

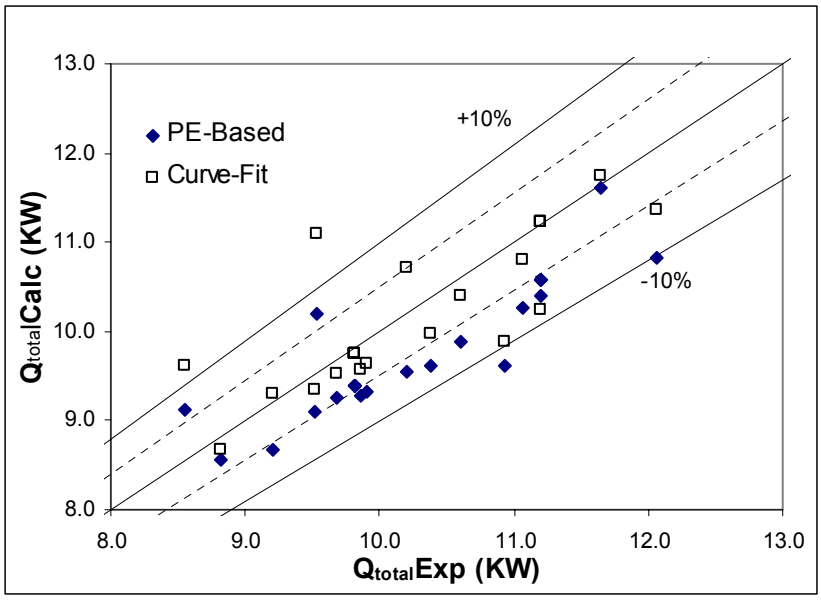

Figure 5.11: Validation of Curve-Fit Model and Jin(2002) for Total Cooling Capacity using Catalog Data for Generating Parameters & Coefficients

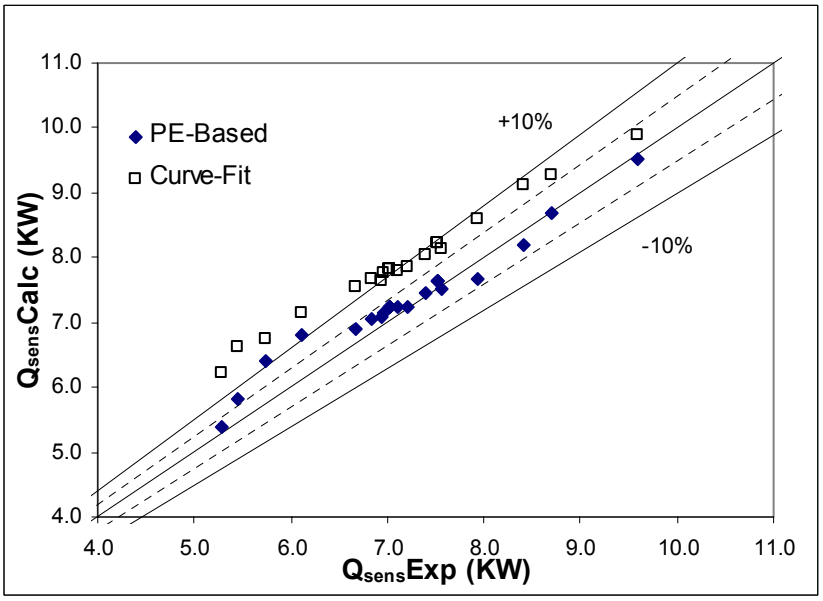

Figure 5.12: Validation of Curve-Fit Model and Jin(2002) for Sensible Cooling Capacity using Catalog Data for Generating Parameters & Coefficients

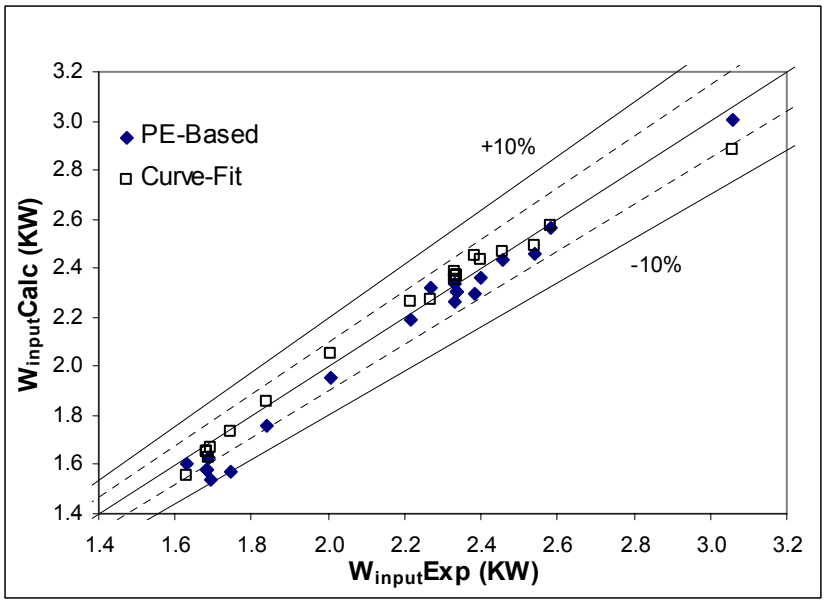

Figure 5.13: Validation of Curve-Fit Model and Jin(2002) for Power Consumption using Catalog Data for Generating Parameters & Coefficients

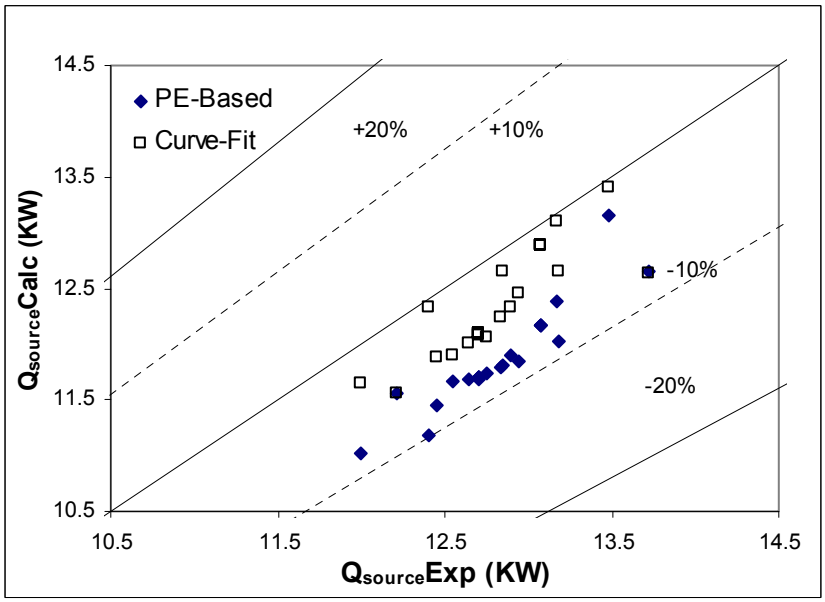

Figure 5.14: Validation of Curve-Fit Model and Jin(2002) for Heat Rejection using Catalog Data for Generating Parameters & Coefficients

From the figures above, both models performed acceptably well with RMS error not exceeding 15%. As expected, the models' uncertainty due to the discrepancies between the catalog data and experimental data can be significantly reduced by using the

experimental data to generate the coefficients or parameters instead of the catalog data. Table 5.4 shows the difference between the parameter/coefficient generator outputs and the experimental data.

	%RMS error	
	Curve-Fit Model	**PE-Based Model**
Number of Data Points	23	23
Total Cooling Capacity	1.60	4.75
Sensible Capacity	8.99	5.70
Heat Rejection	4.95	2.78
Power Input (Cooling)	1.93	1.76

Table 5.4: Parameter/Coefficient Generator Outputs Compared with Experimental Data (Cooling)

Thus Table 5.4 essentially shows the amount of uncertainty due to the model not being able to match the heat pump performance exactly. For only 23 data points, both the curve-fit model and the parameter estimation model match the experimental data within 10%. The largest error(8.99%) is for the sensible capacity predicted by the curve-fit model. As mentioned in Section 4.1.2, the general least square method is sensitive to the input data used for generating the coefficients. Further analysis of the experimental data shows that the air flow rate is generally fixed at 1150CFM except for 4 experimental points. This is a likely cause of the error seen in the curve-fit sensible capacity prediction.

The generated parameters and coefficients are then used in EnergyPlus simulation environment with the same heat pump inlet conditions. As mentioned earlier, the difference in the refrigerant property routines used in EnergyPlus and in the parameter generator will produce slightly different outputs. Table 5.5 shows the RMS error of the EnergyPlus output compared with the experimental data.

	%RMS error	
	Curve-Fit Model	PE-Based Model
Total Cooling Capacity	1.60	2.33
Sensible Capacity	8.99	6.49
Heat Rejection	4.95	5.49
Power Input (Cooling)	1.93	4.58

Table 5.5: Comparison of Water-to-Air Heat Pump Models using Experimental Data with Experimental Measurements (Cooling)

Comparing Table 5.4 and Table 5.5, the uncertainty due to the refrigerant properties and computational uncertainly is about 2-3% and can either reduce or increase the RMS error. The curve-fit model is not affected by this discrepancy because the model does not require refrigerant properties routines. Figure 5.15 to Figure 5.18 shows the performance of both models in the EnergyPlus simulation environment using the parameters/coefficients generated from the experimental data. The four outliers for the curve-fit model in Figure 5.15 which are beyond the 10% region are the four experimental points that have different flow rates than the rest.

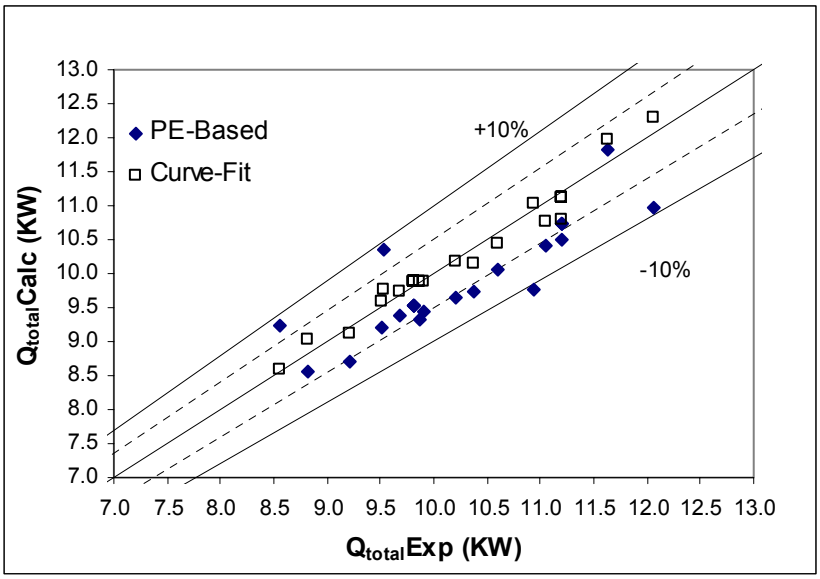

Figure 5.15: Validation of Curve-Fit Model and Jin(2002) for Total Cooling Capacity using Experimental Data for Generating Parameters & Coefficients

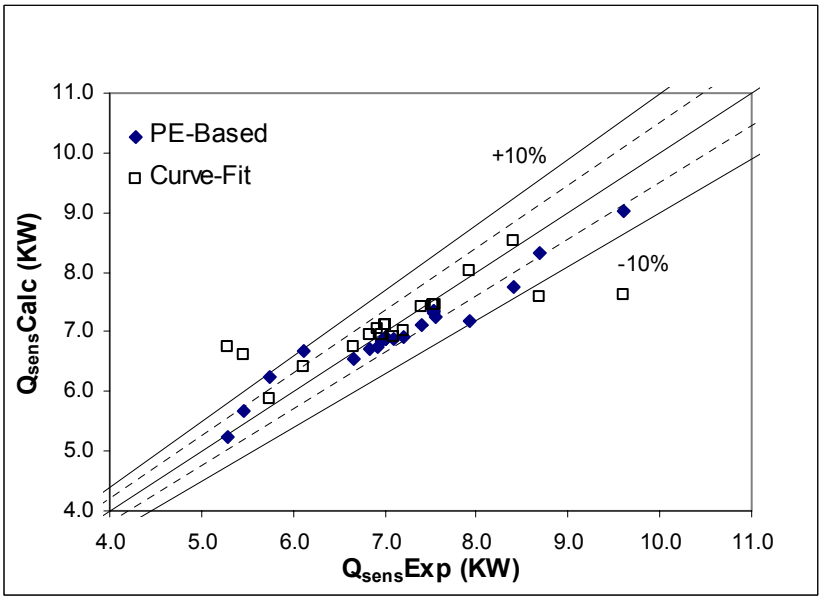

Figure 5.16: Validation of Curve-Fit Model and Jin(2002) for Sensible Capacity using Experimental Data for Generating Parameters & Coefficients

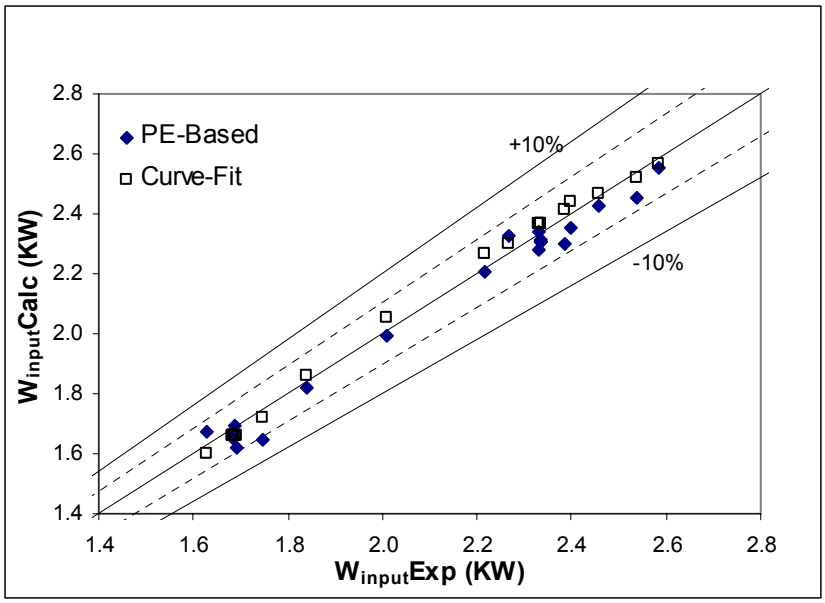

Figure 5.17: Validation of Curve-Fit Model and Jin(2002) for Power Consumption using Experimental Data for Generating Parameters & Coefficients

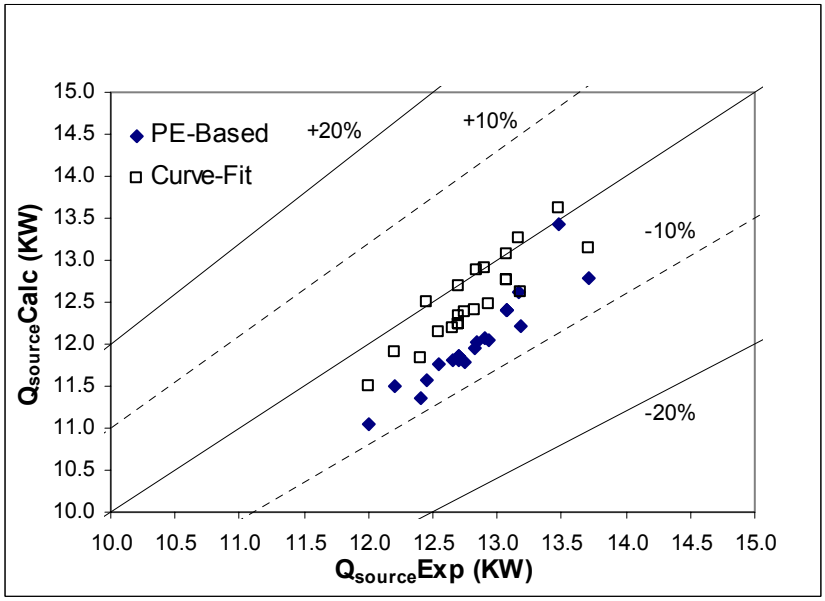

Figure 5.18: Validation of Curve-Fit Model and Jin(2002) for Heat Rejection using Experimental Data for Generating Parameters & Coefficients

5.2.2 Experimental Validation Results for Heating Mode

From the manufacturer's catalog data, 252 data points are used to generate the coefficients for both models. Table 5.6 shows the RMS error of the parameter/coefficient generator output compared to the catalog data. Both models are able to match the catalog data very well with RMS errors of less than 5%.

	%RMS error	
	Curve-Fit Model	**PE-Based Model**
Number of Data Points	252	252
Heating Capacity	0.84	2.93
Heat Absorption	1.70	3.63
Power Input (Heating)	1.47	1.91

Table 5.6: Parameter/Coefficient Generator Outputs Compared with Catalog Data (Heating)

Using the generated parameters and coefficients, the models are simulated in EnergyPlus and compared with 16 experimental data point provided by manufacturer. Table 5.7 shows that RMS error for heat absorption is the highest for both models with RMS error greater than 13%. All 3 categories of uncertainty contribute to the difference between Table 5.6 and Table 5.7. The outputs for each model in the EnergyPlus simulation environment are plotted against the experimental data in Figure 5.19 to Figure 5.21.

	%RMS error	
	Curve-Fit Model	**PE-Based Model**
Heating Capacity	5.54	8.93
Heat Absorption	13.47	18.63
Power Input (Heating)	1.29	2.53

Table 5.7: Comparison of Water-to-Air Heat Pump Models using Catalog Data with Experimental Measurements (Heating)

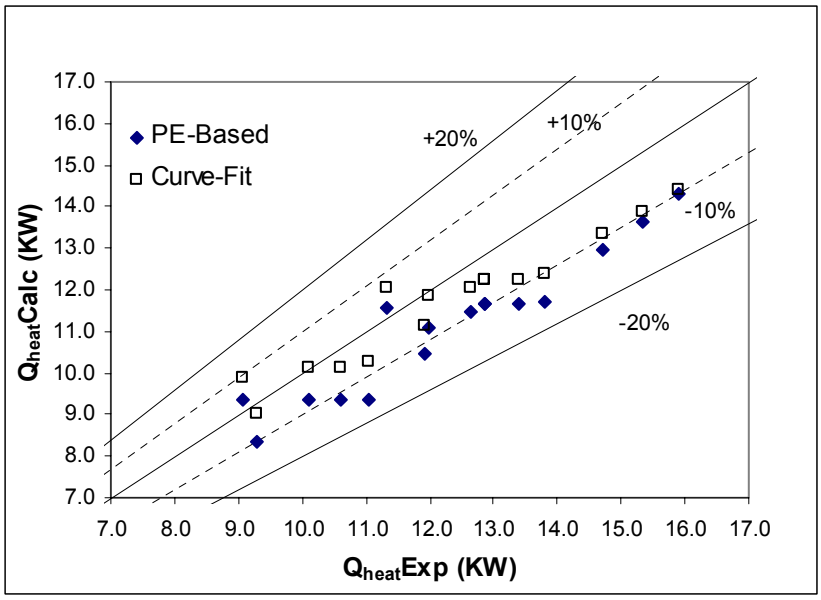

Figure 5.19: Validation of Curve-Fit Model and Jin(2002) for Heating Capacity using Catalog Data for Generating Parameters & Coefficients

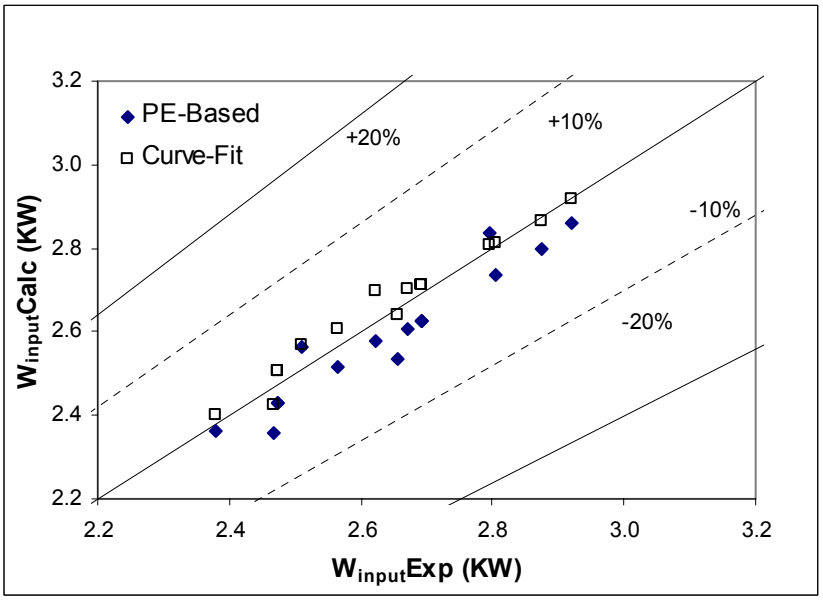

Figure 5.20: Validation of Curve-Fit Model and Jin(2002) for Power Consumption using Catalog Data for Generating Parameters & Coefficients

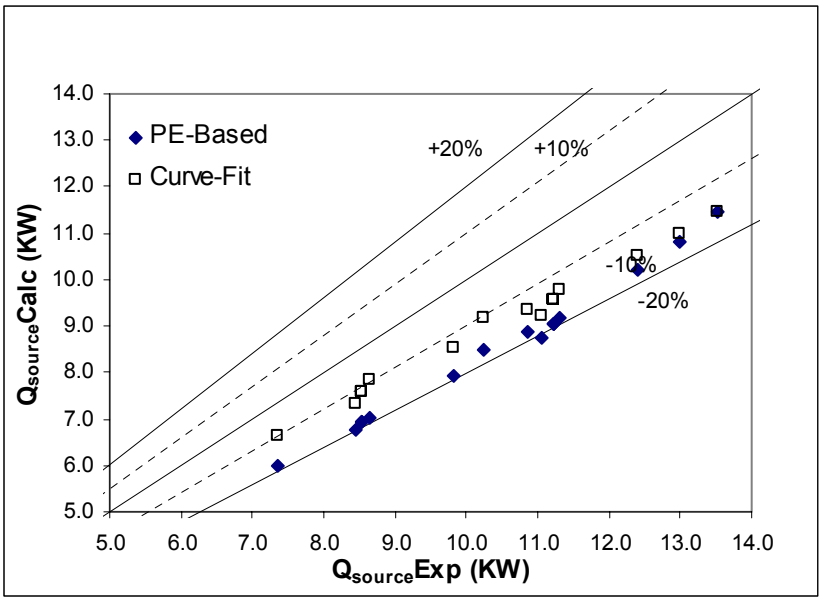

Figure 5.21: Validation of Curve-Fit Model and Jin(2002) for Heat Absorption using Catalog Data for Generating Parameters & Coefficients

Using the same method as the cooling mode, the coefficients and parameters are generated using the 16 experimental data points instead of the catalog data to eliminate the uncertainty due to discrepancies in the catalog data. Table 5.8 shows the RMS error of the parameter/coefficient generator compared to the experimental data.

	%RMS error	
	Curve-Fit Model	**PE-Based Model**
Number of Data Points	16	16
Heating Capacity	0.73	7.60
Heat Absorption	11.49	4.58
Power Input (Heating)	0.56	2.62

Table 5.8: Parameter/Coefficient Generator Outputs Compared with Experimental Data (Heating)

Note that the RMS error is due to the uncertainty of the model not being able to match the experimental data exactly. Both models assume no losses and energy input into the heat pump is always equal to the energy output. However, the experimental results have a heat balance error of about 3% to 5%. For the curve-fit model, the heat absorption

is calculated from the heating capacity and power consumption which are fitted to the curve. The heat balance error in the experimental data causes the heat absorption to be off by 10% although the model is able to simulate the heating capacity and power consumption very accurately. The parameter-estimation based model did a better job of modeling the heat absorption because the model iterates on both the load side and source side heat transfer rates as shown in Figure 4.7. The generated coefficients and parameters are then used in the EnergyPlus simulation environment to estimate the computational uncertainty shown in Table 5.9.

	%RMS error	
	Curve-Fit Model	**PE-Based Model**
Heating Capacity	0.73	2.36
Heat Absorption	11.49	10.09
Power Input (Heating)	0.56	4.92

Table 5.9: Comparison Water-to-Air Heat Pump Models using Experimental Data with Experimental Measurements (Heating)

Comparing Table 5.8 and Table 5.9, the computational uncertainty has no influence on the curve-fit model because the model does not require refrigerant properties. For the parameter estimation based mode, there are 5% difference in the RMS error for heating capacity and heat absorption. As mentioned earlier the computational uncertainty can either reduce or increase the errors of the model. Figure 5.22 to Figure 5.24 shows the performance of both models in the EnergyPlus simulation environment.

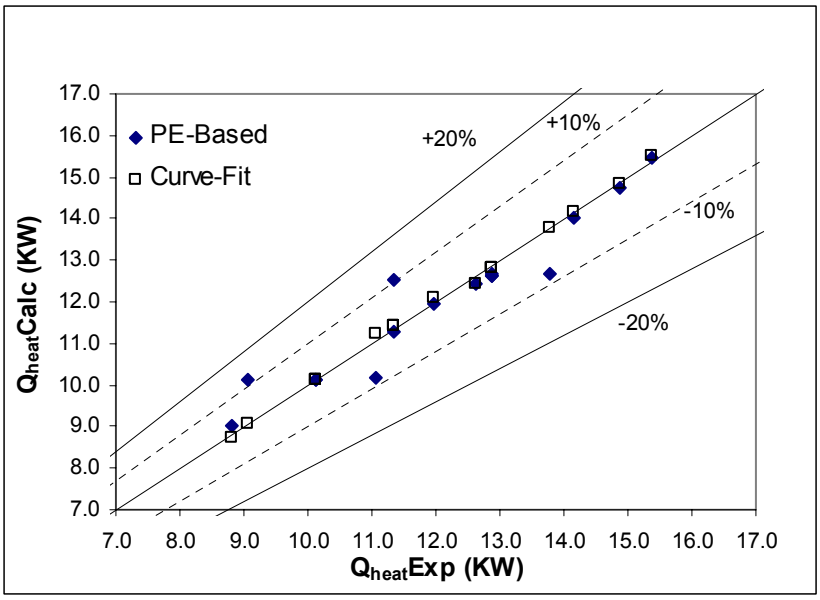

Figure 5.22: Validation of Curve-Fit Model and Jin(2002) for Heating Capacity using Experimental Data for Generating Parameters & Coefficients

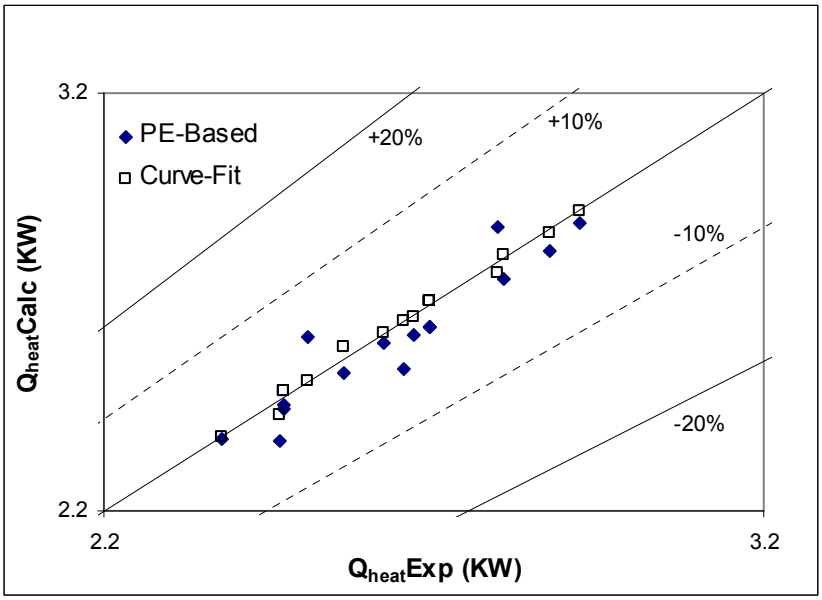

Figure 5.23: Validation of Curve-Fit Model and Jin(2002) for Power Consumption using Experimental Data for Generating Parameters & Coefficients

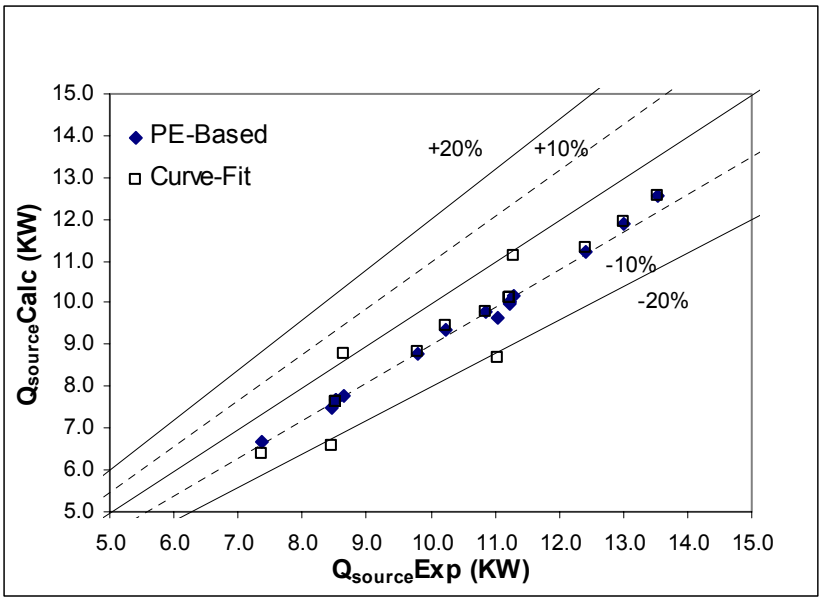

Figure 5.24: Validation of Curve-Fit Model and Jin(2002) for Heat Absorption using Experimental Data for Generating Parameters & Coefficients

5.2.3 Model Performance Beyond Catalog Range

This section compares the performance of the parameter estimation based model and the curve-fit model when they are applied beyond the catalog data. Due to the lack of experimental data at extreme operating conditions, a subset of the catalog data is used as a reference. A simple test is conducted by limiting the inlet conditions for the parameter/coefficient generator to the mid range of the catalog data. The tables below show the catalog data range and the inlet conditions used for generating the coefficients and parameters.

Cooling Mode	Variations in Catalog Data	Used in Generating Parameters/Coefficients
Inlet Air Dry-Bulb Temperature (°F)	70, 80, 85, 95	80, 85
Inlet Air Wet-Bulb Temperature (°F)	60, 65, 67, 75	65, 67
Air Flow Rate (CFM)	975, 1200	975, 1200
Inlet Water Temperature (°F)	30, 40, 50, 60, 70, 80, 90, 100, 110	60, 70, 80
Water Flow Rate (gpm)	4.5, 7.0, 9.0	4.5, 7.0, 9.0

Table 5.10: Catalog Data and Input Data Range for Cooling Mode

Heating Mode	Variations in Catalog Data	Used in Generating Parameters/Coefficients
Inlet Air Dry-Bulb Temperature (°F)	60, 65, 68, 70, 75, 80	70, 75
Air Flow Rate (CFM)	975, 1200	975, 1200
Inlet Water Temperature (°F)	40, 50, 60, 70, 80, 90	60, 70
Water Flow Rate (gpm)	4.5, 7.0, 9.0	4.5, 7.0, 9.0

Table 5.11: Catalog Data and Input Data Range for Heating Mode

The heat pump model used for this analysis is a 3-ton heat pump. In fact, the "catalog data" in this context is the input data used initially for the validation of the water-to-air heat pump models as described in Appendix B and Appendix C. The "half-range" parameters/coefficients are then used to simulate the heat pump performance for the entire catalog data range. This will artificially impose "extreme operating conditions" on the models. Heat pump performance that is beyond the input data range used to generate the parameters is considered to be "extreme operating conditions" as shown in Table 5.12.

Heat Pump Performance	Catalog Range	Input Data Range used for Generating Parameter/Coefficients
Total Cooling Capacity (KW)	8.34-12.66	9.2-11.2
Sensible Capacity (KW)	4.8-11.8	7.2-10.5
Heat Rejection (KW)	10.8-14.0	11.5-13.0
Power Input (Cooling)	1.2-3.2	1.8-2.4
Heating Capacity (KW)	7.5-14.8	10.6-12.5
Heat Absorption (KW)	4.9-12.3	7.8-9.8
Power Input (Heating)	2.0-3.4	2.5-3.0

Table 5.12: Heat Pump Performance Range in Catalog and Input Data

The number of data points used to generate the coefficients and parameters are: 56 data points for cooling mode and 32 for heating mode. The errors associated with the parameter generators' output and the input data are shown in Table 5.13.

	3-ton	
	Curve-Fit Model	**PE-Based Model**
Number of Data Points	56	56
Total Cooling Capacity (%)	0.51	2.29
Sensible Capacity (%)	1.25	1.71
Heat Rejection (%)	0.43	1.88
Power Input (Cooling) (%)	0.69	2.37
Number of Data Points	36	36
Heating Capacity (%)	0.33	1.18
Heat Absorption (%)	0.52	1.63
Power Input (Heating) (%)	0.39	1.50

Table 5.13: Parameter/Coefficient Generator Outputs Compared with Input Data

The generated coefficients or parameters are then used to simulate the entire catalog data range which corresponds to 348 data points for cooling mode and 252 data points for heating mode. The result summary for cooling mode is shown in Figure 5.25 to Figure 5.28.

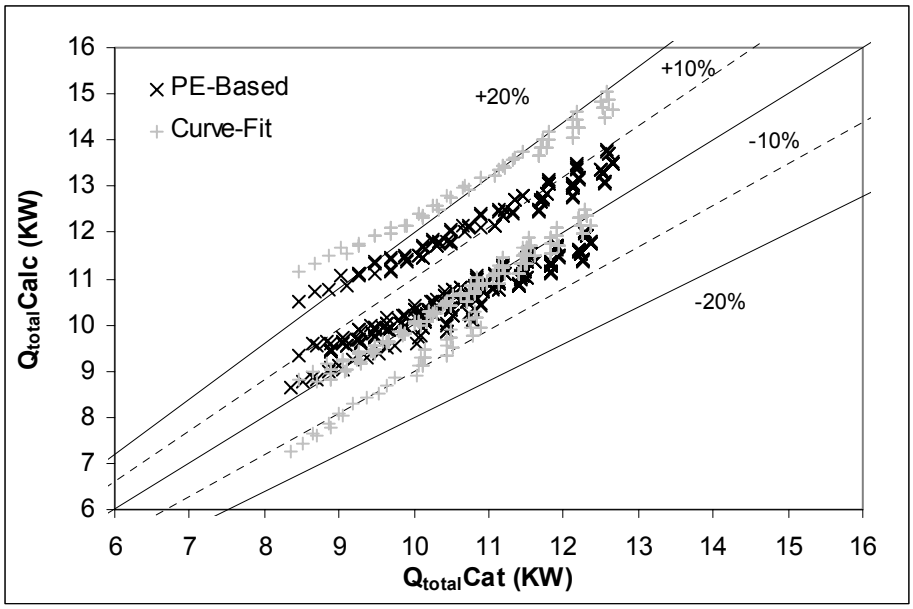

Figure 5.25: Performance of Water-to-Air Heat Pump Models Beyond Catalog Range for Total Cooling Capacity

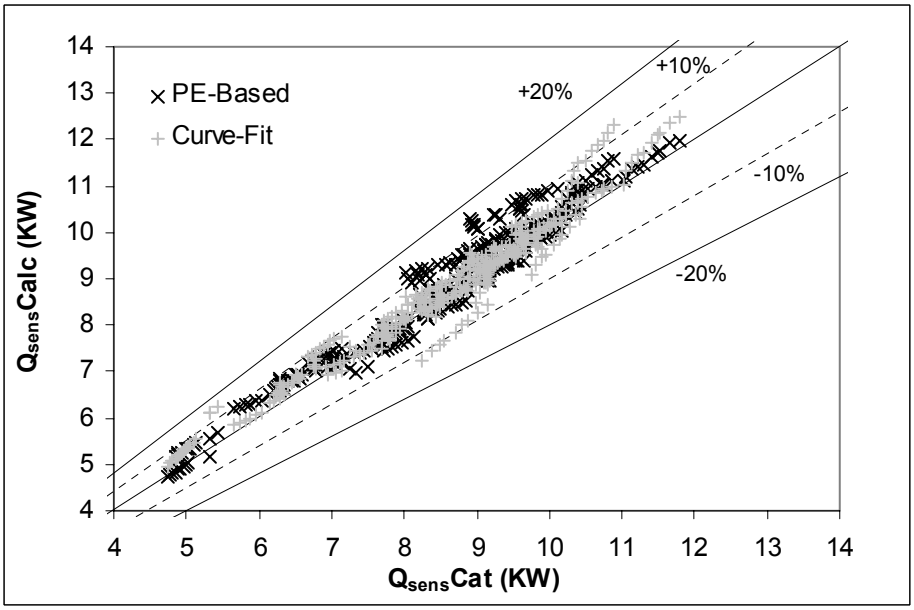

Figure 5.26: Performance of Water-to-Air Heat Pump Models Beyond Catalog Range for Sensible Cooling Capacity

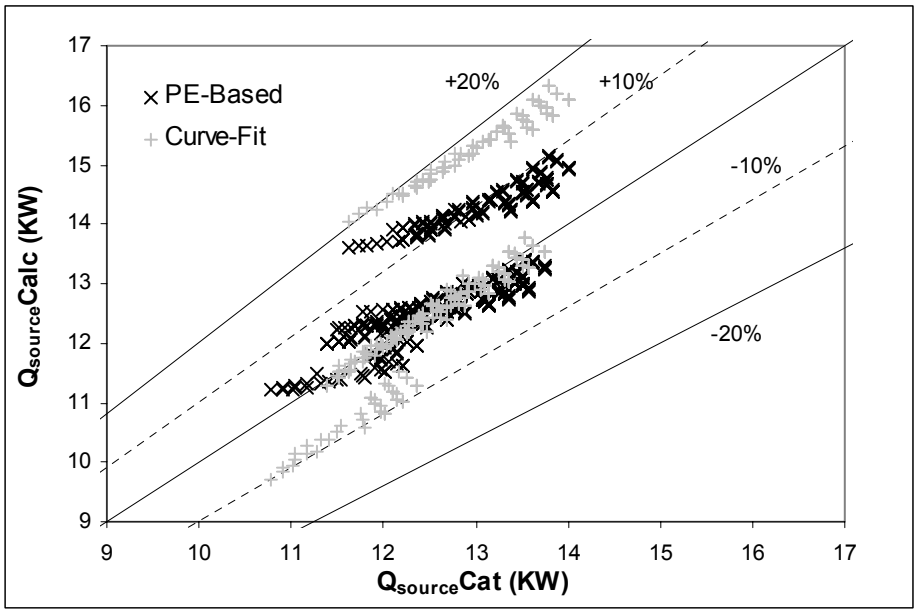

Figure 5.27: Performance of Water-to-Air Heat Pump Models Beyond Catalog Range for Heat Rejection

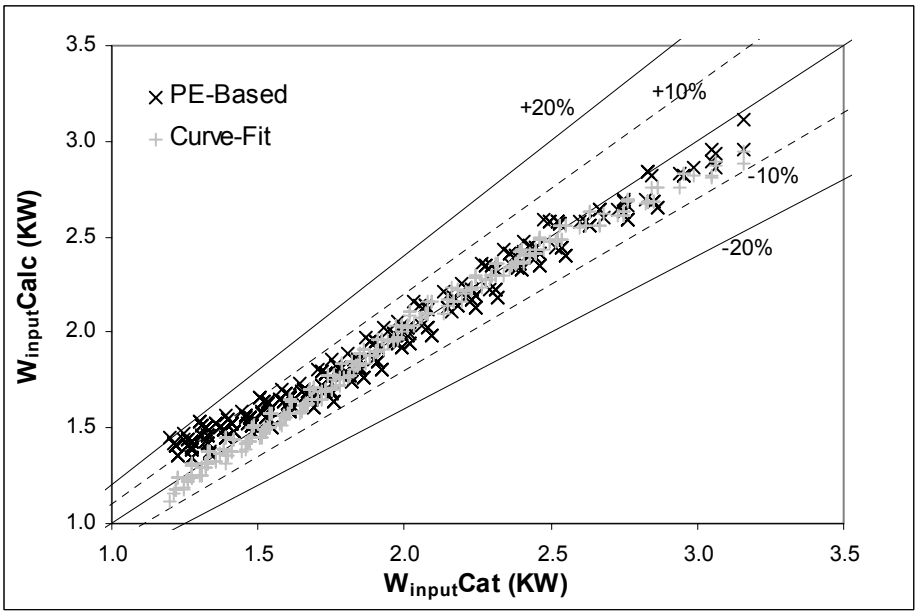

Figure 5.28: Performance of Water-to-Air Heat Pump Models Beyond Catalog Range for Cooling Power Consumption

The graphs above show that both models performed very well except for the total cooling capacity and source side heat transfer rates. For Figure 5.25 and Figure 5.27, there seems to be 2 distinct bands above and below the center line for both models. Further analysis of the data shows that this is due to the effect of higher and lower air wet-bulb temperature (60°F and 75°F) that is unaccounted for in the coefficients and parameters. The catalog data shows that a slight change in the wet bulb temperature has a drastic effect on the total cooling capacity and source side heat transfer rate. Under these conditions, the parameter estimation based model which incorporates the wet bulb temperature in the proper context of the fundamental equations, performs slightly better than the curve-fit model as shown in Table 5.14.

	%RMS error	
	Curve-Fit Model	**PE-Based Model**
Total Cooling Capacity	11.84	7.44
Sensible Capacity	4.57	5.23
Heat Rejection	9.97	5.88
Power Input (Cooling)	2.58	5.94

Table 5.14: Result Summary of Heat Pump Models Operating Beyond Catalog Range for Cooling Mode

Figure 5.29 to Figure 5.31 in the following pages show the result of the curve-fit model and parameter estimation model in heating mode.

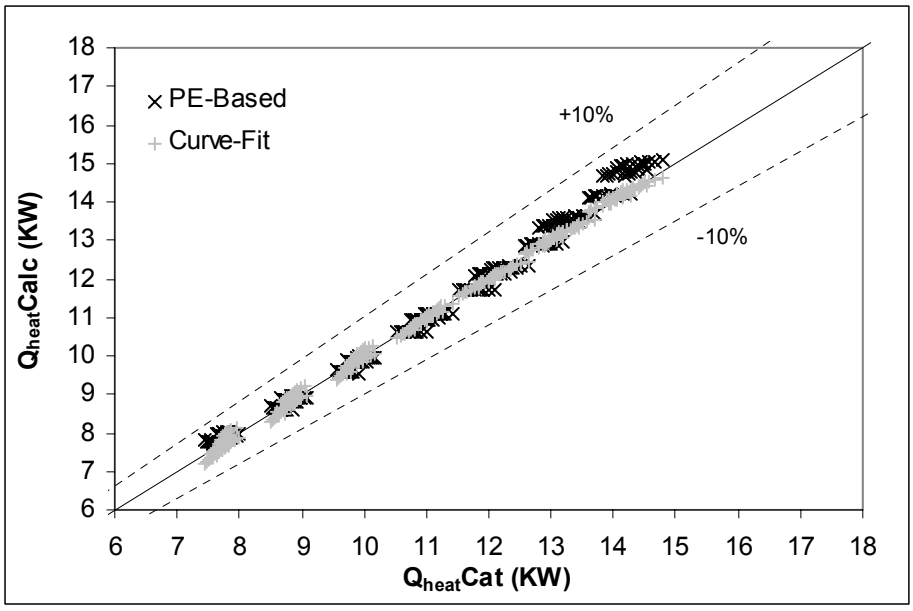

Figure 5.29: Performance of Water-to-Air Heat Pump Models Beyond Catalog Range for Heating Capacity

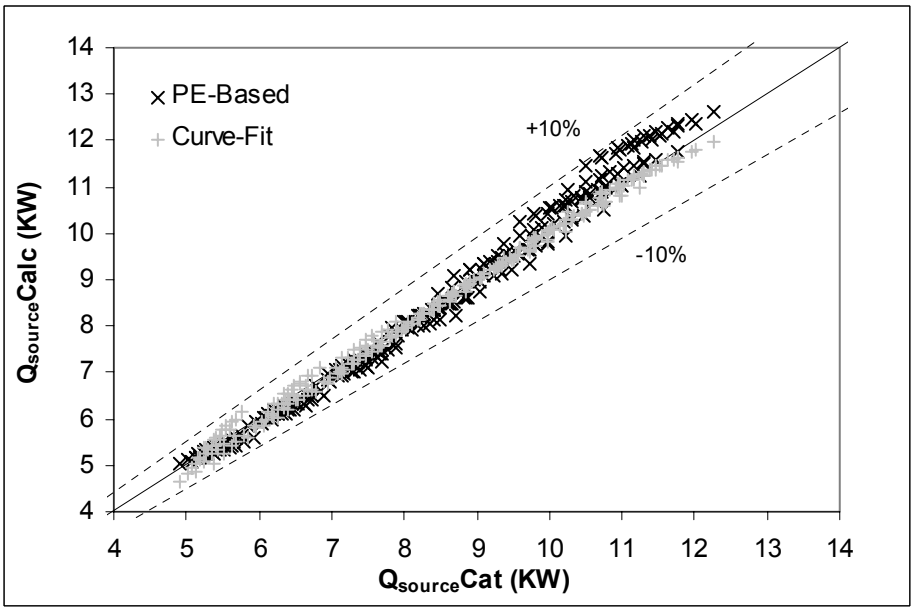

Figure 5.30: Performance of Water-to-Air Heat Pump Models Beyond Catalog Range for Heat Absorption

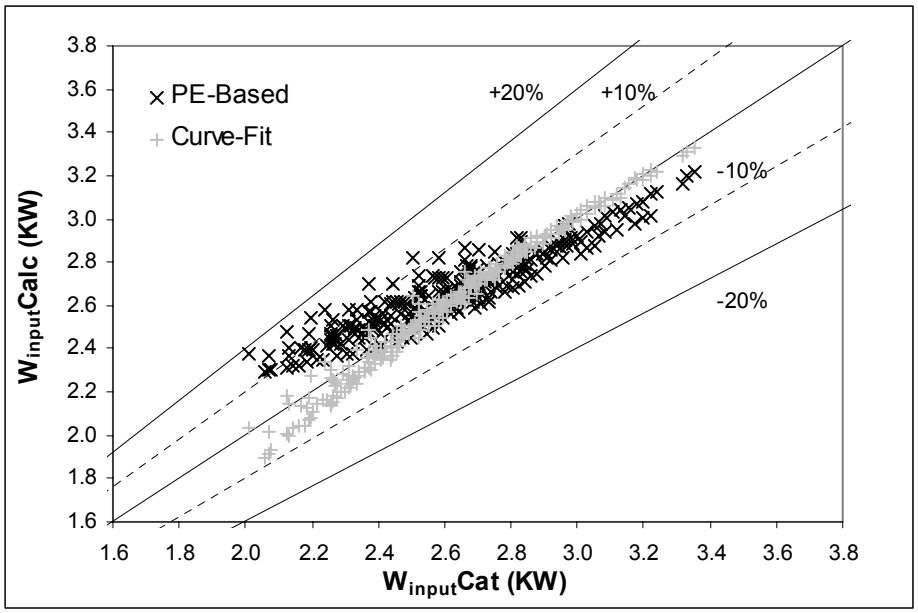

Figure 5.31: Performance of Water-to-Air Heat Pump Models Beyond Catalog Range for Heating Power Consumption

From Figure 5.29 and Figure 5.30, both models are able to simulate the heating capacity and heat absorption very well with errors less than 10%. The parameter estimation based model shows some insensitivity to changes in power consumption with errors for some points exceeding 10%. The summary of the performance for both models is shown in Table 5.15 below:

	%RMS Error	
	Curve-Fit Model	**PE-Based Model**
Heating Capacity (%)	1.06	2.19
Heat Absorption (%)	1.83	3.24
Power Input (Heating) (%)	2.05	5.58

Table 5.15: Result Summary of Heat Pump Models Operating Beyond Catalog Range for Heating Mode

In order to be certain that this study is not a "one case wonder", two more heat pump models are tested. The models tested are 2-ton and 6-ton heat pumps. For the sake of brevity, only the summary of the results are shown without supporting figures. Table

5.16 shows the number of data sets used to generate the parameters/coefficients and the errors of the parameter/coefficient generator outputs compared to the input data. The performance of the heat pump models beyond the catalog data range is shown in Table 5.17.

	2-ton		6-ton	
	Curve-Fit Model	**PE-Based Model**	**Curve-Fit Model**	**PE-Based Model**
Number of Data Points	65	65	72	72
Total Cooling Capacity (%)	0.86	2.36	0.74	2.06
Sensible Capacity (%)	0.86	1.57	1.05	3.21
Heat Rejection (%)	0.81	1.89	0.61	2.08
Power Input (Cooling) (%)	0.80	2.86	0.51	3.99
Number of Data Points	36	36	36	36
Heating Capacity (%)	0.52	1.27	0.33	1.62
Heat Absorption (%)	0.61	1.55	0.42	2.10
Power Input (Heating) (%)	0.37	2.67	0.29	6.46

Table 5.16: Parameter/Coefficient Generator Outputs Compared with Input Data for 2-ton and 6-ton Heat Pumps

	2-ton		6-ton	
	Curve-Fit Model	**PE-Based Model**	**Curve-Fit Model**	**PE-Based Model**
Number of Data Points	510	510	468	468
Total Cooling Capacity (%)	12.85	7.55	14.31	7.59
Sensible Capacity (%)	5.47	7.69	4.21	6.96
Heat Rejection (%)	10.45	5.53	11.19	6.54
Power Input (Cooling) (%)	6.90	12.26	4.28	11.87
Number of Data Points	252	252	252	252
Heating Capacity (%)	1.90	2.33	1.19	6.18
Heat Absorption (%)	2.60	2.34	1.65	9.85
Power Input (Heating) (%)	1.62	8.28	1.69	9.47

Table 5.17: Result Summary of Heat Pump Models Operating Beyond Catalog Range for 2-ton and 6-ton Heat Pumps

From this study, it can be concluded that the parameter estimation based model performed better in general by giving reasonable accuracies. However, the performance of the model in simulating the power consumption is somewhat insensitive to the inlet conditions. This may be attributed to the fact that the fan power is necessarily (but erroneously) included in the parameters as discussed in Section 4.2.4.

The curve-fit model has a tendency to perform either quite well or rather poorly. For the 6-ton heat pump, the curve-fit model is able to simulate the sensible cooling and power consumption very well but failed to capture the total cooling capacity and the heat rejection rate. Thus the performance of the curve-fit model is highly dependent on the range of the input data used for generating the coefficients. In short, the performance of the curve-fit model is more sensitive to the catalog data range compared to the parameter estimation based model.

5.2.4 Summary of Water-to-Air Heat Pump Validation

In general, the curve-fit model captures the trends in the catalog performance data better than the parameter estimation model (even when those trends are not physically correct). This is attributed largely due to the number of coefficients used by the curve-fit model with each model output represented by a separate curve. Based on the comparison between the model outputs and the experimental data, the curve-fit model performs better than the parameter estimation model in most cases except for the sensible cooling capacity. This is likely because the parameter-estimation based model uses a detailed algorithm to split the total heat transfer to sensible and total heat transfer.

It is noted that the parameter-estimation based model performs poorly in the estimating the power consumption. One particular reason is because the compressor model is used to simulate the work done by both the fan and the compressor. This results in a power consumption that is somewhat insensitive to the inlet conditions.

As mentioned by Jin(2002), the curve-fit model cannot simulate the heat pump performance for different working fluids other than the working fluid used in the catalog data. For instance, a degradation factor is required to adjust the source side heat transfer

rate for mixture of water and propylene glycol if the catalog data uses pure water as the working fluid. The degradation factor is not developed for this study. A suggestion on the development of the degradation factor is included in Chapter 6.

From the uncertainty analysis, the parameter estimation based model can be further improved by incorporating the refrigerant property routines from EnergyPlus in the parameter generator program in VBA. Based on the analysis of the 3-ton heat pump model, the uncertainty due to the refrigerant property routines and computational uncertainty is about 2% to 5%. Note that incorporating EnergyPlus refrigerant properties routines requires either conversion of the Fortran 90 code to VBA or compiling the refrigerant property routines into a DLL. Converting the Fortran 90 code to VBA is tedious while using a DLL will restrict accessibility to the debugging environment.

In addition, extending the curve-fit model beyond the catalog range yields good results. The curve-fit model performs surprisingly well even slightly better than the parameter estimation based model in some cases especially in heating mode. The parameter estimation based model tends to give average RMS errors while the curve-fit model tends to either perform quite well or rather poorly. From this study, it can be concluded that the curve-fit model is sensitive to the input data range and it will generally perform as well as the parameter estimation model if the input data covers the entire range.

5.3. Preliminary Verification of Curve-Fit Water-to-Water Heat Pump Model

The proposed curve-fit water-to-water heat pump model is verified using the manufacturer's catalog data. This study is considered preliminary because no experimental data were used to verify the results. The performance of the curve-fit model is compared to the parameter estimation model developed by Jin (2002).

5.3.1 Curve-Fit Model Verification with Catalog Data

The governing equations proposed for the curve-fit water-to-water heat pump model are verified using the catalog data. The main purpose is to determine whether the proposed equations are sufficient to capture the performance variations and profile of a water-to-water heat pump. The model is tested with three heat pump models. The heat pumps selected have varying capacities of 3 ton to 10 ton to ensure that the model is able to simulate any type of heat pumps and to prevent a "one case wonder".

The number of data points obtained from the manufacture is 180 for cooling mode and 189 for heating mode. The catalog data from manufacturer shows the performance of the heat pump at varying load side inlet temperatures, source side inlet temperatures, load side flow rates and source side flow rates. No correction factors are given in the catalog data to extend the number of data points further. Since the catalog data has varying inlet conditions, correction factors are not necessary and the generated performance coefficients should be sensitive to all the inlet conditions. The performance coefficients are generated using the generalized least squares method. The tables below shows the percentage RMS error of the model outputs with the catalog data for cooling mode.

	Cooling		
	3-ton	5-ton	10-ton
Number of Data Points	180	180	180
Qload RMS error (%)	1.23	1.90	1.57
Power RMS error (%)	3.76	3.30	3.32
Qsource RMS error (%)	0.89	1.20	1.11

Table 5.18: Comparison of Cooling Catalog Data and Simulation Results for Curve-Fit Water-to-Water Heat Pump Model

Table 5.18 shows that the load side heat transfer rate and the source side heat transfer rate have RMS error of less than 2% while the power input is slightly higher at about 3-4%. With RMS error of less than 5% for all the heat pump outputs, it should be sufficient to conclude that the governing equations are sufficient to simulate the heat pump in cooling mode. Simulation results for the heating mode are shown in the table below:

	Heating		
	3-ton	5-ton	10-ton
Number of Data Points	189	189	189
Qload RMS error (%)	3.13	1.97	1.93
Power RMS error (%)	6.66	3.21	3.21
Qsource RMS error (%)	3.80	2.09	2.55

Table 5.19: Comparison of Heating Catalog Data and Simulation Results for Curve-Fit Water-to-Water Heat Pump Model

Table 9 shows that the load side heat transfer rate and source side heat transfer rate have errors of less than 4% for all heat pumps simulated. The power input to the heat pump has higher errors especially for the 3-ton heat pump with RMS error of more than 6%. Although the heating mode results have a higher percentage error compared to the cooling mode results, they are still acceptable and have conservative accuracy. The simulation result for 3-ton heat pump has the least satisfactory match with the catalog data especially for the heating mode. A comparison of the simulation results to the catalog data for the 3-ton heat pump is shown in Figure 5.32 to Figure 5.37 below:

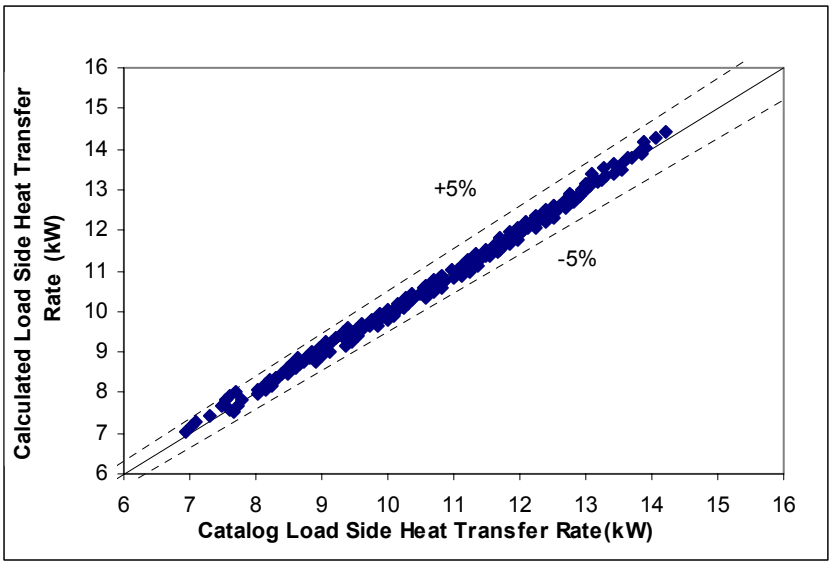

Figure 5.32: Comparison of Cooling Load Side Heat Transfer Rate for Simulation Results with Catalog Data

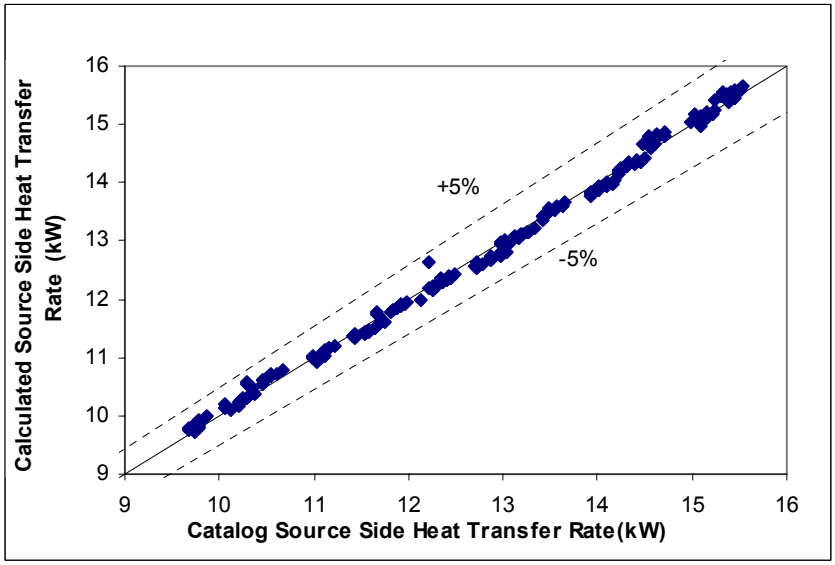

Figure 5.33: Comparison of Cooling Source Side Heat Transfer Rate for Simulation Results with Catalog Data

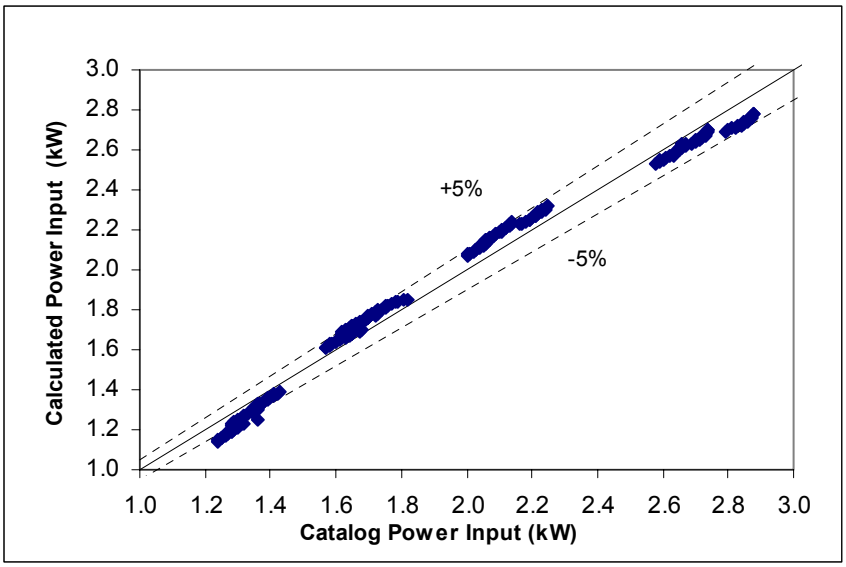

Figure 5.34: Comparison of Cooling Power Input for Simulation Results with Catalog Data

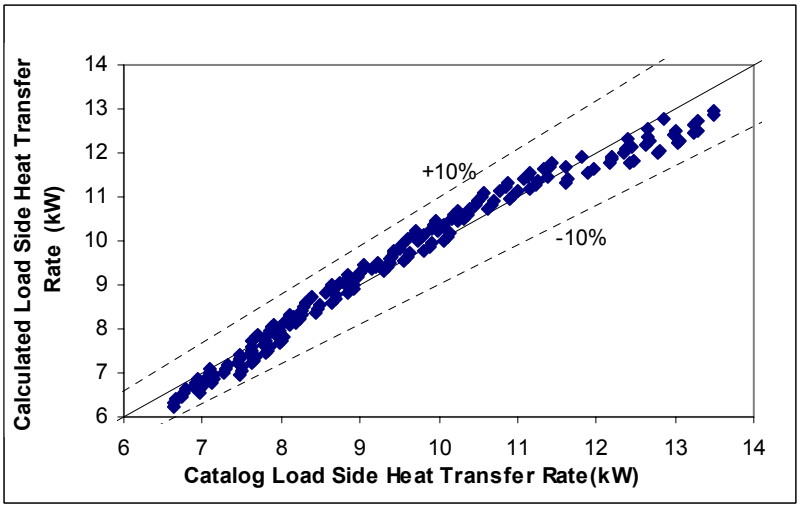

Figure 5.35: Comparison of Heating Load Side Heat Transfer Rate for Simulation Results with Catalog Data

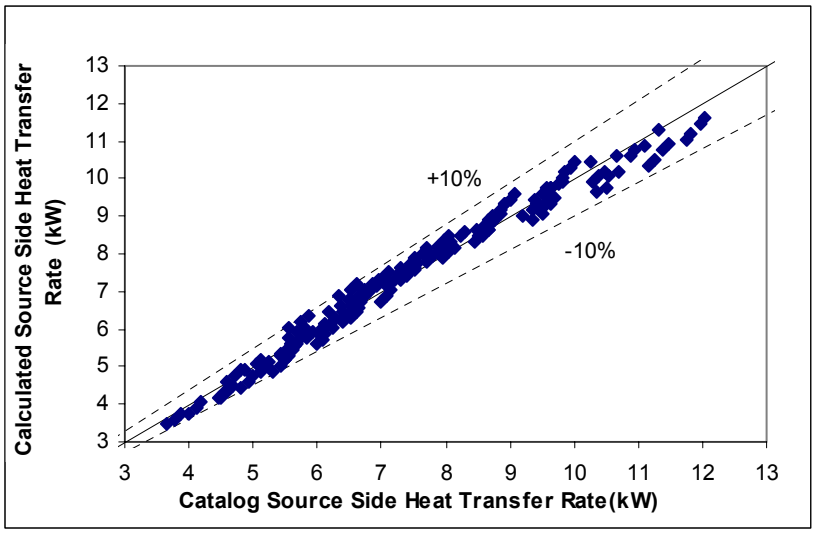

Figure 5.36: Comparison of Heating Source Side Heat Transfer Rate for Simulation Results with Catalog Data

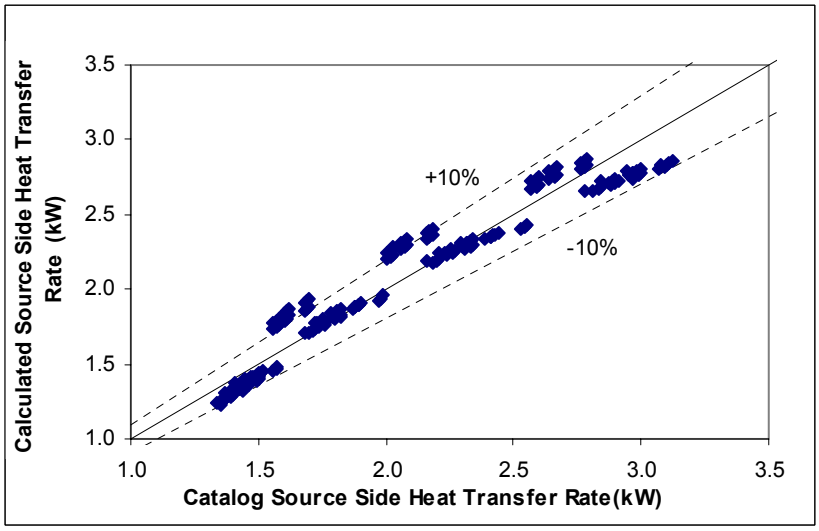

Figure 5.37: Comparison of Heating Power Input for Simulation Results with Catalog Data

5.3.2 Comparisons of Curve-Fit Model and Parameter Estimation Based Model

The performance of the curve-fit model is compared with the parameter estimation based model by Jin (2002). The heat pump model selected for this study is the

3-ton heat pump since the curve-fit model shows the highest error for this model. For generating the coefficients and parameters for both cooling and heating mode, 36 data points covering the entire operating range of the heat pump are selected from the catalog data. Jin(2002) concluded that the parameter-estimation based model requires at least 32 data points to generate "good" parameters that would capture the performance of the heat pump adequately. Jin(2002) also noted that there is only a small significant increase in accuracy when all the data points are used. To prevent uncertainty due to different refrigerant properties used in the parameter generator program and the EnergyPlus simulation environment, the simulation was not conducted in the EnergyPlus simulation environment. The parameters/coefficients used in the verification are shown in Appendix D. Figure 5.38 to Figure 5.40 shows the performance of the models in cooling mode. Figure 5.41 to Figure 5.43 shows the performance of the models in heating mode.

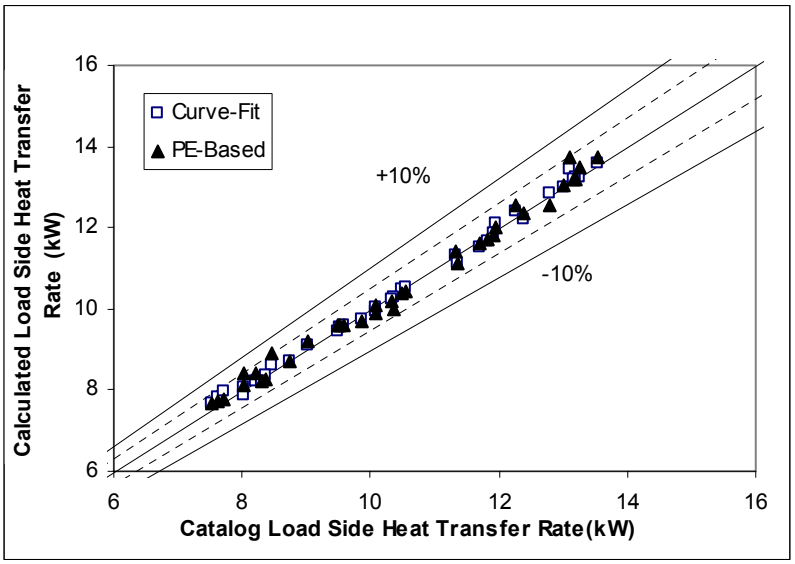

Figure 5.38: Performance of Water-to-Water Heat Pump Models in Simulating Load Side Heat Transfer Rate (Cooling)

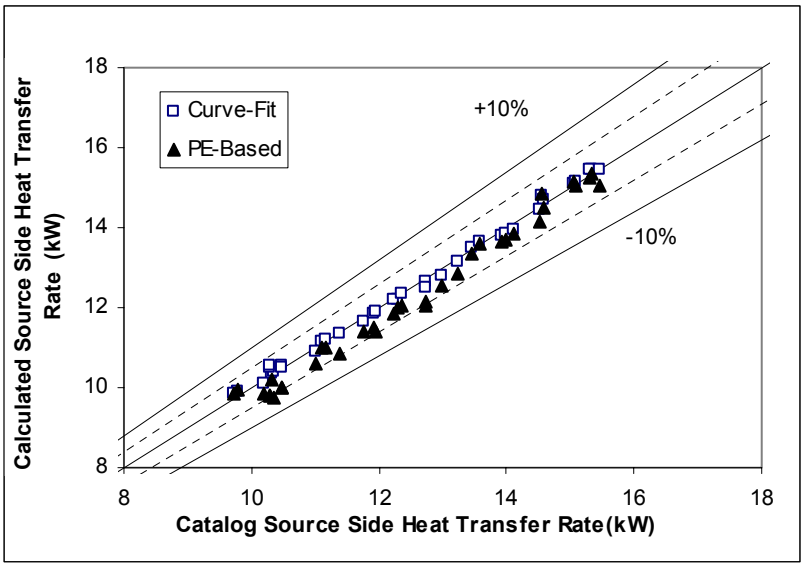

Figure 5.39: Performance of Water-to-Water Heat Pump Models in Simulating Source Side Heat Transfer Rate (Cooling)

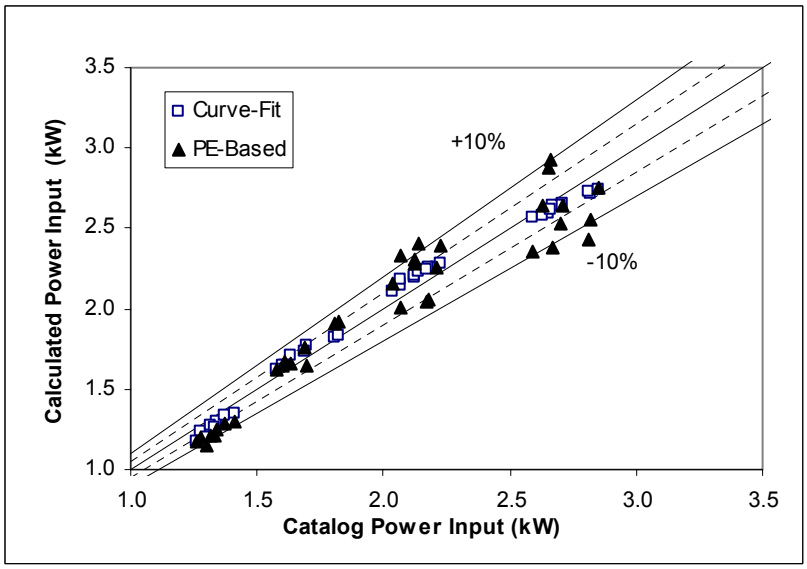

Figure 5.40: Performance of Water-to-Water Heat Pump Models in Simulating Power Consumption (Cooling)

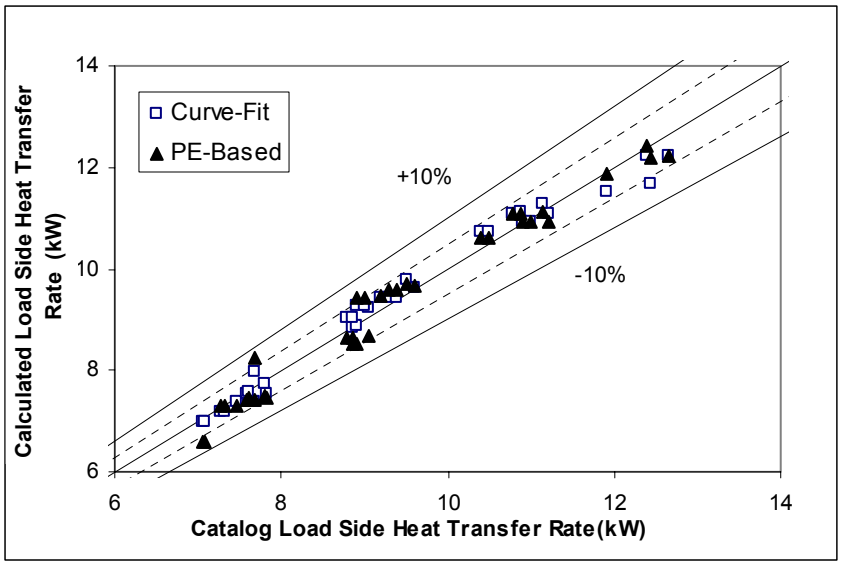

Figure 5.41: Performance of Water-to-Water Heat Pump Models in Simulating Load Side Heat Transfer Rate (Heating)

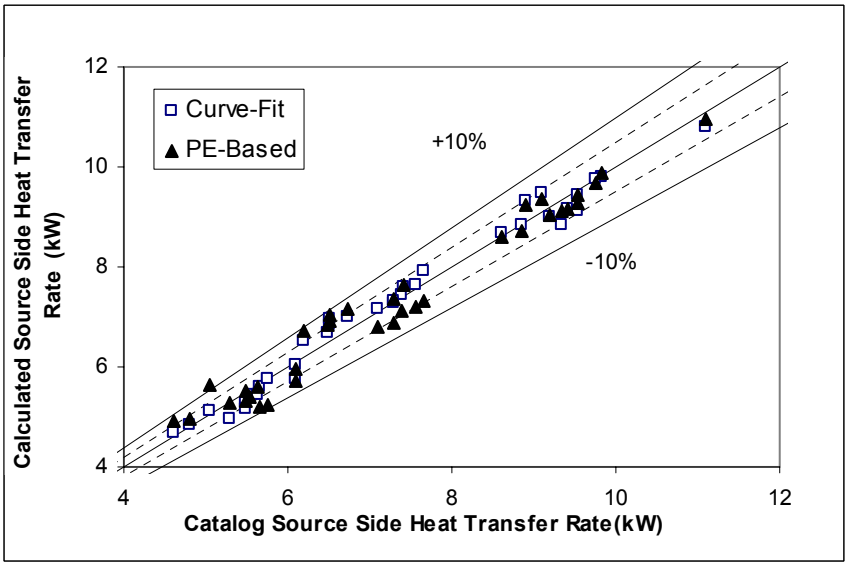

Figure 5.42: Performance of Water-to-Water Heat Pump Models in Simulating Source Side Heat Transfer Rate (Heating)

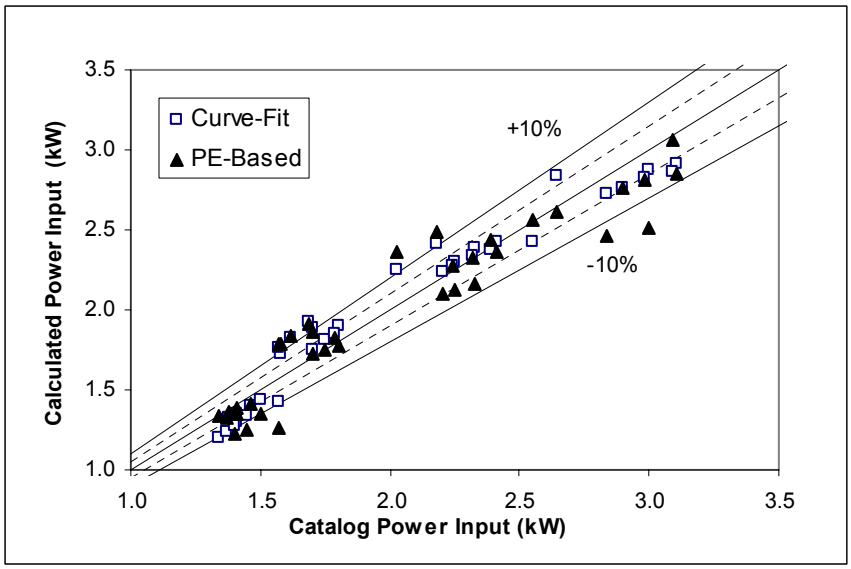

Figure 5.43: Performance of Water-to-Water Heat Pump Models in Simulating Power Consumption (Heating)

	Cooling		Heating	
	Curve-Fit	PE-Based	Curve-Fit	PE-Based
Number of Data Points	36	36	36	36
Qload RMS error (%)	1.30	2.05	2.45	3.33
Power RMS error (%)	3.54	5.91	7.12	8.89
Qsource RMS error (%)	0.97	3.81	3.32	4.81

Table 5.20: Result Summary of Water-to-Water Heat Pump Models Compared with Catalog Data

Unlike the parameter estimation based model, the number of data points used to generate the coefficients does not affect the accuracy of the curve-fit model. This can be seen by comparing Table 5.18, Table 5.19, and Table 5.20. As discussed in Section 4.1.2 the curve-fit model is more sensitive to the type of data points (varying inlet conditions with no abrupt changes in outputs) than the number of data points. Table 5.20 shows that the curve-fit model performs better than the parameter estimation based model for both cooling and heating mode. This might be attributed to the fact that the curve-fit model uses more coefficients. The curve-fit model uses 10 coefficients while the parameter estimation based model uses 8 parameters.

The curve-fit model has 2 dedicated curves: one for load side heat transfer rate and another one for power consumption. The source side heat transfer rate is calculated using the calculated power consumption and load side heat transfer rate. Table 5.20 shows that although the curve-fit model performed rather poorly for power consumption with RMS error 3%-7%, the source side heat transfer rate is still reasonably accurate with RMS error 1%-3%. This is because the error in the power consumption is rather small when compared to the value of the source side heat transfer rate which is between 10-16 KW for cooling and 4-11 KW for heating. This also explains why the source side heat transfer rate for the curve-fit model has a higher RMS error in heating mode than cooling mode.

On the other hand, the parameter estimation model is able to capture the load side and source side rates pretty accurately with RMS error of 2%-5%. The parameter estimation based model iterates on the source side and load side heat transfer rates until both values converged. Similar to the curve-fit model, the source side heat transfer rate is calculated from the load side heat transfer rate and the power consumption. Depending on the convergence tolerance, there is uncertainty in the range of possible values for the calculated source side and load side heat transfer rates. Although this uncertainty has a small effect on the accuracy of the source side heat transfer rates, it has a considerably large effect on the power consumption, with an RMS error of 6%-8%.

5.3.3 Summary of Water-to-Air Heat Pump Validation

From this study, it can be concluded that the curve-fit model is slightly better than the parameter estimation based model at capturing the performance of the water-to-water heat pump model within the specified data set. Both models shows higher errors in

simulating the power consumption with RMS error of 3-9% with the curve-fit model outperforming the parameter estimation based model. More data points used for generating the coefficients/parameters will result in slightly higher accuracy for the parameter estimation based model as noted by Jin (2002). However, this is not the case for the curve-fit model which is more dependent on the type of data points (varying inlet conditions with no abrupt changes in outputs). Based on this study, there is not a significant difference in the performance of the two models.

6.0 Conclusion and Recommendations

6.1. Summary of Results

The results of this study are summarized in the order in which they are presented in this thesis.

1. Comparison of the EnergyPlus air-to-air heat pump model with experimental data showed that the model is capable of simulating the heat pump performance with an RMS error of 4-12%. Most of the error is attributed to the discrepancies in the catalog data and the propagation of error from the curves.
2. Compressor shell heat loss is dependent on the temperature difference between the shell temperature and the condenser outlet air temperature for cooling mode. The measured compressor shell heat loss for a 3-ton air-to-air heat pump accounted for 11%-16% of the compressor power input. Compressor heat loss is generally unaccounted in the manufacturers' catalog data.
3. Based on the parametric study of the part-load latent degradation model, the LHR function is found to be affected most strongly by the fan time delay, $t_{fandelay}$ and the parameter γ (ratio of the initial evaporation rate to the steady-state latent capacity).
4. Both Jin(2002) and the curve-fit water-to-air heat pump models are capable of simulating the performance of water-to-air heat pumps fairly well with RMS error of about 10%. The high number of coefficients used in the curve-fit model improves its performance. Computational uncertainty of 2-5% due to different

refrigerant property routines in the parameter generator and the simulation model can either increase or decrease the error of the parameter estimation based model.

5. Extrapolation of the water-to-air heat pump models beyond the data set shows that the curve-fit model performed rather poorly in total cooling capacity and heat rejection with RMS error of 10%-15%. The curve-fit model is very sensitive to the input data range used in generating the coefficients. Failure to account for the entire range of the wet-bulb temperature cause the model to underestimate or overestimate the total cooling capacity and heat rejection.
6. The constant "averaged" parameters used by Jin(2002) model gives reasonable output beyond the catalog data range. However, the model also shows insensitivity in simulating the heat pump power input with the largest RMS error of about 12%.
7. The curve-fit water-to-water heat pump developed in this study performs adequately well compared to the catalog data with RMS error less than 7%. The curve-fit model is more robust and requires less computation time than the parameter estimation model.

6.2. Future Work

Recommendations for future work include the following:

1. Another curve-fit air-to-air heat pump model can be developed based on Lash (2002) method. The model is expected to perform better than the DOE-2 model

because it has no restriction on the type of data points and there is no propagation of error. The governing equations are proposed in Appendix E. The model requires fewer curves with fewer parameters. The governing equations require validation at least with the catalog data.

2. For this study, the heat pump models are validated for steady-state operation, but they are not validated for part-load operation. The part-load latent degradation model for constant fan has been validated by Henderson et. al (2003) using field measured data. It would be interesting to see the performance of the EnergyPlus water-to-air heat pumps in simulating part-load latent capacity for both constant fan and cycling fan.
3. Incorporate EnergyPlus refrigerant property routines in the parameter generator program for both the Jin (2002) water-to-water and water-to-air heat pump models. This will reduce the computational uncertainty of the model by 2%-5% of the RMS error. As mentioned earlier, the refrigerant properties can be compiled as a DLL or ported to VBA.
4. The current generalized least square method used for calculating the coefficients for the curve-fit models has some problems with input data that have fixed inlet conditions. A more robust numerical method may be proposed or adopted for the calculation of the coefficients.
5. The curve-fit water-to-water and water-to-air heat pump models can only simulate the heat pump performance using the same working fluids as the manufacturer catalog data which is usually pure water. Development of some sort of degradation factor to account for the performance loss due to the usage

of antifreeze is necessary. Some manufacturers provide correction factors for the heat pump performance based on the concentration of antifreeze as mentioned by Jin(2002). However, measured experimental data is still necessary for both development and validation of the heat pump model.

6. In this study, the interaction of the heat pump models with other system components and the zone is not validated experimentally. The overall system performance can be validated experimentally using the facility built by Hern (2004).

REFERENCES

Aaron, D.A. and P.A. Domanski, P.A. 1990. Experimentation, analysis, and correlation of refrigerant-22 flow through short tube restrictors. ASHRAE Transactions. 1(2), pp.729-742.

ARI. 2003. ARI Standard 210/240, Unitary Air-Conditioning and Air-Source Heat Pump Equipment. Arlington, Va.: Air-Conditioning and Refrigeration Institute

ARI. 1999. ARI Standard 540-99, Positive Displacement Refrigerant Compressors and Compressor Units. Arlington, VA: Air-Conditioning and Refrigeration Institute.

ASHRAE. 2000 ASHRAE Handbook – 2000 HVAC Systems and Equipment. Atlanta: American Society of Heating, Refrigerating, and Air-Conditioning Engineering, Inc.

Bonne, U., A.Patani, R.D. Jacobson, D.A. Mueller. 1980. Electric-Driven Heat Pump Systems Simulations and Controls II. ASHRAE Transactions 86(1), pp. 687-705.

Bourdouxhe, J-P H., M. Grodent, J J. Lebrun, C. Saavedra, K. L. Silva.1994. A Toolkit for Primary HVAC System Energy Calculation- Part 2: Reciprocating Chiller Models. ASHRAE Transactions. 100(2), pp. 774-786.

Carrier, H.W., E.R. Cherne, A.W. Grant, and H.W. Roberts. 1959. Modern Air Conditioning, Heating and Ventilating. New York: Pitman Publishing Corp.

DOE. 1982. DOE-2 Engineers Manual, version 2.1A. LBL-11353. Berkeley, CA: Lawrence Berkeley National Laboratory.

EnergyPlus. 2004. Engineering Document: The Reference to EnergyPlus Calculations. US Department of Energy.

Groff, G.C., C.E. Bullock. 1979. A Computer Simulation Model for Air-Source Heat Pump System Seasonal Performance Studies. Proceedings of the 2nd Annual Heat Pump Technology Conference, Stillwater, Oklahoma, pp.18-19.

Henderson, H.I., K. Rengarajan, D.B. Shirey. 1992. The Impact of Comfort Control on Air Conditioner Energy Use in Humid Climates. ASHRAE Transactions 98 (2), pp. 104-112.

Henderson, H.I., K. Rengarajan.1996. A Model to Predict the Latent Capacity of Air Conditioners and Heat Pumps at Part-Load Conditions with Constant Fan Operation ASHRAE Transactions 102 (1), pp. 266-274.

Henderson, H.I. Jr., Y.J. Huang and Danny Parker. 1999. Residential Equipment Part-Load Curves for Use in DOE-2. Environmental Energy Technologies Division, Ernest Orlando Lawrence Berkeley National Laboratory.

Henderson, H.I., D.B. Shirey, R.A. Raustad. 24-26 Sep 2003. Understanding the Dehumidification Performance of Air-Conditioning Equipment at Part-Load Conditions. CIBSE/ASHRAE Conference, Edinburgh, Scotland.

Hern, S.A. 2004. Design of An Experimental Facility for Hybrid Ground Source Heat Pump Systems. M.S. Thesis, Department of Mechanical and Aerospace Engineering, Oklahoma State University.

Iu, I., P.K. Bansal, S.J. Rees, D.E. Fisher, N.A. Weber, and J.D. Spitler. October 8 – 10, 2003. Energy Efficiency Analysis of a Unitary Heat Pump System, Proc. Int. Conf. on Building Systems and Facilities Management - Integrating Innovations and Technologies For a Built Environment, Singapore, pp. 334 – 341.

Jin, Hui. 2002. Parameter Estimation Based Models of Water Source Heat Pumps. Phd. Thesis, Department of Mechanical and Aerospace Engineering, Oklahoma State University.

Jin, H., and J.D. Spitler. 2002. A Parameter Estimation Based Model of Water-To-Water Heat Pumps for use in Energy Calculation Programs. ASHRAE Transactions. 108(1), pp. 3-17.

Katipamula,S., and D.L. O'Neal. 1992. Part-load factor for a heat pump derived from laboratory measurements. Energy and Buildings. 19(2),pp.125-132

Khattar, M.K., N. Ramanan, and M. Swami. 1985. Fan cycling effects on air conditioner moisture removal performance in warm, humid climates. Presented at International Symposium on Moisture and Humidity, Washington, D.C.. 837-842

Kuester, J., and J. H. Mize. 1973. Optimization Techniques with Fortran. Chp 9. New York, McGraw-Hill.

Lash, T. 1992. Simulation and Analysis of a Water Loop Heat Pump System, M.S.Thesis, Department of Mechanical Engineering, University of Illinois at Urbana-Champaign.

McElgin, J., D.C. Wiley. 1940. Calculation of Coil Surface Areas for Air Cooling and Dehumidification. Heating, Piping and Air Conditioning, 12(1), pp. 195-201.

Mulroy, W.J., D.A. Didion. 1985. Refrigerant Migration in a Split-Unit Air Conditioner. ASHRAE Transactions, 91(1A), pp. 193-206

Murugappan, Arun. 2002. Implementing Ground Source Heat Pump and Ground Loop Heat Exchanger Models in the EnergyPlus Simulation Environment, M.S. Thesis, Department of Mechanical and Aerospace Engineering, Oklahoma State University.

O'Neal, D.L., S. Katipamula. 1991. Performance Degradation During On-Off Cycling of Single-Speed Air Conditioners and Heat Pumps - Model Development and Analysis. ASHRAE Transactions 97 (2), pp. 316-323

O'Neal, D.L., S. Katipamula. 1991. Performance Degradation during On-Off Cycling of Single-Speed Air Conditioners and Heat Pumps - Experimental Results. ASHRAE Transactions 97 (2), pp. 331-339

Shenoy,Arun. 2004. Simulation, Modeling and Analysis of Water to Air Heat Pump. M.S. Thesis, Department of Mechanical and Aerospace Engineering, Oklahoma State University.

Taylor, R. D., C.O. Pedersen, D.E. Fisher, R. J. Liesen, L.K. Lawrie. December 3-5, 1990. Simultaneous Simulation of Buildings and Mechanical Systems in Heat Balance Based Energy Analysis Programs, Proceedings of the 3rd International Conference on System Simulation in Buildings, Liege, Belgium.

Taylor, R.D., C.O. Pedersen, D.E. Fisher, R. J. Liesen, L.K. Lawrie. August 20-22, 1991. Impact of Simultaneous Simulation of Buildings and Mechanical Systems in Heat Balance Based Energy Analysis Programs on System Response and Control, Conference Proceedings IBPSA Building Simulation '91, Nice, France.

U.S. Department of Energy, 1979, Test Procedures for Central Air Conditioners, Including Heat Pumps," Federal Register, Vol. 44, No. 249, pp. 76,700-76,763

Weber, N.A. 2003. Performance Effects of Air Velocity Profiles in a Residential Heat Pump. M.S. Thesis, Department of Mechanical and Aerospace Engineering, Oklahoma State University.

APPENDIX A: Generating Coefficients for EnergyPlus Curve-Fit Air-to-Air Heat Pump Model

This section is about the steps taken to generate the coefficients used for validating the model as discussed in Chapter 5.1.

A.1 Temperature Modifying Factors (TMF) and Flow Fraction Modifying Factors (FMF) for Cooling Mode

Two sets of TMF and FMF functions are required for simulating the total cooling capacity and the COP. The rated conditions for the model is as following; (80˚F [26.7˚C] indoor dry bulb and 67˚F [19.4˚C] wet bulb; 95˚F [35.0˚C] outdoor dry bulb; 350~450 cfm/ton [0.047~0.06 m^3/s kW]). Since this is a 3-ton heat pump, 1200cfm is regarded as the rated air flow rate.

Q(CFM)	idb(F)	iwb(F)	odb(F)	Qtotal (MBH)	iwb(C)	odb(C)	Qtotal/Qtotal,rated
1200	80	72	85	41.2	22.22	29.44	1.198
1200	80	67	85	37.2	19.44	29.44	1.081
1200	80	62	85	34.5	16.67	29.44	1.003
1200	80	57	85	33.7	13.89	29.44	0.980
1200	80	72	95	38.8	22.22	35.00	1.128
1200	80	67	95	34.4	19.44	35.00	1.000
1200	80	62	95	32.7	16.67	35.00	0.951
1200	80	57	95	31.6	13.89	35.00	0.919
1200	80	72	105	35.7	22.22	40.56	1.038
1200	80	67	105	31.4	19.44	40.56	0.913
1200	80	62	105	30.2	16.67	40.56	0.878
1200	80	57	105	29.2	13.89	40.56	0.849
1200	80	72	115	32.6	22.22	46.11	0.948
1200	80	67	115	28.4	19.44	46.11	0.826
1200	80	62	115	27.7	16.67	46.11	0.805
1200	80	57	115	26.8	13.89	46.11	0.779

Table A.1: Dataset for generating $f_C\left(iwb, odb\right)$ function (Cooling)

Table A.1 shows the dataset used to generate the $f_C\left(iwb, odb\right)$ function with the baseline condition highlighted. The temperatures are converted from IP units to SI units since EnergyPlus uses SI units. The total cooling capacity is divided by the rated total

cooling capacity of 34.4 KBtu/hr. General Least Square Method is used to solve for the coefficients a_1 to a_6 of the equations below,

$$f_c(iwb, odb) = \frac{C_C}{C_{C,rated}} = a_1 + a_2(iwb) + a_3(iwb)^2 + a_4(odb) + a_5(odb)^2 + a_6(iwb)(odb)$$

The coefficients calculated are shown in Table A.5 with an average error of 0.73%.

Coefficient	F_C(iwb,odb)
a1	1.572337E+00
a2	-7.154010E-02
a3	3.084594E-03
a4	2.935484E-03
a5	-1.118462E-04
a6	-4.502094E-04
Average Error(%)	0.73%

Table A.2: Coefficients for $f_C(iwb, odb)$ (Cooling)

Q(CFM)	idb(F)	iwb(F)	odb(F)	Qtotal (MBH)	Q/Qrated	Qtotal/Qtotal,rated
900	80	67	95	32.1	0.750	0.933
1050	80	67	95	33.3	0.875	0.968
1200	80	67	95	34.4	1.000	1.000
1350	80	67	95	35.3	1.125	1.026
1500	80	67	95	36.2	1.250	1.052

Table A.3: Dataset for generating $f_C(Q/Q_{rated})$ function (Cooling)

Table A.3 shows the dataset used to generate the $f_C(Q/Q_{rated})$ function with the baseline condition highlighted. Coefficients b_1 to b_3 of the equations below are calculated by plotting the flow faction, Q/Q_{rated} against capacity fraction, $Q_{total}/Q_{total,rated}$ in Excel using the 2nd order polynomial. Coefficients b_1 to b_3 obtained from Figure A.1 are shown in Table A.4.

$$f_c(Q/Q_{rated}) = \frac{C_C}{C_{C,rated}} = b_1 + b_2(Q/Q_{rated}) + b_3(Q/Q_{rated})^2$$

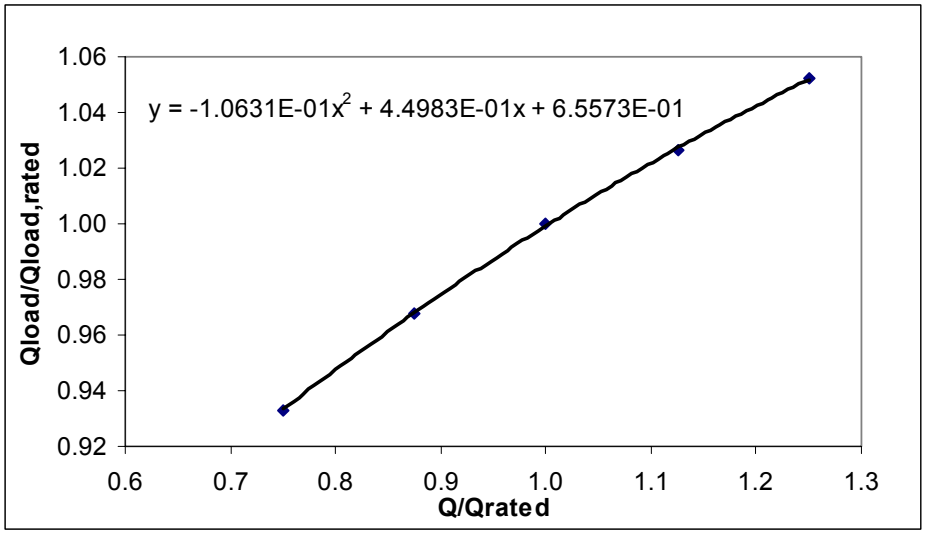

Figure A.1: Q/Q_{rated} against $Q_{total}/Q_{total,rated}$ for $f_C\left(Q/Q_{rated}\right)$ function (Cooling)

Coefficient	F_C(Q/Qrated)
b1	6.5573E-01
b2	4.4983E-01
b3	-1.0631E-01

Table A.4: Coefficients for $f_C\left(Q/Q_{rated}\right)$ (Cooling)

The procedure used to compute the coefficients for $f_C\left(iwb,odb\right)$ and $f_C\left(Q/Q_{rated}\right)$ is used for computing $f_{EIR}\left(iwb,odb\right)$ and $f_{EIR}\left(Q/Q_{rated}\right)$. Table A.5 and Table A.6 are the datasets used for computing $f_{EIR}\left(iwb,odb\right)$ and $f_{EIR}\left(Q/Q_{rated}\right)$. For the sake of brevity, only the datasets and the coefficients are shown below;

Q(CFM)	idb(F)	iwb(F)	odb(F)	iwb(C)	odb(C)	Power Input (kW)	Qtotal (W)	EIR	EIR/EIRrated
1200	80	72	85	22.22	29.44	3140	12075.72	0.260	0.762
1200	80	67	85	19.44	29.44	3110	10903.32	0.285	0.836
1200	80	62	85	16.67	29.44	3090	10111.95	0.306	0.896
1200	80	57	85	13.89	29.44	3090	9877.47	0.313	0.917
1200	80	72	95	22.22	35.00	3470	11372.28	0.305	0.894
1200	80	67	95	19.44	35.00	3440	10082.64	0.341	1.000
1200	80	62	95	16.67	35.00	3430	9584.37	0.358	1.049
1200	80	57	95	13.89	35.00	3410	9261.96	0.368	1.079
1200	80	72	105	22.22	40.56	3860	10463.67	0.369	1.081
1200	80	67	105	19.44	40.56	3800	9203.34	0.413	1.210
1200	80	62	105	16.67	40.56	3770	8851.62	0.426	1.248
1200	80	57	105	13.89	40.56	3770	8558.52	0.440	1.291
1200	80	72	115	22.22	46.11	4250	9555.06	0.445	1.304
1200	80	67	115	19.44	46.11	4170	8324.04	0.501	1.468
1200	80	62	115	16.67	46.11	4120	8118.87	0.507	1.487
1200	80	57	115	13.89	46.11	4130	7855.08	0.526	1.541

Table A.5: Dataset for generating $f_{EIR}\left(iwb, odb\right)$ function (Cooling)

Q(CFM)	idb(F)	iwb(F)	odb(F)	Power Input (W)	Qtotal (W)	EIR	EIR/EIRrated
900	80	67	95	3300	9408.51	0.3508	1.028
1050	80	67	95	3370	9760.23	0.3453	1.012
1200	80	67	95	3440	10082.64	0.3412	1.000
1350	80	67	95	3520	10346.43	0.3402	0.997
1500	80	67	95	3600	10610.22	0.3393	0.994

Table A.6: Dataset for generating $f_{EIR}\left(Q/Q_{rated}\right)$ function (Cooling)

Coefficient	F_{EIR}(iwb,odb)	F_{EIR}(Q/Qrated)
a1	5.296651E-02	1.2307E+00
a2	8.919838E-02	-3.9331E-01
a3	-2.634651E-03	1.6387E-01
a4	-1.083157E-02	
a5	7.247208E-04	
a6	-4.445318E-04	
Average Error(%)	0.80%	

Table A.7: Coefficients for $f_{EIR}\left(iwb, odb\right)$ and $f_{EIR}\left(Q/Q_{rated}\right)$ functions (Cooling)

A.3 Temperature Modifying Factors (TMF) and Flow Fraction Modifying Factors (FMF) for Heating Mode

The rating conditions for heating mode are as following: (70˚F [21.1˚C] indoor dry bulb and 60˚F [15.5˚C] indoor wet bulb; 47˚F [8.33˚C] outdoor dry bulb and 43˚F [6.11˚C] outdoor dry bulb; 350~450 cfm/ton [0.047~0.06 m3/s kW]). For the sake of brevity, only the datasets and the coefficients calculated for the heating capacity TMF

and FMC ($f_H\left(idb,odb\right)$, $f_H\left(Q/Q_{rated}\right)$) and the heating energy input ratio TMF and FMF ($f_{EIR}\left(idb,odb\right)$, $f_{EIR}\left(Q/Q_{rated}\right)$) are shown.

Q(CFM)	idb(F)	odb(F)	Qheat(W)	Total Power (W)	idb (C)	odb(C)	Qheat/Qheat,rated	EIR/EIRrated
1200	55	-10	4142.38	1886	12.78	-23.33	0.430	1.475
1200	55	0	4818.86	2026	12.78	-17.78	0.500	1.362
1200	55	10	5621.66	2166	12.78	-12.22	0.583	1.248
1200	55	20	6574.53	2305	12.78	-6.67	0.682	1.136
1200	55	30	7705.31	2445	12.78	-1.11	0.799	1.028
1200	55	40	9047.70	2584	12.78	4.44	0.939	0.925
1200	55	50	10641.00	2724	12.78	10.00	1.104	0.829
1200	55	60	12532.08	2863	12.78	15.56	1.300	0.740
1200	70	-10	3618.32	2180	21.11	-23.33	0.375	1.952
1200	70	0	4294.79	2320	21.11	-17.78	0.446	1.750
1200	70	10	5097.60	2460	21.11	-12.22	0.529	1.563
1200	70	20	6050.46	2599	21.11	-6.67	0.628	1.392
1200	70	30	7181.24	2739	21.11	-1.11	0.745	1.236
1200	70	40	8523.64	2878	21.11	4.44	0.884	1.094
1200	70	47	9640.06	2976	21.11	8.33	1.000	0.966
1200	70	50	10116.93	3018	21.11	10.00	1.049	0.852
1200	70	60	12008.01	3157	21.11	15.56	1.246	2.453
1200	80	-10	3188.05	2414	26.67	-23.33	0.331	2.141
1200	80	0	3864.52	2554	26.67	-17.78	0.401	1.870
1200	80	10	4667.32	2694	26.67	-12.22	0.484	1.633
1200	80	20	5620.19	2833	26.67	-6.67	0.583	1.427
1200	80	30	6750.97	2973	26.67	-1.11	0.700	1.246
1200	80	40	8093.37	3112	26.67	4.44	0.840	1.088
1200	80	50	9686.66	3252	26.67	10.00	1.005	0.949
1200	80	60	11577.74	3391	26.67	15.56	1.201	0.981

Table A.8: Dataset for generating $f_H\left(idb,odb\right)$ and $f_{EIR}\left(idb,odb\right)$ functions (Heating)

Q(CFM)	idb(F)	odb(F)	Qheat(W)	Total Power (W)	Q/Qrated	Qheat/Qheat,rated	EIR/EIRrated
900	70	47	9138.86	3085.00	0.75	0.95	1.09
1200	70	47	9640.06	2976.00	1.00	1.00	1.00
1500	70	47	10144.19	3077.58	1.25	1.05	0.98

Table A.9: Dataset for generating $f_H\left(Q/Q_{rated}\right)$ and $f_{EIR}\left(Q/Q_{rated}\right)$ functions (Heating)

Coefficient	F_H(idb,odb)	F_H(Q/Qrated)
1	8.825666E-01	7.9386E-01
2	-2.837969E-03	2.0371E-01
3	-1.087553E-04	2.4324E-03
4	2.467141E-02	
5	3.355738E-04	
6	3.903128E-18	
%Average Error	0.72%	

Table A.10: Coefficients for $f_H\left(idb,odb\right)$ and $f_H\left(Q/Q_{rated}\right)$ functions (Heating)

Coefficient	F_{EIR}(idb,odb)	F_{EIR}(Q/Qrated)
1	9.306693E-01	1.8312E+00
2	-8.845850E-03	-1.4410E+00
3	1.016505E-03	6.0974E-01
4	1.014525E-03	
5	2.563606E-04	
6	-1.364867E-03	
%Average Error	1.91%	

Table A.11: Coefficients for $f_{EIR}\left(idb, odb\right)$ and $f_{EIR}\left(Q/Q_{rated}\right)$ functions (Heating)

A.3 Post Calculation of Simulation Results

Cooling Mode

The total cooling and sensible capacity in the catalog data has the indoor fan heat deducted. Thus in order to figure out the actual coil capacity, the indoor fan power has to be added to the calculated total and sensible cooling capacity. It can be assumed that the total fan heat is equaled to the fan power input. Besides that, the total power reflected in the catalog data includes the compressor power, and both the indoor and outdoor fan. Thus the actual compressor power is calculated by deducting the indoor and outdoor fan power from the calculated heat pump power consumption. Since the indoor fan speed is not specified, it is assumed that the fan is running at MEDIUM speed and fan curve can be obtained from the manufacturer catalog. The graph below shows the indoor fan power consumption at MEDIUM speed setting, operating with 230VAC against the air flow rate.

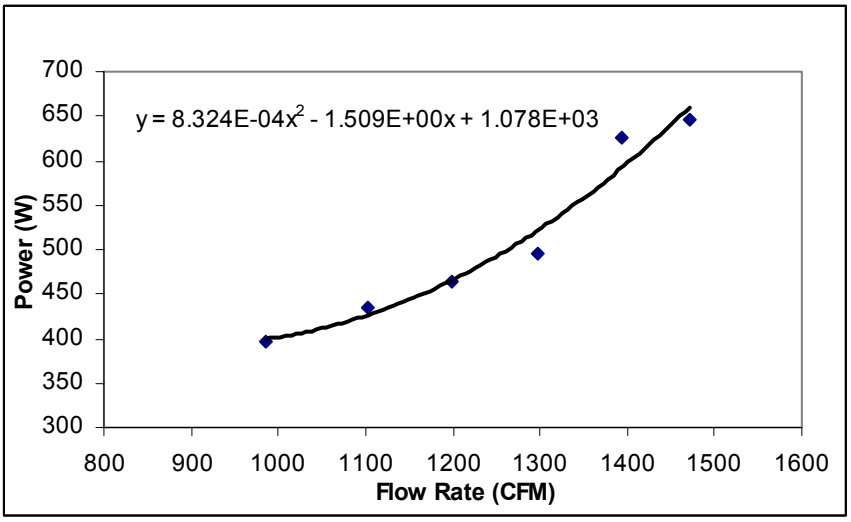

Figure A.2: Indoor Fan Performance Curve

The fan curve shown in Figure A.2 is used for estimating the indoor fan power consumption at various flow rates. The outdoor fan power however was not specified in the catalog data. The outdoor fan power is obtained from the manufacturer's experimental data which is about constant at 182W. In addition to that, the performance data in the catalog was at 230VAC but the experimental data conducted in OSU was at 208VAC. An empirical correction factor of, $\dot{W}_{208V} \cong \frac{\dot{W}_{230V}}{1.25}$ calculated by Iu et. al(2003) is required to adjust for the compressor power. Changes in the compressor power will affect the heat pump capacity as well but it is assumed to be very minimal. The table below shows EnergyPlus results and the adjustments made to the results;

	EnergyPlus Output						Adjusted for Fan Power			
	Qtotal (KW)	Qsen (KW)	Total Power (KW)	CFM	Indoor Fan (W)	Outdoor Fan (W)	Qtotal (KW)	Qsen (KW)	Wcomp@230 (KW)	Wcomp@208 (KW)
TCND82	10.594	7.626	3.090	1217.45	474.64	182.00	11.069	8.100	2.434	1.947
TCND88	10.367	7.516	3.185	1220.13	476.03	182.00	10.843	7.992	2.527	2.021
TCND95	9.845	7.361	3.407	1223.18	477.63	182.00	10.322	7.839	2.748	2.198
TCND105	9.115	7.039	3.745	1221.77	476.89	182.00	9.592	7.516	3.086	2.469
TCND115	8.250	6.684	4.081	1216.27	474.03	182.00	8.724	7.158	3.425	2.740
TEVP69	9.045	7.163	3.361	1222.75	477.41	182.00	9.522	7.641	2.701	2.161
TEVP73	9.165	7.140	3.360	1224.13	478.14	182.00	9.643	7.618	2.700	2.160
TEVP76	9.409	7.207	3.383	1224.11	478.13	182.00	9.887	7.685	2.723	2.178
TEVP80	9.845	7.361	3.407	1223.18	477.63	182.00	10.322	7.839	2.748	2.198
TEVP84	10.473	7.507	3.408	1216.08	473.93	182.00	10.947	7.981	2.752	2.202
CFM760	9.436	6.164	3.311	763.34	411.15	182.00	9.848	6.575	2.718	2.174
CFM950	9.452	6.539	3.310	948.58	395.59	182.00	9.848	6.935	2.733	2.186
CFM1090	9.619	6.937	3.349	1095.09	423.74	182.00	10.043	7.361	2.743	2.194
CFM1200	9.820	7.258	3.379	1198.23	465.00	182.00	10.285	7.723	2.733	2.186
CFM1330	10.023	7.625	3.459	1329.46	543.08	182.00	10.567	8.168	2.734	2.187

Table A.12: Post Calculations for EnergyPlus Air-to-Air Heat Pump Results in Cooling Mode

Heating Mode

The heating capacity listed in the catalog data includes contribution from the indoor fan heat. The indoor fan is assumed to be operating with MEDIUM speed setting at 230VAC and the fan power can be calculated based on Figure A.2. Thus the heating capacity of the coil is calculated by deducting the fan heat from the heating capacity outputs from EnergyPlus. The compressor power is calculated by deducting the indoor and outdoor fan power from the total power. The outdoor fan power is assumed to be at 182W based on the experimental data provided by the manufacturer. No correction factor is required to adjust for the compressor power because the results are compared to the manufacturer experimental data which are ran at 230VAC. Table A.13 below shows the adjustments made to EnergyPlus outputs for heating mode.

EnergyPlus Output					Adjusted for Fan Power	
Heating Capacity (W)	Total Power (W)	CFM	Indoor Fan (W)	Outdoor Fan (W)	Heating Capacity (W)	Wcomp (KW)
9423.52	2964.82	1209.57	470.61	182.00	8952.91	2312.21
9893.71	2952.38	1534.63	722.62	182.00	9171.09	2047.76
9034.73	3278.10	1234.69	483.81	182.00	8550.92	2612.29
9155.85	3041.59	902.09	394.13	182.00	8761.72	2465.46
9922.05	2750.78	1203.06	467.36	182.00	9454.69	2101.42
11612.78	3080.89	1203.40	467.53	182.00	11145.25	2431.37

Table A.13: Post Calculations for EnergyPlus Air-to-Air Heat Pump Results in Heating Mode

APPENDIX B: Generating Coefficients for EnergyPlus Curve-Fit Water-to-Air Heat Pump Model

B.1 Procedure for Generating Cooling Coefficients

The cooling catalog data is extended using the air correction table provided by the manufacturer. The catalog data is extended from 54 data points to 810 data points. The data points are then filtered by checking for unrealistic relative humidity (>100%) of the air exiting the cooling coil as mentioned in Jin(2002). In addition to that, data points with zero latent capacity, which seldom occurs under normal heat pump operations are deleted. From 810 possible data points, only 348 data points are considered to be good data points.

Initially the rated conditions are specified and the values are obtained from the catalog data. The general rule of thumb by Shenoy (2002) is to use the values corresponds to the largest cooling capacity listed in the catalog. Output from an Excel VBA program below shows the rated conditions required by the model listed in SI units together with the coefficients generated.

Number of Data Set	348
TREF (fixed at 283.15K) 10C	283.15
RatedAirVolFlowRate (m3/s)	5.66E-01
RatedWaterVolFlowRate (m3/s)	2.84E-04
RatedTotalCap (W)	12368.82
RatedSensCap (W)	8529.21
RatedPower (W)	1380.00

	TotalCoolCapCoeff	SensCoolCapCoeff	CoolPowerCoeff
Coefficient 1	-1.27373428	4.27615968	-7.66308745
Coefficient 2	3.73053580	13.90195633	1.13961086
Coefficient 3	-1.75023168	-17.28090511	7.57407956
Coefficient 4	0.04789060	-0.70050924	0.30151440
Coefficient 5	0.015777882	0.51366014	-0.091186547
Coefficient 6		0.017194205	

Error Analysis	Error
Qtotal RMS error	0.28
Qsens RMS error	0.37
HeatRej RMS error	0.28
Power RMS error	0.04
Qtotal RMS error (%)	2.68
Qsens RMS error (%)	4.49
HeatRej RMS error (%)	2.19
Power RMS error (%)	1.86
Qtotal Average error (%)	2.30
Qsens Average error (%)	3.75
HeatRej Average error (%)	1.95
Power Average error (%)	1.52

Figure B.1: Screenshot of Excel Interface with Cooling Coefficients Generated Using Catalog Data

Based on experience and observations, a slightly different rated conditions used will change only the coefficients with no apparent difference in the outputs or the error. However, unreasonably low or high rated conditions will results in high RMS error. Thus it is advisable to stick to the recommended guidelines. Note that the same rated conditions should be used in the EnergyPlus simulation environment together with the coefficients. As mentioned in Chapter 5.2, the coefficients generated using experimental data from manufacturer are as follows:

Number of Data Set	23
TREF (fixed at 283.15K) 10C	283.15
RatedAirVolFlowRate (m3/s)	5.66E-01
RatedWaterVolFlowRate (m3/s)	2.84E-04
RatedTotalCap (W)	12368.82
RatedSensCap (W)	8529.21
RatedPower (W)	1380.00

	TotalCoolCapCoeff	**SensCoolCapCoeff**	**CoolPowerCoeff**
Coefficient 1	-4.77186397	-1730.59710214	-6.10883054
Coefficient 2	6.41736364	1639.98229451	-0.08902097
Coefficient 3	-1.40852854	-4.95569700	7.43661983
Coefficient 4	0.45599722	-0.54508385	0.19599418
Coefficient 5	0.005198137	0.591504054	-0.110411869
Coefficient 6		0.023427522	

Error Analysis	Error
Qtotal RMS error	0.17
Qsens RMS error	0.62
HeatRej RMS error	0.63
Power RMS error	0.05
Qtotal RMS error (%)	1.60
Qsens RMS error (%)	8.99
HeatRej RMS error (%)	4.95
Power RMS error (%)	1.93
Qtotal Average error (%)	1.23
Qsens Average error (%)	4.82
HeatRej Average error (%)	4.19
Power Average error (%)	1.60

Figure B.2: Screenshot of Excel Interface with Cooling Coefficients Generated Using Experimental Data

B.3 Procedure for Generating Heating Coefficients

Using the air correction table, the heating data points are extended from 44 data points to 252 data points. The entire air correction table is used and the scenario of "bad data points" does not occur for the heating data points. Then the rated heat pump conditions are entered into the Excel interface and the coefficients generated are shown in Figure B.3. The rated heat pump conditions are the values corresponds to the highest heating capacity listed in the catalog data. Figure B.4 shows the coefficients generated using 16 experimental data points as described in Chapter 5.2.

Number of Data Set	252
TREF (fixed at 283.15K) 10C	283.15
RatedAirVolFlowRate (m3/s)	5.66E-01
RatedWaterVolFlowRate (m3/s)	2.84E-04
RatedTotalCap (W)	7591.29
RatedPower (W)	2300.00

	TotalHeatCapCoeff	**HeatPowerCoeff**	**HeatQSourceCoeff**
Coeffcient 1	-5.12650150	-7.73235249	-4.26360426
Coeffcient 2	-0.93997630	6.43390775	-3.859190823
Coeffcient 3	7.21443206	2.29152262	9.328284919
Coeffcient 4	0.121065721	-0.175598629	0.245312227
Coeffcient 5	0.051809805	0.005888871	0.071490214

Error Analysis	Error
HeatCap RMS error	0.09
HeatAbs RMS error	0.12
Power RMS error	0.04
HeatCap RMS error (%)	0.84
HeatAbs RMS error (%)	1.70
Power RMS error (%)	1.47
HeatCap Average % error	0.66
HeatAbs Average % error	1.21
Power Average % error	1.06

Figure B.3: Screenshot of Excel Interface with Heating Coefficients Generated Using Catalog Data

Number of Data Set	16
TREF (fixed at 283.15K) 10C	283.15
RatedAirVolFlowRate (m3/s)	5.66E-01
RatedWaterVolFlowRate (m3/s)	2.84E-04
RatedTotalCap (W)	7591.29
RatedPower (W)	2300.00

	TotalHeatCapCoeff	**HeatPowerCoeff**	**HeatQSourceCoeff**
Coeffcient 1	12.26592225	-9.87672886	-14.33926632
Coeffcient 2	-20.10456930	8.27426368	3.23992199
Coeffcient 3	9.05169962	2.40800781	12.19630665
Coeffcient 4	0.751440956	-0.121038077	0.088595113
Coeffcient 5	0.09316979	0.033021799	0.15617671

Error Analysis	Error
HeatCap RMS error	0.09
HeatAbs RMS error	1.16
Power RMS error	0.01
HeatCap RMS error (%)	0.73
HeatAbs RMS error (%)	11.49
Power RMS error (%)	0.56
HeatCap Average % error	0.59
HeatAbs Average % error	10.17
Power Average % error	0.41

Figure B.4: Screenshot of Excel Interface with Heating Coefficients Generated Using Experimental Data

APPENDIX C: Generating Parameters for EnergyPlus Parameter Estimation Based Water-to-Air Heat Pump Model

The parameter estimation program as described in Chapter 4.2 was developed by Jin(2002) in Fortran 90. The code was converted into Excel Visual Basic for Application which has a nice user interface for setting the initial guesses and comparing the outputs from the parameter generator. As mentioned in Chapter 5.2, the same catalog data is used for generating the parameters/coefficients for Jin(2002) and the curve-fit model. Refer to Appendix B for the steps taken to prepare the inputs for the parameter generator from the catalog data.

VBA provides a nice environment for generating the parameters because the outputs from the parameter generator can be directly compared to the catalog data. Initially, the convergence tolerance is set to be very low for example, 0.001 and initial guesses of 1.0 is used for all the parameters. Then the parameter generator is run and the parameters generated from the "first" initial guesses are used as the "second" initial guesses. The convergence tolerance is then set to be higher for example, 0.000001. The errors associated with the "second" initial guesses will be lower and these steps are repeated until there are no significant changes in the errors, which mean that one has obtained the "best" parameters.

This process can also be programmed as an iterative loop but requires a huge amount of computational time. Using a Intel P4 3.0 GHz equipped with 1GB of DDR2 RAM, the VBA parameter generator takes about 526.39 seconds to generate the "first" cooling parameters using 348 data points. The required computational time will reduce as the initial guesses are closer to the "best" parameters thus requiring less iteration for

convergence. For the sake of brevity, only the parameters generated and used in the EnergyPlus simulation environment for the validation of the heat pump model are shown in this section.

C.1 Parameters Generated Using Catalog Data

E+ Input Parameter	SCROLL
LoadSideOutsideUACoeff (W/K)	1.34066E+03
LoadSideTotalUACoeff (W/K)	8.53502E+02
SuperheatTemp (C)	7.55724E-01
PowerLosses (W)	1.13223E+03
LossFactor (~)	8.75497E-01
RefVolFlowRate (m^3/s)	1.92499E-03
VolumeRatio (~)	1.74056E+00
LeakRateCoeff (~)	6.16688E-05
SourceSideUACoeff (W/K)	1.89091E+03

Table C.1: Cooling Parameters Generated Using Catalog Data

E+ Input Parameter	SCROLL
LoadSideUACoeff (W/K)	9.71732E+02
SuperheatTemp (C)	2.73653E+00
PowerLosses (W)	6.81431E+02
LossFactor (~)	6.02057E-01
RefVolFlowRate (m^3/s)	1.79491E-03
VolumeRatio (~)	2.51099E+00
LeakRateCoeff (~)	3.24397E-09
SourceSideUACoeff (W/K)	2.39362E+03

Table C.2: Heating Parameters Generated Using Catalog Data

C.2 Parameters Generated Using Experimental Data

E+ Input Parameter	SCROLL
LoadSideOutsideUACoeff (W/K)	1.00001E+03
LoadSideTotalUACoeff (W/K)	7.96727E+02
SuperheatTemp (C)	7.01624E-01
PowerLosses (W)	1.21571E+03
LossFactor (~)	9.83378E-01
RefVolFlowRate (m^3/s)	2.01482E-03
VolumeRatio (~)	1.77279E+00
LeakRateCoeff (~)	7.73228E-04
SourceSideUACoeff (W/K)	1.92032E+03

Table C.3: Cooling Parameters Generated Using Experimental Data

E+ Input Parameter	SCROLL
LoadSideUACoeff (W/K)	1.03355E+03
SuperheatTemp (C)	2.70803E+00
PowerLosses (W)	6.36551E+02
LossFactor (~)	6.79090E-01
RefVolFlowRate (m^3/s)	2.03767E-03
VolumeRatio (~)	2.43994E+00
LeakRateCoeff (~)	4.11545E-07
SourceSideUACoeff (W/K)	2.45493E+03

Table C.4: Heating Parameters Generated Using Experimental Data

APPENDIX D: Coefficients and Parameters for Water-to-Water Heat Pump Models

The procedure for generating the parameters and coefficients for water-to-water heat pump models are similar to the water-to-air heat pump models. Table D.1 shows the parameters for the parameter-estimation based model. Table D.2 shows the coefficients for the curve-fit model.

Simulation Parameter	Cooling	Heating
UA Load Side (W/K)	6.83994E+02	1.66575E+03
UA Source Side (W/K)	1.33916E+03	2.14113E+03
Superheat Temp (C)	1.15210E+00	3.64937E-01
W_{loss} (W)	2.29473E+01	2.36407E+02
LossFactor (~)	8.65341E-01	6.33162E-01
Piston Displacement (m^3/s)	2.98787E-03	1.96328E-03
Pressure Drop (Pa)	9.31427E+02	1.18454E+03
Clearance Factor (~)	3.07970E-02	1.56224E-02

Table D.1: Cooling and Heating Parameters for a 3-ton Heat Pump

Simulation Coefficient	Cooling	Heating
RatedLoadVolFlowRate (m3/s)	5.678E-04	5.678E-04
RatedSourceVolFlowRate (m3/s)	5.678E-04	5.678E-04
RatedQLoad (W)	14215.35	13482.60
RatedPower (W)	1320.00	1460.00
CapacityCoeff 1	-2.8581E+00	-3.2495E+00
CapacityCoeff 2	4.3425E+00	-3.4165E-01
CapacityCoeff 3	-9.6592E-01	4.2434E+00
CapacityCoeff 4	1.0978E-01	1.6876E-03
CapacityCoeff 5	4.6779E-02	1.1998E-01
PowerCoeff 1	-8.3346E+00	-8.2237E+00
PowerCoeff 2	4.3775E-01	8.7855E+00
PowerCoeff 3	9.0091E+00	3.9891E-01
PowerCoeff 4	3.6343E-02	-2.3708E-01
PowerCoeff 5	-2.6220E-01	-4.9596E-02

Table D.2: Cooling and Heating Coefficients for a 3-ton Heat Pump

APPENDIX E: Proposal for New Curve-Fit Air-to-Air Heat Pump Model Based on Lash (1992) Approach

As Lash (1992) approach is adapted to water-to-water heat pump, the governing equations can be easily manipulated to simulate the performance of air-to-air heat pump. The outdoor coil heat transfer with the environment is not of interest to the simulation and only 3 curves are required for cooling mode and 2 curves for heating mode. The governing equations for both cooling and heating mode are as following;

Cooling Mode

$$\frac{Q_{total}}{Q_{total,ref}} = A1 + A2\left[\frac{T_{db,ODC}}{T_{ref}}\right] + A3\left[\frac{T_{wb,IDC}}{T_{ref}}\right] + A4\left[\frac{\dot{V}_{air}}{\dot{V}_{air,ref}}\right] \tag{E.1}$$

$$\frac{Q_{sens}}{Q_{sens,ref}} = B1 + B2\left[\frac{T_{db,ODC}}{T_{ref}}\right] + B3\left[\frac{T_{db,IDC}}{T_{ref}}\right] + B4\left[\frac{T_{wb,IDC}}{T_{ref}}\right] + B5\left[\frac{\dot{V}_{air}}{\dot{V}_{air,ref}}\right] \tag{E.2}$$

$$\frac{Power_c}{Power_{c,ref}} = C1 + C2\left[\frac{T_{db,ODC}}{T_{ref}}\right] + C3\left[\frac{T_{wb,IDC}}{T_{ref}}\right] + C4\left[\frac{\dot{V}_{air}}{\dot{V}_{air,ref}}\right] \tag{E.3}$$

Heating Mode:

$$\frac{Q_h}{Q_{h,ref}} = D1 + D2\left[\frac{T_{db,ODC}}{T_{ref}}\right] + D3\left[\frac{T_{db,IDC}}{T_{ref}}\right] + D4\left[\frac{\dot{V}_{air}}{\dot{V}_{air,ref}}\right] \tag{E.4}$$

$$\frac{Power_h}{Power_{h,ref}} = E1 + E2\left[\frac{T_{db,ODC}}{T_{ref}}\right] + E3\left[\frac{T_{db,IDC}}{T_{ref}}\right] + E4\left[\frac{\dot{V}_{air}}{\dot{V}_{air,ref}}\right] \tag{E.5}$$

Where:

$A1$ - $E4$ = Equation fit coefficients for the cooling and heating mode

T_{ref} = 283K

$T_{db,ODC}$ = Outdoor coil inlet dry-bulb temperature, K

$T_{db,IDC}$ = Indoor coil inlet dry-bulb temperature, K

$T_{wb,IDC}$ = Indoor coil inlet wet-bulb temperature, K

$\dot{V}_{air}$ = Indoor air volumetric flow rate, m^3/s

Q_{total} = Total cooling capacity, W

Q_{sens} = Sensible cooling capacity, W

$Power_c$ = Power input for cooling mode, W

Q_h = Total heating capacity, W

$Power_h$ = Power input for heating mode, W

For cooling mode, the reference conditions; reference indoor air volumetric flow rate, $\dot{V}_{air,ref}$, reference sensible capacity, $Q_{sens,ref}$, and reference power input, $Power_{c,ref}$ are the conditions when the heat pump is operating at the highest total cooling capacity indicated in the manufacturer catalog which is also the reference total cooling capacity, $Q_{total,ref}$. The same procedure is used to specify the reference total heating capacity, $Q_{h,ref}$ and reference power input, $Power_{h,ref}$ for the heating mode. The governing equations still requires validation at least using the catalog data to determine if the model is capable of capturing the heat pump performance accurately.

APPENDIX F: Failure in Generalized Least Square Method (GLSM) for Fixed Inlet Conditions

To illustrate the reason why Generalized Least Square Method (GLSM) is not able to generate the coefficients for data points with fixed inlet conditions, the illustration is done using MathCad. Initially, data points with varying inlet conditions are used to illustrate the algorithm of the GLSM. Then data points with fixed conditions are used to illustrate where the failure occurs. The coefficients calculated are for the total cooling capacity represented by the following equations:

$$\frac{Q_{total}}{Q_{total,ref}} = A1 + A2\left[\frac{T_{wb}}{T_{ref}}\right] + A3\left[\frac{T_{w,in}}{T_{ref}}\right] + A4\left[\frac{\dot{V}_{air}}{\dot{V}_{air,ref}}\right] + A5\left[\frac{\dot{V}_{w}}{\dot{V}_{w,ref}}\right]$$

GLSM is used to calculate for the coefficients A1 to A5. The term for the inlet conditions is represented by Matrix F and the ratio of the total capacity to the rated capacity is represented by Matrix Y. For the initial test, 8 data points are selected with varying inlet conditions. Thus Matrix F has a size of 8x5 and Matrix Y has a size of 8x1. The computational procedure in GLSM is illustrated in MathCad as following:

$$F := \begin{pmatrix} 1 & 1.033354939 & 1.058861637 & 0.609374979 & 0.569105671 \\ 1 & 1.01962056 & 0.960758943 & 0.609374979 & 0.731707339 \\ 1 & 1.033354939 & 1.000000022 & 0.74999998 & 0.36585367 \\ 1 & 1.029430833 & 1.058861637 & 0.609374979 & 0.731707339 \\ 1 & 1.049051371 & 0.980379483 & 0.609374979 & 0.569105671 \\ 1 & 1.033354939 & 1.117723252 & 0.74999998 & 0.731707339 \\ 1 & 1.033354939 & 1.000000022 & 0.74999998 & 0.36585367 \\ 1 & 1.01962056 & 1.01962056 & 0.609374979 & 0.36585367 \end{pmatrix} \quad Y := \begin{pmatrix} 0.552112644 \\ 0.589933142 \\ 0.63098591 \\ 0.529577441 \\ 0.665909028 \\ 0.484506981 \\ 0.63098591 \\ 0.523282007 \end{pmatrix}$$

Step 1:GLSM compute the transpose of Matix F, resulting in Matrix Ftrans

$$Ftrans := F^{T} \qquad Ftrans = \begin{pmatrix} 1 & 1 & 1 & 1 & 1 & 1 & 1 & 1 \\ 1.033 & 1.02 & 1.033 & 1.029 & 1.049 & 1.033 & 1.033 & 1.02 \\ 1.059 & 0.961 & 1 & 1.059 & 0.98 & 1.118 & 1 & 1.02 \\ 0.609 & 0.609 & 0.75 & 0.609 & 0.609 & 0.75 & 0.75 & 0.609 \\ 0.569 & 0.732 & 0.366 & 0.732 & 0.569 & 0.732 & 0.366 & 0.366 \end{pmatrix}$$

Step 2:GLSM compute the product of Matrix Ftrans x Matix F, resulting in Matrix Ftrans_F

$$Ftrans\_F := Ftrans \cdot F \qquad Ftrans\_F = \begin{pmatrix} 8 & 8.251 & 8.196 & 5.297 & 4.431 \\ 8.251 & 8.511 & 8.454 & 5.464 & 4.57 \\ 8.196 & 8.454 & 8.416 & 5.433 & 4.561 \\ 5.297 & 5.464 & 5.433 & 3.544 & 2.906 \\ 4.431 & 4.57 & 4.561 & 2.906 & 2.655 \end{pmatrix}$$

Step 3:GLSM compute the inverse of Ftrans_F,resulting in Matrix Ftrans_F_inv

$$Ftrans\_F\_inv := Ftrans\_F^{-1} \qquad Ftrans\_F\_inv = \begin{pmatrix} 1.823 \times 10^{3} & -1.73 \times 10^{3} & -65.011 & 36.484 & 6.446 \\ -1.73 \times 10^{3} & 1.698 \times 10^{3} & 8.398 & -42.365 & -4.062 \\ -65.011 & 8.398 & 74.116 & -20.634 & -10.694 \\ 36.484 & -42.365 & -20.634 & 36.788 & 7.209 \\ 6.446 & -4.062 & -10.694 & 7.209 & 7.089 \end{pmatrix}$$

Step 4: GLSM compute the product of Matrix Ftrans x Matrix Y, resulting in Matrix Ftrans_Y

$$Ftrans\_Y := Ftrans \cdot Y \qquad Ftrans\_Y = \begin{pmatrix} 4.607 \\ 4.754 \\ 4.702 \\ 3.053 \\ 2.52 \end{pmatrix}$$

Step 5: GLSM compute the Matrix C **Check if FxC=Y**

$$Cmatrix := Ftrans\_F\_inv \cdot Ftrans\_Y$$

$$Cmatrix = \begin{pmatrix} -2.022 \\ 3.472 \\ -1.048 \\ 0.154 \\ -0.02 \end{pmatrix} \qquad F \cdot Cmatrix = \begin{pmatrix} 0.538 \\ 0.59 \\ 0.626 \\ 0.521 \\ 0.675 \\ 0.495 \\ 0.626 \\ 0.536 \end{pmatrix}$$

To illustrate where the failure occurs, the water flow rates and air flow rates are fixed to the rated conditions. This is the case for catalog data that shows the heat pump performance at fixed flow rates. With fixed flow rates, values at column 4 and column 5 of matrix F are equal to 1.0. The failure occurs at Step 3, because the matrix Ftrans_F is a singular matrix.

$$F := \begin{pmatrix} 1 & 1.033354939 & 1.058861637 & 1 & 1 \\ 1 & 1.01962056 & 0.960758943 & 1 & 1 \\ 1 & 1.033354939 & 1.000000022 & 1 & 1 \\ 1 & 1.029430833 & 1.058861637 & 1 & 1 \\ 1 & 1.049051371 & 0.980379483 & 1 & 1 \\ 1 & 1.033354939 & 1.117723252 & 1 & 1 \\ 1 & 1.033354939 & 1.000000022 & 1 & 1 \\ 1 & 1.01962056 & 1.01962056 & 1 & 1 \end{pmatrix} \qquad Y := \begin{pmatrix} 0.552112644 \\ 0.589933142 \\ 0.63098591 \\ 0.529577441 \\ 0.665909028 \\ 0.484506981 \\ 0.63098591 \\ 0.523282007 \end{pmatrix}$$

Step 1: GLSM compute the transpose of Matix F, resulting in Matrix Ftrans

$$Ftrans := F^{T} \qquad Ftrans = \begin{pmatrix} 1 & 1 & 1 & 1 & 1 & 1 & 1 & 1 \\ 1.033 & 1.02 & 1.033 & 1.029 & 1.049 & 1.033 & 1.033 & 1.02 \\ 1.059 & 0.961 & 1 & 1.059 & 0.98 & 1.118 & 1 & 1.02 \\ 1 & 1 & 1 & 1 & 1 & 1 & 1 & 1 \\ 1 & 1 & 1 & 1 & 1 & 1 & 1 & 1 \end{pmatrix}$$

Step 2: GLSM compute the product of Matrix Ftrans x Matix F, resulting in Matrix Ftrans_F

$$Ftrans\_F := Ftrans \cdot F \qquad Ftrans\_F = \begin{pmatrix} 8 & 8.251 & 8.196 & 8 & 8 \\ 8.251 & 8.511 & 8.454 & 8.251 & 8.251 \\ 8.196 & 8.454 & 8.416 & 8.196 & 8.196 \\ 8 & 8.251 & 8.196 & 8 & 8 \\ 8 & 8.251 & 8.196 & 8 & 8 \end{pmatrix}$$

Step 3: GLSM compute the inverse of Ftrans_F, resulting in Matrix Ftrans_F_inv

$Ftrans\_F\_inv := Ftrans\_F^{-1}$ $\qquad Ftrans\_F\_inv =$

Matrix is singular.
Cannot compute its inverse.

VITA

Tang, Chih Chien

Candidate for the Degree of

Master of Science

Thesis: MODELING PACKAGED HEAT PUMPS IN A QUASI-STEADY STATE ENERGY SIMULATION PROGRAM

Major Field: Mechanical Engineering

Biographical:

Education: Graduated from La Salle High School, Sabah, Malaysia; received Bachelor of Science degree in Mechanical Engineering from Oklahoma State University in May 2003.Completed the requirements for the Master of Science degree with a major in Mechanical Engineering at Oklahoma State University in May, 2005

Experience: Employed by Oklahoma State University, Department of Mechanical Engineering as a graduate research assistant and teaching assistant, June 2003 to May 2005

Professional Memberships: Phi Kappa Phi, Tau Beta Pi Association, Pi Tau Sigma Honor Society, Golden Key International Honor Society, The National Society of Collegiate Scholars, American Society of Heating, Refrigerating and Air-Conditioning Engineers (ASHRAE).

Name: Tang, Chih Chien Date of Degree: May, 2005

Institution: Oklahoma State University Location: Stillwater, Oklahoma

Title of Study: MODELING PACKAGED HEAT PUMPS IN A QUASI-STEADY STATE ENERGY SIMULATION PROGRAM

Page of Study: 172 Candidate for the Degree of Master of Science

Major Field: Mechanical Engineering

Scope and Method of Study: The purpose of this study is to validate steady-state heat pump models implemented in EnergyPlus. The heat pump models include air-to-air, water-to-air heat and water-to-water. Part load models are used to adjust the models' full load outputs to part load conditions. New curve-fit heat pump models are proposed and compared to existing parameter estimation based models using experimental data. Uncertainties in the models are analyzed and quantified. A short study is also conducted on the compressor shell heat loss that is often neglected by the manufacturer.

Findings and Conclusions: The EnergyPlus heat pump models agree with experimental data with an error of less than 12%. Most of the errors are attributed to the discrepancies between the catalog and the experimental measurement. The curve-fit models in EnergyPlus agree with detailed and parameter estimation based models within 6%. Curve-fit heat pump models also allow extrapolation beyond the catalog data without catastrophic error and require less computation time and are more robust than parameter estimation based models. The current drawback of curve-fit models is the inability to simulate the degradation effect of antifreeze on water source heat pump performance. The heat pump component models in EnergyPlus have been validated but the control algorithm and system interactions still require further validation with measured data.

ADVISER'S APPROVAL: _____